

Test Methods to Quantify Cracking Resistance of Asphalt Binders and Mixtures

David Newcomb, Principal Investigator
Texas A&M Transportation Institute

JANUARY 2021

Research Project
Final Report 2021-02

To request this document in an alternative format, such as braille or large print, call [651-366-4718](tel:651-366-4718) or [1-800-657-3774](tel:1-800-657-3774) (Greater Minnesota) or email your request to ADArequest.dot@state.mn.us. Please request at least one week in advance.

Technical Report Documentation Page

1. Report No. MN 2021-02	2.	3. Recipients Accession No.	
4. Title and Subtitle Test Methods to Quantify Cracking Resistance of Asphalt Binders and Mixtures		5. Report Date January 2021	
		6.	
7. Author(s) David E. Newcomb, Poura Arabali, Haydar Al-Khayat, and Fujie Zhou		8. Performing Organization Report No.	
9. Performing Organization Name and Address Texas A&M Transportation Institute 3135 TAMU College Station, Texas 77845		10. Project/Task/Work Unit No.	
		11. Contract (C) or Grant (G) No. (C) 1003324 (WO) 5	
12. Sponsoring Organization Name and Address Minnesota Department of Transportation Office of Research & Innovation 395 John Ireland Boulevard, MS 330 St. Paul, Minnesota 55155-1899		13. Type of Report and Period Covered Final Report	
		14. Sponsoring Agency Code	
15. Supplementary Notes http://mndot.gov/research/reports/2021/202102.pdf			
16. Abstract (Limit: 250 words) Incorporating cracking tests and criteria in binder acceptance, mix design, and construction quality control (QC and quality assurance (QA) offer a way to improve pavement performance. The objective of this research is to identify and, if necessary, refine binder and mixture tests capable of addressing asphalt cracking in Minnesota asphalt pavements. The tests/criteria selected for evaluation are the IDEAL-CT and the DCT for asphalt mixtures, and the ΔT_c and the G-R parameter for binders. These tests are relatively simple to perform in standard agency and contractor laboratories, require minimal time to perform and produce results, are repeatable and reproducible, and provide a distinction between brittle and ductile behavior. Additionally, binders are tested using the multiple stress creep recovery procedure to characterize their elastic recovery. Mixtures and binders from projects constructed in the 2018 and 2019 construction seasons are tested using these methods. It is found that all the mixtures and binders exhibit good cracking resistance. The mixture results from 2018 are robust for periods of up to two weeks after mixing and molding, but the mixing and molding needs to take place at the same time for both QC and QA samples as reheating QA samples will lead to a degradation in cracking resistance. The main conclusion from the 2019 mixture testing is that cracking resistance is directly related to asphalt content. Binder testing shows that all of the sources used possess good aging properties.			
17. Document Analysis/Descriptors binders, asphalt mixtures, performance tests, mix design, thermal degradation, reflection cracking		18. Availability Statement	
19. Security Class (this report) Unclassified	20. Security Class (this page) Unclassified	21. No. of Pages 110	22. Price

TEST METHODS TO QUANTIFY CRACKING RESISTANCE OF ASPHALT BINDERS AND MIXTURES

FINAL REPORT

Prepared by:

David E. Newcomb, P.E., Ph.D.
Poura Arabali
Haydar Al-Khayat
Fujie Zhou, P.E., Ph.D.
Texas A&M Transportation Institute

January 2021

Published by:

Minnesota Department of Transportation
Office of Research & Innovation
395 John Ireland Boulevard, MS 330
St. Paul, Minnesota 55155-1899

This report represents the results of research conducted by the authors and does not necessarily represent the views or policies of the Minnesota Department of Transportation or the Texas A&M Transportation Institute. This report does not contain a standard or specified technique.

The authors, the Minnesota Department of Transportation, and the Texas A&M Transportation Institute do not endorse products or manufacturers. Trade or manufacturers' names appear herein solely because they are considered essential to this report.

ACKNOWLEDGMENTS

The authors would like to thank the Minnesota Department of Transportation and specifically the Technical Advisory Panel (TAP) for the opportunity to perform this research. Their guidance and support throughout this work was key to its success. We sincerely appreciate David Van Deusen's leadership as chair of the TAP and the input, guidance and technical support provided by John Garrity, Chelsea Bennett, James Bittman, Gerald Geib, Dusty Ordorff of Bituminous Roadways, Inc., and Curt Turgeon. The technical feedback and logistical efforts of Joe Voels and Chelsea Bennet were crucial to the Texas A&M Transportation Institute's efforts.

TABLE OF CONTENTS

CHAPTER 1: Introduction.....	1
1.1 Background.....	1
1.1.1 Asphalt Binders and Performance Grade System	2
1.1.2 Asphalt Mixtures	3
1.2 Scope	3
1.3 Objectives	4
CHAPTER 2: Background and Literature Review	5
2.1 Low Temperature Behavior of Asphalt Binders.....	5
2.2 Cracking Parameters.....	5
2.3 Cracking Mechanism.....	8
2.4 Laboratory Asphalt Binder Test Methods.....	10
2.4.1 Bending Beam Rheometer (BBR)	10
2.4.2 Direct Tension Test (DTT)	11
2.4.3 Single-Edged Notched Bend (SENB) Test	12
2.4.4 Double-Edged Notched Tension (DENT) Test.....	13
2.4.5 Dynamic Shear Rheometer (DSR) Testing for Calculation of Glover-Rowe Parameter	14
2.5 Laboratory Asphalt Mixture Test Methods	16
2.5.1 Disk-Shaped Compact Tension (DCT) Test	16
2.5.2 Semi-Circular Bend (SCB) Test (Low Temperature).....	19
2.5.3 Indirect Tensile (IDT) Test.....	22
2.5.4 Illinois Flexibility Index Test (I-FIT or IL-SCB)	24
2.5.5 Thermal Stress Restrained Specimen Test (TSRST)	27
2.5.6 Texas Overlay Test.....	29
2.5.7 IDEAL Cracking Test (IDEAL-CT)	30

2.6 Summary and Recommendations for Performance Testing	34
CHAPTER 3: Materials and Methods.....	35
3.1 Construction Projects and Studied Materials.....	35
3.2 Asphalt Mixtures Cracking Tests.....	37
3.2.1 IDEAL Cracking Test Procedure	39
3.2.2 DCT Test Procedure for MnDOT Mixtures	39
3.3 Asphalt Mixtures Testing Plan	40
3.3.1 Designed Experimental Plan for Application of IDEAL Cracking Test.....	40
3.3.2 Correlation between DCT Test and IDEAL Cracking Test Results	41
3.4 Asphalt Binders Testing Plan	46
CHAPTER 4: Results and Discussions of Asphalt Binders and Mixtures Testing.....	48
4.1 Introduction.....	48
4.2 Sample Preparation and Testing of MnDOT Project Materials	48
4.2.1 Asphalt Mixture Volumetric Properties	48
4.3 Asphalt Mixture Testing Results	49
4.3.1 MnDOT 2018 Mixtures	49
4.3.2 MnDOT 2019 Mixtures	59
4.4 Asphalt Binder Testing Results	60
4.4.1 Bending Beam Rheometer	60
4.4.2 High Temperature Performance Grade (PG).....	64
4.4.3 Glover-Rowe Parameter.....	65
4.4.4 Multiple Stress Creep Recovery (MSCR) Test.....	68
CHAPTER 5: Research Benefits and Implementation.....	71
5.1 Background.....	71
5.2 Economic Aspects	71

5.3 Environmental Aspects	72
5.4 Social Aspects	73
CHAPTER 6: Economic Potential of Cracking Performance Tests	75
6.1 Life Cycle Cost Analysis	75
6.2 Potential Project Level Savings	76
6.3 Potential Statewide Savings	78
CHAPTER 7: Field Validation Plan	81
7.1 Introduction	81
7.2 Factorial Design	81
7.2.1 Thermal Cracking.....	83
7.2.2 Reflection Cracking.....	83
7.3 Demonstration Projects.....	84
CHAPTER 8: Summary and Conclusions	86
REFERENCES.....	89

LIST OF FIGURES

Figure 1.1. Predominant asphalt cracking mechanisms in Minnesota	2
Figure 1.2. Concept of balanced mix design (Newcomb & Zhou, 2018).....	3
Figure 2.1. Relationship between ductility and DSR parameter (Glover et al., 2005).....	6
Figure 2.2. Relationship between ductility and ΔT_c (Anderson et al., 2011)	7
Figure 2.3. Black space diagram, specification limits and Glover-Rowe parameter limit besides master curves with different aging conditions (Rowe et al., 2014).....	8
Figure 2.4. Temperature gradient and thermal stress gradient in the pavement during cooling process (Hass et al. 1987)	9
Figure 2.5. Thermal stress and tensile strength and fracture temperature for an asphalt mixture specimen (Hills and Brien 1966)	9

Figure 2.6. BBR test equipment and typical results (Pavement Interactive, Asphalt Institute, 2003)	11
Figure 2.7. DTT equipment and specimen (Asphalt Institute, 2003)	12
Figure 2.8. SENB test specimen (ASTM E399-90 2002).....	12
Figure 2.9. DENT test specimen (Marasteanu and Falchetto, 2018)	13
Figure 2.10. DCT test setup and disk-shaped specimen	17
Figure 2.11. DCT test specimen configuration and typical experimental results (Wagoner et al., 2005)	17
Figure 2.12. Field cracking performance data versus DCT fracture energy for defining a specification limit (Marasteanu et al., 2012)	18
Figure 2.13. SCB test experimental setup and specimen (Li and Marasteanu, 2004, Li et al., 2008a, Marasteanu et al., 2012)	20
Figure 2.14. Typical load versus LLD curves (a) at different temperatures (Li et al., 2008a), (b) for three replicates (Marasteanu et al., 2012)	21
Figure 2.15. Field cracking performance data versus SCB fracture energy for defining a specification limit (Marasteanu et al., 2012)	22
Figure 2.16. Field cracking performance data versus SCB fracture toughness for defining a specification limit (Marasteanu et al., 2012)	22
Figure 2.17. IDT test setup and specimen (Buttlar and Roque, 1994).....	23
Figure 2.18. Typical creep compliance results from the IDT creep test (Roque and Buttlar 1992).....	23
Figure 2.19. Different load-displacement curves of two asphalt mixtures with the same fracture energy obtained from IL-SCB tests (Al-Qadi et al., 2015)	25
Figure 2.20. Parameters in a typical load displacement curve from IL-SCB test (Al-Qadi et al., 2015)	26
Figure 2.21. Comparison of flexibility index to field performance (Al-Qadi et al., 2015)	27
Figure 2.22. TSRST experimental setup (Jung and Vinson, 1994)	28
Figure 2.23. Typical results of the TSRST including fracture temperature and fracture strength (Jung and Vinson, 1994)	28
Figure 2.24. Overlay tester.....	29

Figure 2.25. Typical results of overly test (Walubita et al., 2012)	30
Figure 2.26. IDEAL cracking test setup and typical test results (Zhou et al., 2017)	31
Figure 3.1. Correlation between the DCT and IDEAL cracking test results	42
Figure 3.2. DCT test vs. IDEAL cracking test results for RH PMLC mixtures conducted by NCAT/MnROAD	44
Figure 3.3. DCT test vs. IDEAL cracking test results for CA PMLC mixtures conducted by NCAT/MnROAD	44
Figure 3.4. Comparison of CT Index from IDEAL cracking tests performed by TTI and NCAT/MnROAD	45
Figure 3.5. Relation between NCAT/MnDOT DCT test results vs. TTI IDEAL cracking test results for RH PMLC mixtures	46
Figure 3.6. Asphalt binder testing plan	47
Figure 4.1. Comparison of IDEAL cracking test results at different testing time intervals after compaction for Mixture P2	50
Figure 4.2. Comparison of IDEAL cracking test results at different testing time intervals for Mixture P3	51
Figure 4.3. Comparison of IDEAL cracking test results at different testing time intervals for Mixture P4	51
Figure 4.4. Comparison of IDEAL cracking test results at different testing time intervals for Mixture P5-A	52
Figure 4.5. Comparison of IDEAL cracking test results at different testing time intervals for Mixture P5-B	52
Figure 4.6. Comparison of IDEAL cracking test results at different times for Mixture P6	53
Figure 4.7. Mean CT Index from IDEAL cracking test conducted at different time intervals from compaction for the 2018 MnDOT mixtures	55
Figure 4.8. Mean CT Index from IDEAL cracking test conducted at 22 hours after molding for the 2018 MnDOT mixtures	55
Figure 4.9. COV of CT Index results for the MnDOT 2018 mixtures at different timings	56
Figure 4.10. Asphalt binder content vs. CT Index for 2018 mixtures	57
Figure 4.11. DCT fracture energy vs. CT Index from IDEAL cracking test	58

Figure 4.12. IDEAL cracking test results for 2019 mixtures with different binder contents.....	59
Figure 4.13. High temperature and low temperature PG grading results for binders of 2018 and 2019 projects	61
Figure 4.14. Black space diagram and the Glover-Rowe parameter testing results.....	66
Figure 4.15. MSCR cycle and determination of the J_{nr} value	69
Figure 4.16. MSCR elastic recovery curve and asphalt binder test results	70
Figure 5.1. Pavement performance curve and different M&R treatments (Peshkin et al., 2011)	72
Figure 6.1. Life cycle cost analysis results and present worth value for different scenarios using the average annual HMA quantity on a project level basis.	77
Figure 6.2. Life cycle cost analysis results and present worth value for different scenarios using the 75% quartile annual HMA quantity on a project level basis	78
Figure 6.3. Estimated cost savings with the application of cracking tests statewide using the average annual HMA quantity.	79
Figure 6.4. Estimated cost savings with the application of cracking tests statewide using the 75% quartile annual HMA quantity	79

LIST OF TABLES

Table 2.1. Summary of asphalt binder tests	15
Table 2.2. Suggested low temperature cracking specification limits for DCT test results for loose mixtures (Marasteanu et al., 2012)	19
Table 2.3. Summary of asphalt mixture tests	32
Table 3.1. Summary description of MnDOT construction projects and the asphalt materials used in this study.....	36
Table 3.2. Criteria suggested for cracking performance tests (Newcomb and Zhou, 2018)	38
Table 3.3. Suggested low temperature cracking performance criteria for DCT Test (Marasteanu et al., 2012)	39
Table 3.4. Timing matrix for IDEAL cracking test	40
Table 3.5. IDEAL and DCT tests experimental data (after Newcomb and Zhou, 2018)	41
Table 3.6. IDEAL cracking and DCT tests results from NCAT/MnROAD partnership (Taylor, 2018)	43

Table 3.7. IDEAL cracking test results for RH PMLC mixtures conducted by TTI and NCAT/MnROAD	45
Table 4.1. MnDOT and TTI maximum specific gravity (G_{mm}) results.....	49
Table 4.2. Timing for performing IDEAL cracking test conducted on MnDOT mixtures received in 2018	49
Table 4.3. IDEAL cracking test results for 2019 Mixtures P2 in Project 8607-63.....	53
Table 4.4. IDEAL cracking test results for Mixture P3 in Project 0304-37	53
Table 4.5. IDEAL cracking test results for Mixture P4 in Project 1118-21	54
Table 4.6. IDEAL cracking test results for Mixture P5-A in Project 6904-46.....	54
Table 4.7. IDEAL cracking test results for Mixture P5-B in Project 6904-46.....	54
Table 4.8. IDEAL cracking test results for Mixture P6 in Project 0704-100	54
Table 4.9. Results of DCT test and IDEAL cracking test for 2018 mixtures	57
Table 4.10. Results of IDEAL cracking on 2019 projects	60
Table 4.11. BBR test results of MnDOT asphalt binder from 2018 and 2019 projects.....	61
Table 4.12. Continuous PG low grading and the ΔT_c of the tested binders	62
Table 4.13. PG high temperature testing results for original binders using DSR.....	62
Table 4.14. PG high temperature testing results for RTFO aged binders using DSR	64
Table 4.15. Frequency sweep test results for G-R parameter conducted at 15 C and 0.005 rad/s	67
Table 4.16. MSCR test results conducted at 58°C.....	70
Table 6.1. Parameter used in the life cycle cost analysis.....	76
Table 6.2. Statistical analysis of the HMA quantity and price on the provided data.....	76
Table 6.3. Estimate of the annual number of projects in the state	80
Table 7.1. Experimental matrix for thermal cracking test sites	82
Table 7.2. Experimental matrix for reflection cracking test sites	82

EXECUTIVE SUMMARY

Cracking generated by two mechanisms, thermal stresses and reflective cracking from lower layers, are the primary distresses found on Minnesota asphalt roads and, subsequently, the primary cause of asphalt pavement roughness in the state. There has been a movement in asphalt technology since 2007 (Zhou et al., 2007) to integrate performance testing into asphalt mixture design. The current Superpave method of mixture design is based solely on the concepts of volumetric proportioning, and thus does not provide any direct indication of cracking resistance in mixtures. Likewise, binder parameters measured in the Superpave grading system provided an improvement over previous specifications but did not correlate well with cracking tendencies.

The objective of this research was to identify and, if necessary, refine binder and mixture tests capable of addressing cracking in Minnesota asphalt pavements during mixture design and construction. Binder characterization using the difference in critical low temperatures (ΔT_c) for relaxation (m-value) and stiffness (S) was used as an indication of thermal cracking susceptibility based on work by Anderson et al (2011). For cracking at intermediate temperatures where reflection cracking is likely, the Glover-Rowe (G-R) parameter was used, which had been correlated to aging and loss of ductility. Both these values relate well to a loss in relaxation of asphalt binders in different temperature regimes, and aside from the G-R parameter requiring an extra 20 hours of aging in the pressure air vessel (PAV), they do not require any greater complexity or new equipment.

The IDEAL cracking test was selected for asphalt mixture testing. It is a fast, monotonic indirect tensile test performed at 77°F (25°C) with readily available laboratory equipment and minimal sample preparation and no instrumentation (Zhou et al., 2017). These features make the IDEAL test suitable for mixture design and quality control/quality assurance (QC/QA). The disc-shaped compact tension (DCT) test (Marasteanu et al., 2012) has proven to be correlated to low-temperature cracking and was performed by the Minnesota Department of Transportation (MnDOT) for this study. Due to the time required for sample preparation and temperature conditioning, this test may be most suited to asphalt mixture design.

Five projects from MnDOT's 2018 construction season and three projects from 2019 were identified for cracking test validation. The asphalt binders and loose mixtures were shipped to the Texas A&M Transportation Institute (TTI) laboratory where the research team performed binder testing for these projects for obtaining the G-R parameter and ΔT_c . Moreover, the IDEAL cracking test was conducted to evaluate the mixtures' cracking resistance. DCT test results for the materials from these projects were provided by MnDOT.

Although a previous study (Newcomb & Zhou, 2018) showed good correlation between the IDEAL and DCT test results, another study (Taylor, 2018) involving MnDOT asphalt mixtures tested at the National Center for Asphalt Technology showed the opposite with a poor correlation. The latter results were for reheated and critically aged plant mixtures while the previous ones were for laboratory-aged mixture design samples. In this study, a comparison between IDEAL-CT Index testing performed by TTI and DCT

values from testing done at the MnDOT Materials Laboratory showed no correlation. Thus, further examination of the relationship between these two cracking tests is warranted.

In this research, the time between mixing and molding asphalt samples and testing them was studied to see if a difference in results could be detected. This was an important question for QC/QA testing as QC samples would most likely be tested on the day of production and QA samples would be tested later at a different laboratory. Results showed that a time period of up to two weeks did not significantly affect the testing values. However, it is important to note that the samples were compacted at the same time and that the "QA" samples were not reheated before testing. Reheating the material before QA testing could negatively affect the IDEAL-CT Index. The coefficients of variation (COV) were less than 15 percent for more than 75 percent of the testing done for the 2018 samples, and only two out of the 24 cases showed COVs over 20 percent. This indicates that the test was very repeatable.

Raw materials for mixture design from the 2019 construction season were tested to validate the effect of asphalt binder content on the cracking resistance. As shown in a previous study (Newcomb & Zhou, 2018), cracking resistance increased with asphalt content. The IDEAL-CT Index results showed that, for these three 2019 projects, when the asphalt content was at the optimum or above as determined volumetrically, the IDEAL-CT Index was higher than the proposed benchmark of 80. The plant mix samples from all three projects also passed this criterion with values that were equal to or greater than those for the lab mixed and compacted optimum asphalt contents. This provides some confidence in the proposed use of the IDEAL-CT in QC/QA.

All the binders from the 2018 and 2019 construction seasons were tested according to the protocols for ΔT_c and G-R parameter. Typically, ΔT_c is considered sufficient if the value is greater than -5.0, and for the materials tested, the lowest value was -2.2 and the greatest value was 1.4. For G-R, the onset of cracking is considered to be when the stiffness (G^*) crosses 180 kPa and the presence of block cracking occurs when G^* crosses 600 kPa at a temperature of 15°C and a rotational velocity of 0.005 rad/sec. It has been suggested that a good criterion is considered to be 450 kPa at 40 hours of aging in a PAV. For the binders in this study, the maximum stiffness at 40-hr PAV was 113 kPa. All of the binders showed excellent resistance to intermediate and low temperature cracking.

A further field validation plan was developed and presented as a part of the implementation for this work. There were two approaches that could be taken in the design and construction of test sites. The first would be to use a factorial experiment design and the second would be a demonstration project with shadow specifications. The factorial experiment design would be the more rigorous scientific approach, although it would be costlier. Factorial levels would be set according to the degree of binder cracking resistance for thermal cracking (ΔT_c) or reflection cracking (G-R). Mixture design would be set according to asphalt content, which is one of the most sensitive cracking resistance parameters. The levels for the experiment design would be the optimum asphalt content minus 0.4 percent and the optimum asphalt content. Thus, there would be four sections for each test site for each type of cracking. Demonstration projects have been conducted to introduce new materials and construction technology to industry and agency personnel. They are used to build confidence in new processes and procedures for participants and spectators, and they normally include an educational component. Successful

demonstration projects are sponsored jointly between contractors and DOTs, highlighting the need for the new technology, benefits for public, advantages to the industry, and the plan for implementation. Incorporation of shadow specifications provides an opportunity for the industry to learn about the testing involved and the application of specifications to materials typically used in the state.

The need for better asphalt binder characterization is due to past observations that the Superpave fatigue cracking parameter $G^*\sin \delta$ does not adequately differentiate cracking and non-cracking susceptible binders (Hajj & Bhasin, 2017). The ΔT_c and the G-R parameters have been directly tied to ductility and field cracking. Using one or both of these parameters in place of the $G^*\sin \delta$ will provide a more meaningful binder cracking specification for the industry. The only drawback is the need for 40-hr PAV aging, which could result in some shipping delays for binder suppliers.

The use of cracking tests during mixture design and QC/QA could be used as a springboard for contractor innovation. Performance testing could be used as a means of determining asphalt content on cracking resistance criteria rather than typical volumetric approaches. Some elements of volumetric requirements would need to remain to ensure that pavements do not rut or flush. For instance, it may be desirable to maintain a minimum air void requirement, e.g., 2 percent, at the maximum number of gyrations (N_{max}). Also, a minimum voids in mineral aggregate (VMA) requirement or asphalt film thickness could help to ensure that mixtures do not become “choked.”

The implementation of performance testing may lead to the use of higher-quality materials than what have been used and help construct and preserve a more sustainable pavement network. Application of performance testing can bring about substantial economic, environmental, and social benefits. It can lead to higher service lives of pavements, reduce the costs of maintenance and rehabilitation, and save raw materials and resources. It can enhance the safety and reduce the costs of the work zones through a lesser need to repair pavements and work zones. It also lowers the adverse environmental effects of materials production.

CHAPTER 1: INTRODUCTION

1.1 BACKGROUND

Cracking of asphalt pavements has a variety of causes. These include traffic-related bottom-up cracking and top-down cracking due to fractures from repeated strains, thermally induced stresses (repeated or single-event) causing top-down cracking in cold temperatures, or horizontal movements of lower overlaid cracked layers creating reflection cracks that propagate to the surface. Typically, cracking appears after a number of years of damage accumulation on materials that have become embrittled. Therefore, in addition to the mechanics that dictate cracking, there is also a component of material aging that should be accounted for.

There has been a movement in asphalt technology since 2007 (Zhou et al., 2007) to integrate performance testing into asphalt mixture design. The current Superpave method of mixture design is based solely on the concepts of volumetric proportioning. While the heuristics found in the volumetric approaches are valid for the mixtures for which they were developed, there have been numerous changes over the years. Starting immediately after the initial development of Superpave in the 1990s, the greatly increased use of polymer modified asphalt binders and lower asphalt content, initially resulting from Superpave to overcome rutting problems, led to cracking problems in some asphalt pavements. The rising price of asphalt binders in the 2000s resulted in the use of increased amounts of reclaimed asphalt pavement (RAP) and recycled asphalt shingles (RAS). Increasing the use of recycled materials and binder additives resulted in further cracking problems (Zhou et al., 2017). In addition to this, some suppliers began to use excessive amounts of Recycled Engine Oil Bottoms (REOB) to modify the asphalt so that it would meet low-temperature requirements. This excess amount of REOB tended to make the asphalt binder susceptible to aging. Considering these problems in recent years, state DOTs have been trying to address them with new performance tests for asphalt binders and mixtures.

The cracking generated by two mechanisms, thermal stresses and reflective cracking from lower layers, are the primary distresses found on Minnesota asphalt roads and, subsequently, the primary cause of asphalt pavement roughness in Minnesota. Low temperature or thermal cracking has two fundamental mechanisms: 1) a steady increase in embrittlement through oxidative aging and tensile stresses in the pavement created through contraction due to cold temperatures; and 2) physical hardening that occurs when cold temperatures over an extended period of time cause the precipitation of wax in the asphalt binder, which embrittles the binder in the winter. Oxidative aging is not reversible, but physical hardening subsides completely as temperature increases. Low temperature cracking (Figure 1.1a) mostly occurs in occasions when there are no existing cracks in a lower substrate, while reflective cracking (Figure 1.1b) occurs due to the movements associated with existing cracks in a lower substrate such as an old concrete or asphalt layer. During periods of transition from warm to cold weather or periods of high-temperature fluctuations, the contraction of the material forming the lower layer creates tensile stress or repeated stress that may cause the overlay material to crack. Reflective cracking is exacerbated by the oxidative aging and physical hardening (if present) in the overlay material. A number of binder

and mixture tests have been identified in the literature to characterize these materials. The question is which ones might be suitable in terms of practicality and simplicity and correlation to performance.



(a) Thermal Cracking

(b) Reflective Cracking

Figure 1.1. Predominant asphalt cracking mechanisms in Minnesota

1.1.1 Asphalt Binders and Performance Grade System

Asphalt binder provides cohesion in asphalt concrete. The consistency of asphalt binder is time and temperature dependent. It acts like a solid or semi-solid at ordinary temperatures and liquefies when subjected to heat or dissolved in solvents. Mechanical and rheological properties of the asphalt cement play a crucial role in the performance, durability and mechanical behavior of asphalt concrete pavements.

The Performance Grade (PG) system was developed during the Strategic Highway Research Program (SHRP) to characterize asphalt binder behavior. SHRP began in the late 1980s with research funding of \$50,000,000 with an emphasis on asphalt pavements (McDaniel et al., 2011). The Superpave PG system improved the binder specification through required binder testing at low service temperature, high service temperature, and at the construction temperature. The PG system assigns cold and hot temperature limits to each binder, which must pass the defined testing criteria. The first temperature limit provides information on the binder behavior at high service temperature, and the second one is associated with the response of the binder under low service temperature. The two temperature limits are determined using the Dynamic Shear Rheometer (DSR), Rotational Viscometer, Bending Beam Rheometer (BBR), and Direct Tension Tester (DTT) (Asphalt Institute, 2003).

Moreover, new aging protocols were applied in the PG system to simulate pavement materials in the field more realistically. The Rolling Thin Film Oven (RTFO) simulates the chemical and physical processes, which the binder goes through during mixing, compaction and construction, defined as short-term aging (Asphalt Institute, 2003; Anderson & Bonaquist, 2012). The Pressure Aging Vessel (PAV) simulates the

continuous oxidation that takes place during the entire life of the asphalt material, defined as long-term aging (Asphalt Institute; 2003, Bahia & Anderson, 1995).

1.1.2 Asphalt Mixtures

The Superpave specification and new asphalt mixture design required the selection of suitable materials, volumetric parameters criteria, and application of gyratory compaction as a new laboratory compaction method. Quality criteria of the materials and the original compaction levels were associated with the traffic classification. Compaction levels, in terms of the number of gyrations, were later modified by many states to more closely match field compaction efforts. In addition to high-temperature stiffness, more emphasis was placed on aggregate structure for resistance against rutting.

However, the asphalt industry has faced some problems in recent years regarding the cracking performance of asphalt materials, as mentioned before. Considering these problems, state DOTs have been trying to address them with various performance tests for rutting and cracking. The application of a rutting test to determine a maximum asphalt content for controlling rutting, and a cracking test that would indicate a minimum asphalt content formed the framework known as a balanced mix design (BMD) (Newcomb & Zhou, 2018). Asphalt contents greater than a given maximum might result in rutting failures and asphalt contents less than a given minimum value might result in cracking failure. The objective of the BMD approach is to identify a range or a minimum asphalt content that will satisfy the demands for cracking resistance as well as those for rutting resistance. The BMD concept is illustrated in Figure 1.2.

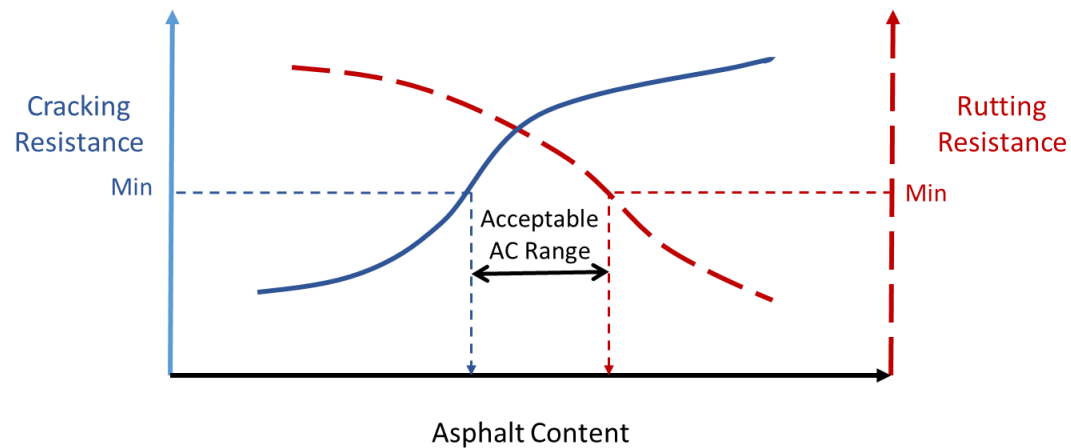


Figure 1.2. Concept of balanced mix design (Newcomb & Zhou, 2018)

1.2 SCOPE

The Minnesota Department of Transportation is interested in adopting asphalt binder and mixture tests that correspond to the performance of asphalt pavements in terms of cracking generated by two mechanisms: thermal stresses and reflective cracking from lower layers.

A review of current literature and technology available for testing materials in terms of cracking resistance is presented in this report. A brief description of the mixture and binder cracking tests and cracking parameters is also provided. This report investigates and presents the experimental plan performed in this study on the MnDOT asphalt mixtures and binders from selected construction projects undertaken in 2018 and 2019. This plan includes the testing plan to perform the IDEAL Cracking Test (IDEAL CT) on the MnDOT mixtures. This report contains the literature review, research methods, materials, results, data analysis, recommended test methods and criteria, conclusions and recommendations, and implementation plans.

One of the challenges in quality assurance (QA) procedures is the storage time between sample fabrication at the plant and testing in the laboratory. This time interval may cause changes in mixtures and the volumetric properties and result in discrepancies between results of quality control (QC) and QA testing. Therefore, the effect of time interval between compaction and cracking test is investigated for a series of mixtures. For another series of mixtures, the differences between the IDEAL Cracking Test results of the lab-mixed and plant-mixed mixtures is studied. The effect of different binder contents is also studied for these mixtures.

1.3 OBJECTIVES

The objective of this research was to identify and, if necessary, refine binder and mixture tests capable of addressing asphalt cracking in Minnesota asphalt pavements. The concept of balanced mix design applies a rutting test to define a maximum asphalt binder content for rutting and a cracking test to determine a minimum asphalt content (Newcomb & Zhou, 2018). This work focused on the cracking aspect. The effort to improve cracking performance tests in this project could lead to improved asphalt binder and mixture specifications. The tests should be relatively simple to perform in standard agency and contractor laboratories, require minimal time to perform and produce results, be repeatable and reproducible, and provide a distinction between brittle and ductile behavior.

The objectives of this project were to: 1) suggest an integrated mix design approach to improve cracking performance testing that may be used in mixture design and field control; and 2) validate and refine the approach to balanced mix design. From the literature, the cracking tests for both binders and mixtures were identified for evaluation of materials. Binder testing has been performed on asphalts used in Minnesota having a range of aging and physical hardening characteristics. Construction projects were identified for evaluation of mixture testing procedures considering pavement structure, climate, traffic, and mix design. The products of this project were test methods and criteria to evaluate asphalt binders and mixtures in terms of cracking potential. Furthermore, an approach to field validation of asphalt binder and mixture testing is proposed for future work.

CHAPTER 2: BACKGROUND AND LITERATURE REVIEW

2.1 LOW TEMPERATURE BEHAVIOR OF ASPHALT BINDERS

Asphalt binder becomes stiffer and more brittle at low temperature and thus, it becomes more susceptible to fracture leading to low temperature cracking. Low temperature cracking is the primary distress and mode of failure for many asphalt pavements constructed in cold climates. The assumption that the severity of thermal cracking in the field is correlated with the asphalt mixture creep stiffness after 2 hours of loading is the basis of the proposed testing conditions and criterion for low temperature behavior of asphalt binder (Readshaw, 1972, Anderson and Kennedy, 1993). Based upon the time-temperature superposition principle, the binder creep stiffness at 2 hrs. of loading at temperature (T) in °C is approximately equivalent to the stiffness at 60 s at T+10 °C. Therefore, using this principle, the low temperature tests in the PG system may be conducted faster and more conveniently. The PG system defines a maximum value of 300 MPa for creep stiffness at 60 s, obtained from BBR test, to limit the stiffness at low temperature.

Furthermore, the m-value or slope of the binder creep stiffness versus time curve at 60 s with both of the axes on logarithmic scale was investigated for low temperature behavior in the PG system in order to control the rheological property of binder. This control was instigated to avoid the use of heavily blown binders which were related to poor fatigue performance. A low m-value is associated with a lower relaxation rate which leads to accumulating thermal stresses resulting in thermal cracking (Marasteanu and Falchetto, 2018). The PG system defines a minimum value of 0.3 for m-value at 60 s. Thus, the asphalt binder needs to pass the two limiting criteria at the PG low temperature. For simplicity of the PG system, the effect of physical hardening (Bahia, 1991) is not considered in the low temperature behavior of the asphalt binder despite its potentially important effect on binder properties (Marasteanu and Falchetto, 2018).

Additionally, the tensile failure stress and strain of a dog-bone-shaped specimen under tension in DTT is determined based on the SHRP PG system. The critical temperature is the temperature at which the failure tensile strain is 1%. Since the variability of this test is high, this has been changed to an optional test.

2.2 CRACKING PARAMETERS

Thermal stresses can cause two types of distresses in asphalt pavement, transverse cracking and block cracking. Transverse cracking may be observed in newer pavements, while block cracking may take place in older aged pavements. While the “Limiting Stiffness” concept as used in the Superpave PG asphalt binder specification according to AASHTO M 320 explains transverse cracking, observations made by Kandhal (1977) indicated that block cracking and concurrent surface raveling were associated with low binder ductility after binder aging.

The “Limiting Stiffness” concept, used for prediction of transverse cracking, assumes that asphalt binder exhibits a unique curve in a Black Space Diagram (complex modulus G^* vs. phase angle δ). This concept

is only true for some limiting conditions. Predictions from limiting stiffness concepts can only be applied for binders cooled quickly with limited reaction times, which are not m-controlled. This concept can be used for prediction of transverse cracking in new pavements. However, this concept becomes inaccurate as binders age. At slower cooling rates and for materials under thermal cycling, thermal stresses cannot relax as quickly as expected in aged binders. Thus, more thermal stresses and damage may build up (Anderson et al., 2011). Oxidative aging leads to slower relaxation of binders and makes the binder more m-controlled as aging takes place.

Historical research has concluded that there is a relationship between durability of asphalt pavements and ductility at intermediate temperatures. Two parameters were developed that were related to ductility and loss of flexibility with aging (Glover et al., 2005, Anderson et al., 2011). Glover et al. (2005) developed the parameter $G' / (\eta' / G')$ determined through DSR testing. Another parameter is the difference between the temperature determined for controlling creep stiffness (S-value) and temperature determined for controlling relaxation properties (m-value), called ΔT_c (Anderson et al., 2011). Both these parameters could track and reflect the loss of relaxation properties as a result of binder aging. The research results indicated that the DSR parameter, $G' / (\eta' / G')$ at 15 °C and 0.005 rad/s was correlated with ductility at 15 °C and at a rate of 1 cm/min (Glover et al., 2005) as shown in Figure 2.1.

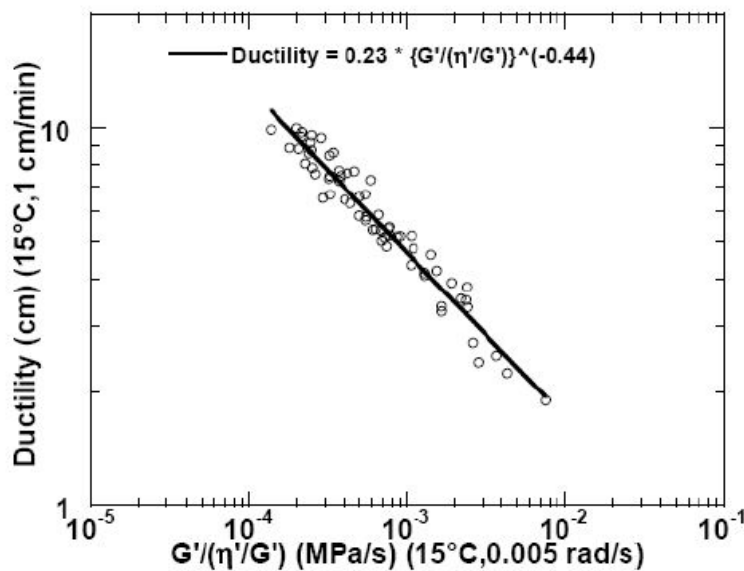


Figure 2.1. Relationship between ductility and DSR parameter (Glover et al., 2005)

It has been suggested that binders which have a ductility of 5 cm are close to a point where cracking occurs and binders with ductility of 3 cm will experience cracking. Using the experimental results, Glover et al., (2005) could find two cracking threshold values for the DSR parameter, $G' / (\eta' / G')$ corresponding to the ductility of 5 cm and 3 cm. The $G' / (\eta' / G')$ values obtained at 15 °C and 0.005 rad/s corresponding to these mentioned warning and cracking limits are 0.0009 and 0.003 MPa/s.

Anderson et al. (2011) conducted BBR low temperature tests according to AASHTO T 313 for different asphalt binders and PAV aging times. The critical temperature for creep stiffness at 60 s, $S(60)$, and the

critical temperature for m-value, $m(60)$, were determined. The critical temperature, T_c , is defined as the temperature where the BBR creep stiffness or m-value are equal to specification limits. $T_{c,S}$ is the temperature where the BBR creep stiffness at 60 s of loading, $S(60)$, is equal to 300 MPa. $T_{c,m}$ is the temperature where the BBR m-value at 60 s of loading, $m(60)$, is equal to 0.3. The equations for calculation of $T_{c,S}$ and $T_{c,m}$ are presented here (Anderson et al., 2011):

$$T_{c,S} = T_1 + \left[\frac{\log(300) - \log(S_1)}{\log(S_1) - \log(S_2)} \times (T_1 - T_2) \right] - 10 \quad (1)$$

$$T_{c,m} = T_1 + \left[\frac{0.30 - m_1}{m_1 - m_2} \times (T_1 - T_2) \right] - 10 \quad (2)$$

where T_1 is Temperature No. 1 in °C, T_2 is Temperature No. 2 in °C, S_1 is Stiffness at 60 s of loading at Temperature No. 1 in MPa, S_2 is Stiffness at 60 s of loading at Temperature No. 2 in MPa, m_1 is m-value at 60 s of loading at Temperature No. 1, and m_2 is m-value at 60 s of loading at Temperature No. 2.

A relatively good correlation between ductility and ΔT_c , the difference $T_{c,m}$ and $T_{c,S}$, were observed for different binders (Anderson et al., 2011) as shown in Figure 2.2. ΔT_c was calculated as $T_{c,m} - T_{c,S}$ in that research study. If the ΔT_c increases, the binder becomes more m-controlled and the binder ductility declines. Recently this parameter has been changed to $T_{c,S} - T_{c,m}$, so that a more negative number indicates greater aging.

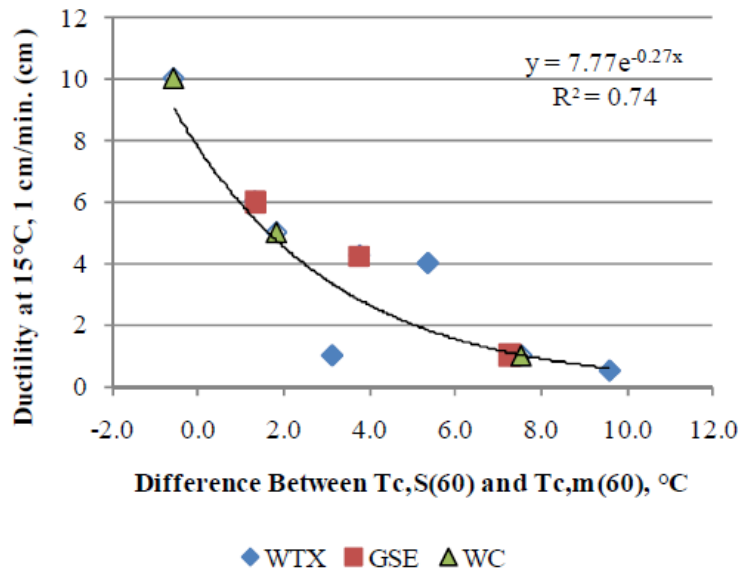


Figure 2.2. Relationship between ductility and ΔT_c (Anderson et al., 2011)

Rowe (2011) modified the DSR parameter developed by Glover et al. (2005). He simplified the DSR parameter $G' / (\eta' / G')$ equation and proposed that the frequency ω be removed from the equation since it had a fixed value of 0.005 rad/s:

$$\frac{G'}{(\eta' / G')} = G^* (\cos \delta)^2 \times \omega / \sin \delta \quad (3)$$

Therefore, he suggested the parameter below, known as Glover-Rowe parameter. It can be obtained by using binder rheological parameters in Black Space diagrams (G^* and δ) with DSR testing at the same testing conditions used for Glover parameter (Rowe, 2011; Rowe et al., 2014):

$$GR = G^*(\cos\delta)^2/\sin\delta \quad (4)$$

Using the cracking limit value of 0.0009 MPa/s for the Glover DSR parameter, Rowe (2011) proposed a limiting value of 180 kPa for the Glover-Rowe parameter ($\frac{G^*(\cos\delta)^2}{\sin\delta} \leq 180 \text{ kPa}$). The format and variables of this parameter are similar to the parameters proposed in the PG system specifications in AASTO M320. Figure 2.3 plots the shows Glover-Rowe functions along with the other two parameters used in PG system.

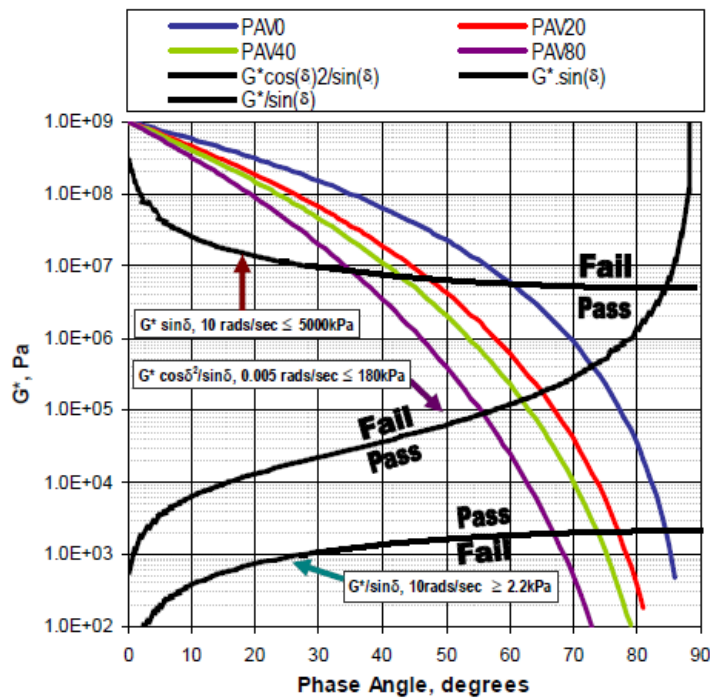


Figure 2.3. Black space diagram, specification limits and Glover-Rowe parameter limit besides master curves with different aging conditions (Rowe et al., 2014).

2.3 CRACKING MECHANISM

The overall cause of initiation of thermal cracks is the tensile stress in asphalt concrete layers which exceeds tensile strength and resistance of the asphalt concrete. Cooling the pavement layers results in the contraction of the asphalt concrete materials. Since the asphalt layer in the pavement is restrained and the contraction cannot freely occur, thermal stresses are generated in the cooled asphalt layer. Based on the amount of induced thermal stress and fracture characteristics of the asphalt concrete materials, thermal cracks initiate in the pavement. Since asphalt pavement layers are more restrained in the longitudinal direction of the pavement, higher thermal stresses are developed in this direction, and thermal cracking usually initiates in the transverse direction. Moreover, the level of friction and bonding

between asphalt layer and lower unbound layers affects the restriction of the movement of layers and may influence the level of cracking. The lower level of bonding and friction between layers result in increased crack spacing and wider thermal cracks. The asphalt layer surface experiences the coldest temperatures during cooling time based on the temperature gradient in depth of the pavement. Therefore, highest thermal stresses are induced in the pavement surface (Zhou et al. 2016). The temperature gradient and thermal stress gradient are shown in Figure 2.4.

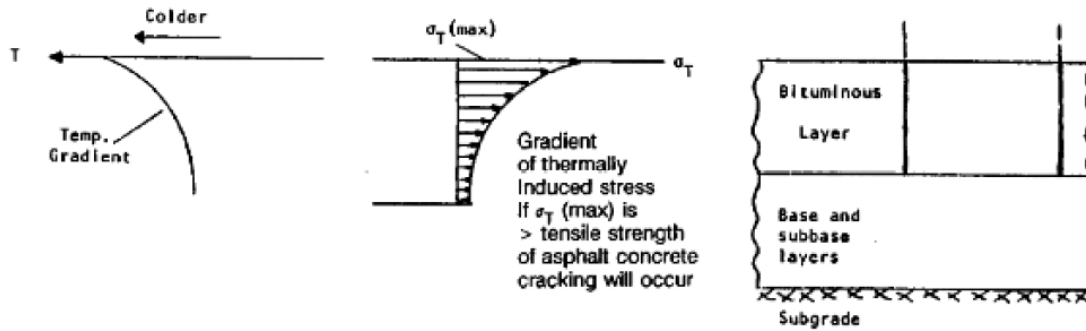


Figure 2.4. Temperature gradient and thermal stress gradient in the pavement during cooling process (Hass et al. 1987)

When the pavement temperature decreases during cooling, the thermal tensile stresses start to increase. When the induced tensile stress at one point exceeds the tensile strength of the asphalt material, cracking is initiated at that point on the pavement surface (Figure 2.5). Then, one or more additional thermal cycles can propagate this crack into the depth of the asphalt layer depending upon the relaxation properties of the mixture, cooling rate, etc. Low temperature cracking may occur every 100-200 ft. on new pavements. However, the spacing may decrease to 10-20 ft. for the aged pavements (Zhou et al. 2016).

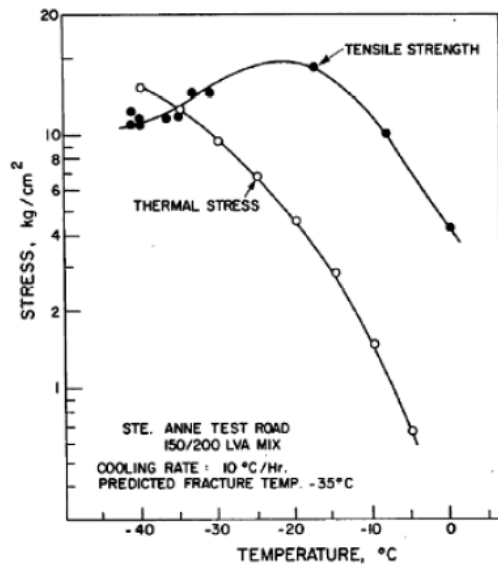


Figure 2.5. Thermal stress and tensile strength and fracture temperature for an asphalt mixture specimen (Hills and Brien 1966)

Thermal fatigue stress occurs when the pavement goes through significant temperature fluctuations diurnally. The pavement experiences colder temperature at night causing higher tensile stresses which decrease during the daytime. This is a type of fatigue cracking that appears on the pavement surface over time and temperature cycles. This type of cracking is hard to characterize and simulate in the laboratory. Few research studies have been conducted regarding this type of cracking (Sugawara and Moriyoshi, 1984; Epps, 1997).

Carpenter (1983) suggested a threshold of $-7\text{ }^{\circ}\text{C}$ ($20\text{ }^{\circ}\text{F}$) for identifying the dominant type of thermal cracking. For temperatures below this threshold, low temperature cracking may be more predominant, and for the ones above this criterion, thermal fatigue cracking may be more likely to occur.

The primary parameters which affect the occurrence of thermal cracking are pavement temperature, asphalt binder type, aging, cooling rate, the coefficient of thermal expansion, pavement thickness, and subgrade type. The pavement surface temperature is mostly a function of air temperature and wind speed. Most of the low temperature cracks develop when the asphalt pavement is subject to temperatures below glass transition temperature for a period of time. The relationship between stiffness and temperature is known to be one of the most significant factors in pavement performance in terms of thermal cracking. A binder with lower PG low grade generally shows better resistance against thermal cracking. If the asphalt concrete is aged, it is more susceptible to thermal cracking due to the poor relaxation properties and increased stiffness. A higher cooling rate leads to a higher probability of thermal cracking. A higher coefficient of thermal contraction results in larger level of thermal cracking. Generally, pavements with greater asphalt layer thickness are less prone to thermal cracking. This is most likely due to the dissipation of stress through a thicker cross-section of material. If the underlying base or subgrade layer provides interlayer friction and bonding, the sliding between layers lessens but the frequency of thermal cracking decreases.

2.4 LABORATORY ASPHALT BINDER TEST METHODS

The PG system applies two low temperature cracking tests for evaluation of the low temperature behavior of asphalt. These two tests are the Bending Beam Rheometer (BBR) and the Direct Tension Test (DTT). Many researchers have realized there are some limitations and restrictions regarding prediction of behavior and failure properties using stiffness concepts. Therefore, they have also studied cracking properties of asphalt binder through fracture tests including Single Edged Notched Bend (SENB) Test, and Double-Edge Notched Tension (DENT) test (Marasteanu and Falchetto, 2018) (Lee and Hesp, 1994) (Anderson, 2005).

2.4.1 Bending Beam Rheometer (BBR)

Researchers developed the BBR test during SHRP to perform low temperature creep tests on small asphalt binder beams in three-point bending. The binder beam has the length of 102 mm, width of 12.5 mm, and height of 6.25 mm. The BBR data are used to measure how much the beam deflects under constant load. This test is conducted according to AASHTO test method 313-12. The binder undergoes short term aging using RTFO and then long term aging using PAV, so that the lab conditioning simulates

the critical field conditions of aged asphalt binders at low temperature. The binder beam is temperature conditioned for 60 minutes in the test bath. The test is conducted in ethanol bath. The BBR equipment and typical results are shown in Figure 2.6.

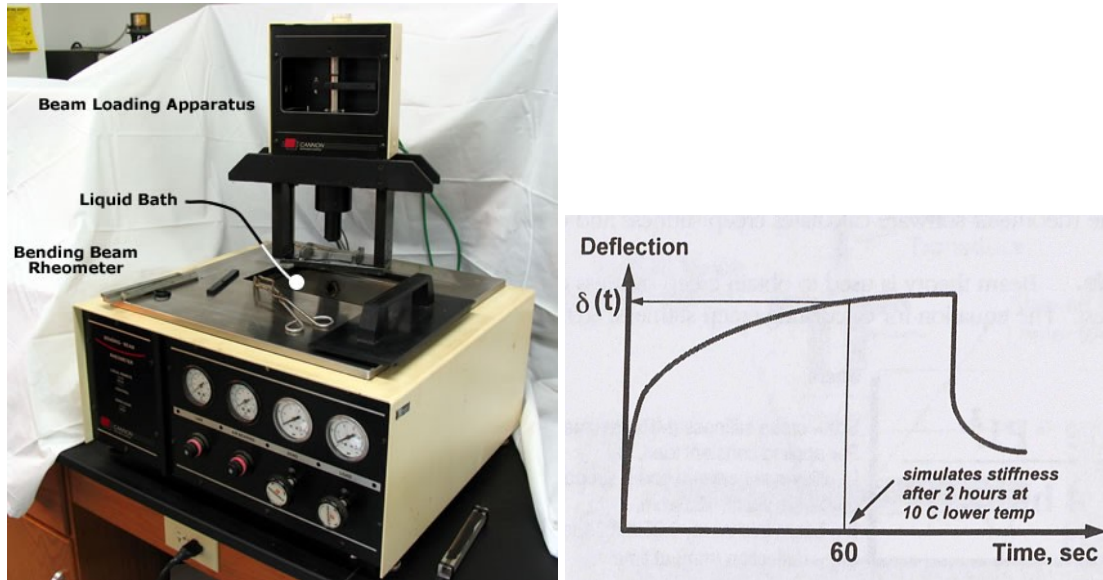


Figure 2.6. BBR test equipment and typical results (Pavement Interactive, Asphalt Institute, 2003)

A constant load of 980 mN is exerted on the middle point of the beam for 240 s. The deflection of the beam is recorded as a function of time. Creep stiffness, $S(t)$, and the slope of the creep stiffness versus time in double logarithmic scale, $m(t)$, are determined as functions of time. As mentioned before, two criteria are defined for creep stiffness and m -value at 60 s in the PG system for evaluation of low temperature behavior of asphalt binder or grading. These two criteria are: $S(60\text{ s}) < 300\text{ MPa}$, and $m(60\text{ s}) > 0.30$. These criteria are assumed to provide a balance of material stiffness and relaxation behavior. The current specification procedure is to select the highest of the two limiting temperatures obtained from the two criteria for low temperature grading. The BBR test can also be applied to obtain ΔT_c as mentioned previously.

The m -value indicates the development of thermal stresses at cold temperatures. Lower m -values are not desirable as they indicate lower stress relaxation. In other words, a higher m -value indicates slower generation of thermal stresses, which is favorable (Marasteanu and Falchetto, 2018).

2.4.2 Direct Tension Test (DTT)

The Direct Tension Test (DTT) may be performed if the BBR test limiting criteria of S and m are not met. This test is conducted according to AASHTO 314-12. The specimens undergo short term aging using RTFO and then long term aging using PAV. Uniaxial tension is exerted on the specimen at a constant rate of 3% per minute. The nominal failure stress and strain are recorded and calculated up to the point of failure. With the DTT records, the nominal failure stress and strain are determined. The cross sectional area of the specimen is 6×6 mm as shown in Figure 2.7. Conditioning and testing take place when the

specimen is in the in potassium acetate cooling medium (Asphalt Institute, 2003, Marasteanu and Falchetto, 2018). There are some concerns regarding the variability and repeatability of this test.

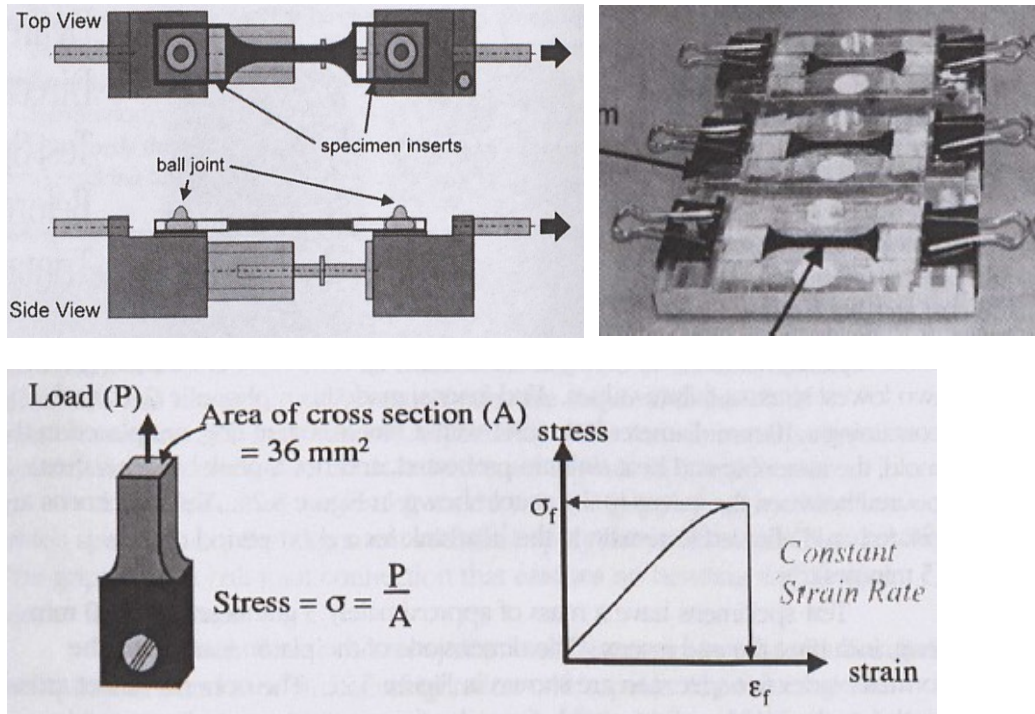


Figure 2.7. DTT equipment and specimen (Asphalt Institute, 2003)

2.4.3 Single-Edged Notched Bend (SENB) Test

Lee and Hesp (1994) and Lee et al. (1995) applied the Single-Edged Notched Bend (SENB) test to characterize the fracture properties of asphalt binders. The dimensions of the beam specimen were 25 mm in depth by 12.5 mm in thickness by 175 mm in length. The beam span was 100 mm. A notch was made at the bottom side and in the middle of the beam before testing. The notch was 5 mm long, and was perpendicular to the beam length. The tests were conducted at temperature of -20 °C with 12 hrs. of conditioning. The specimen configuration in SENB test is shown in Figure 2.8.

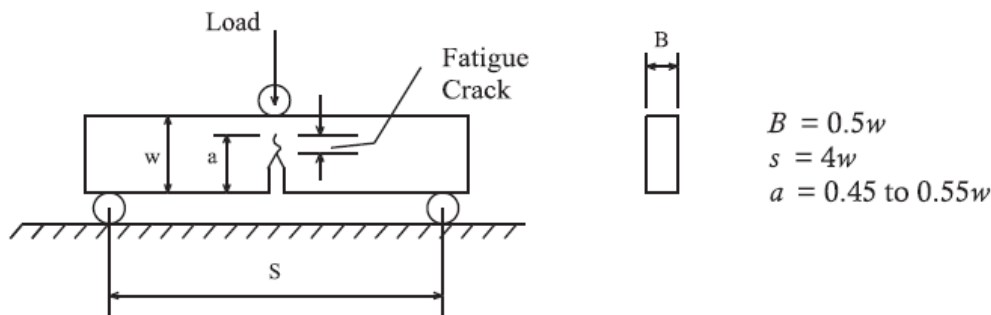


Figure 2.8. SENB test specimen (ASTM E399-90 2002)

The load was applied on top side of the beam. There was a high stress concentration near the crack tip. The stress intensity factor of mode I fracture, K_{Ic} , was used to analyze the stress field near the crack tip using linear elastic fracture mechanics (Bažant and Planas, 1998, Marasteanu and Falchetto, 2018). Experimental results indicated that modified binders had higher fracture toughness, but not a higher stiffness (Lee and Hesp, 1994, and Lee et al., 1995).

Different notch lengths were used in SENB test based on the method proposed by Dongre et al. (1989) in order to measure the fracture energy. It was found that modified binders had improved fracture resistance of asphalt binders, but not failure temperature of the asphalt mixtures. The results indicated that fracture properties are better tools for distinguishing asphalt binders (Marasteanu and Falchetto, 2018). Hoare and Hesp (2000) investigated the impact of specimen size on SENB test results, and no noticeable difference in fracture toughness was observed.

Anderson et al. (2001) applied the SENB test to measure the fracture toughness of modified binders with one control unmodified binder. They concluded that the stress intensity factor of mode I fracture was a more effective tool than PG system in distinguishing the binders in terms of resistance to low temperature cracking (Anderson et al., 2001, Marasteanu and Falchetto, 2018).

2.4.4 Double-Edged Notched Tension (DENT) Test

Double-Edged Notched Tension (DENT) Test is another fracture test used for fracture resistance of asphalt binders at low temperature. The geometry of the DENT test is presented in Figure 2.9. The Ontario Ministry of Transportation has a standard test method (LS-299) for the DENT test. There is an equation available to compute the critical stress intensity factor of DENT specimens (Anderson 2005, Marasteanu and Falchetto, 2018).

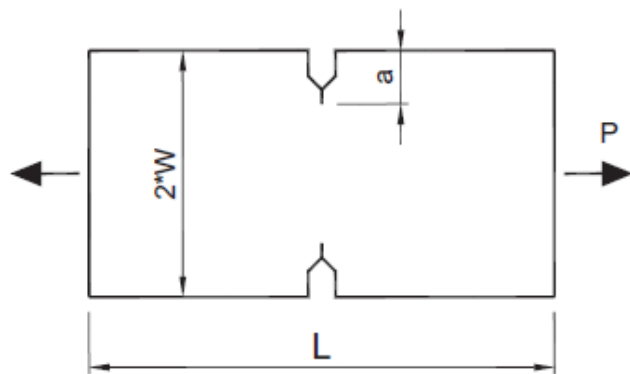


Figure 2.9. DENT test specimen (Marasteanu and Falchetto, 2018)

Dongre et al. (1989) performed the DENT test using DTT equipment. The results indicated that the stress intensity factor K_{Ic} was dependent on the initial crack depth. Therefore, they suggested the application of J-Integral (J_{Ic}) concept and elastic plastic fracture mechanics for characterization of low temperature behavior of asphalt binders.

Gauthier and Anderson (2006) applied both DENT and SENB tests studying the fracture behavior of binders at low temperature. They found that the ranking of binder behavior obtained from fracture tests on notched specimens is different from the ranking made by the PG specification at low temperature. They concluded that linear elastic fracture mechanics could only be applied to the asphalt binders below glass transition temperature. Time-dependent fracture mechanics should be applied to binders above this temperature, since the binder behaves as a time-dependent viscoelastic material (Gauthier and Anderson, 2006, Marasteanu and Falchetto, 2018).

2.4.5 Dynamic Shear Rheometer (DSR) Testing for Calculation of Glover-Rowe Parameter

As mentioned before, DSR testing is required for calculation of the Glover-Rowe parameter, presented in Equation (4), since this parameter is a function of complex modulus and phase angle (G^* and δ). The Glover DSR parameter $G' / (\eta' / G')$ (Glover et al., 2005) is determined at 15°C and 0.005 rad/s to correlate with the ductility at 15°C and 1 cm/min (Anderson et al., 2011). The Glover-Rowe parameter is calculated at the same conditions.

Anderson et al. (2011) applied two approaches for calculation of the Glover parameter $G' / (\eta' / G')$. The DSR test was conducted at 44.7°C and 10 rad/s. Parallel plate geometry (25 mm) with a gap of 1 mm at a test strain of 10% was applied. Then, $G' / (\eta' / G')$ was calculated using G^* and δ derived from DSR test. To obtain the parameter at 15°C and 0.005 rad/s, the calculated value was divided by 2000. The other approach was to run DSR frequency sweep tests at three temperatures (5, 15, and 25°C) for development of the master curve. The DSR test was performed from 0.1 to 100 rad/s at each temperature. A parallel plate geometry (8 mm) with a 2 mm gap at a test strain of 1% was used. The master curve for the reference temperature of 15°C was generated and used for calculation of the Glover DSR parameter.

Rowe (2011) concluded that the approach of generating a master curve could decrease the error in analysis and calculation. Therefore, the master curve can be generated by running DSR frequency sweep tests for computation of G^* and δ at the target temperature and frequency as the input data for calculation of the Glover-Rowe parameters.

A summary of the binder tests is presented in Table 2.1.

Table 2.1. Summary of asphalt binder tests

Test Method	Cracking Mode	Standard Method	Test Specimen	Testing Equipment	Testing Measurement and Dominant Testing/ Cracking Parameter	Relationship to Performance
Bending Beam Rheometer (BBR)	Low Temperature Cracking	AASHTO T 313-12	Beam: L= 4.02 in. (102 mm) b=0.5 in. (12.5 mm) H= 0.25 in. (6.25 mm)	Commercially available	Creep Stiffness (S) and m-value	Defined criteria for Creep Stiffness (S) and m-value
Single-edge notched bending (SENB)	Low Temperature Cracking	ASTM E399-90	Beam L= 6.9 in (175 mm) W= 1 in (25 mm) H= 0.25 in. (12.5 mm)		Stress intensity factor/ Fracture toughness/ Fracture energy	Please refer to the SENB section in the text.
Double-edge notched tension (DENT)	Low Temperature Cracking	Ontario Ministry of Transportation, LS-299	Please refer to the DENT section in the text		Stress intensity factor/ Fracture toughness/ Fracture energy	Please refer to the DENT section in the text.
Direct Tension Test (DTT)	Low Temperature Cracking	AASHTO T 314-12	Le= 1.33 in. (33.8 mm) b=b=0.23 in. (6 mm) (Dog-bone shaped specimen)	DTT device Commercially available	Failure Stress and Strain	Defined criteria for maximum failure strain
DSR Frequency Sweep	Cracking	AASHTO T 315-12	Parallel plate geometry (8 mm) with a 2 mm gap	DSR- Commercially available	Glover-Rowe Parameter	Defined pass/fail criterion for Glover-Rowe Parameter

2.5 LABORATORY ASPHALT MIXTURE TEST METHODS

There are generally two types of test methods for investigation of thermal cracking in asphalt mixtures. One group of the test methods produce engineering indices, and apply failing and passing criteria to assess the thermal cracking resistance of asphalt material. The second group of tests provides results or properties used as input data in thermal cracking models in order to predict the field performance of the asphalt concrete (Zhou et al. 2016).

In this section, the laboratory cracking tests used for thermal cracking and reflection cracking are described. The test methods selected are those most suitable to the purpose of this project. Factors such as test specimen, cracking mode, available test standard, testing condition, test equipment, and cracking test parameter are described.

Different aspects or criteria can be considered for selection and refinement of the cracking tests, such as:

- Test variability.
- Cracking test outcome and interpretation of results.
- Correlation to field performance.
- Test simplicity.
- Availability and cost of the device.
- Sensitivity to mixture design parameters.

2.5.1 Disk-Shaped Compact Tension (DCT) Test

Wagoner et al. (2005) developed the disk-shaped compact tension (DCT) test for determination of the fracture energy of the of asphalt mixtures. This test can be used for characterization of the mixture mechanical behavior against low temperature cracking. The DCT test can be conducted based on ASTM D7313-13. The DCT test is usually performed at a temperature 10 °C higher than the PG low temperature. A disk-shaped specimen with a notch size of 2.46 in. and two holes of 1 in. diameter is loaded and pulled from sides of the notch. Loading continues until the post peak load reaches 0.1 kN. The crack mouth opening displacement (CMOD) is measured using a clip-on gage at the face of the crack mouth (Wagoner et al., 2005, Marasteanu et al., 2012). The test is run in a CMOD-controlled mode. The crack opening rate is 1 mm/min. Test experimental setup, specimen configuration, and typical experimental results are presented in Figure 2.10 and Figure 2.11. The load versus CMOD curve is displayed in Figure 2.11.

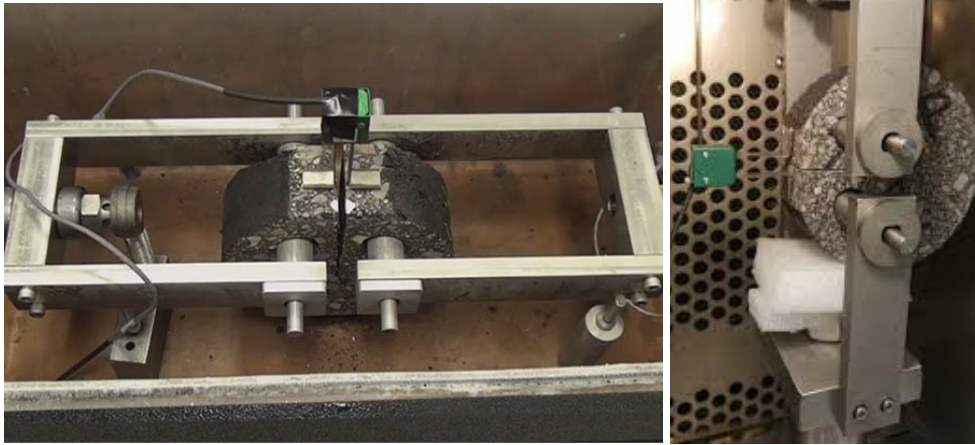


Figure 2.10. DCT test setup and disk-shaped specimen

Recommended Dimensions (mm)	
D	150
W	110
ϕ	25
a	27.5
d	25
C	35

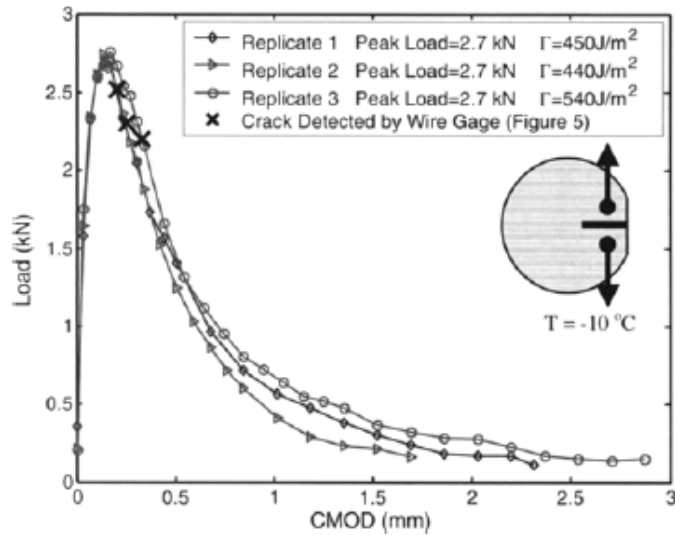
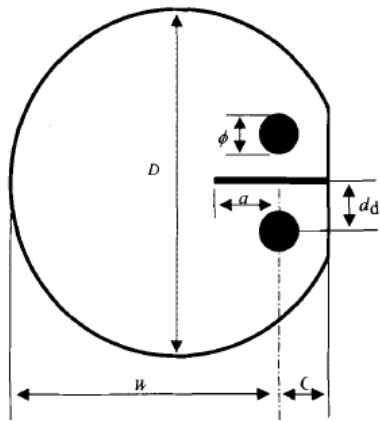


Figure 2.11. DCT test specimen configuration and typical experimental results (Wagoner et al., 2005)

The fracture energy (G_f) is obtained by computing the area under the load versus CMOD curve normalized by the ligament length and thickness (Marasteanu et al., 2012). A mixture with higher fracture energy has a better resistance to cracking. The coefficient of variation (COV) of the DCT test is reported to be in the range 10% to 15% which is a relatively low variability (Zhou et al., 2016). The DCT test results can be used in a defined failing/passing criterion correlated with low temperature cracking field performance.

The DCT specimen is placed in a temperature control chamber and conditioned for at least 2 hours at the desired test temperature before running the test (Marasteanu et al., 2012). Preparation of the DCT specimens requires four cuts and two coring holes. Two cuts are required to make the 2 in. thick sample, one cut for flattening the surface for placing the CMOD gauge, one cut for creating the notch, and two drilling operations for the cored holes. The DCT test can also be performed on field samples.

Braham et al. (2007) conducted DCT tests on 28 asphalt mixtures and studied the effect of four parameters: test temperature, asphalt binder content, air voids, and aggregate type. The results showed that the fracture energy obtained from DCT test is sensitive to temperature, aggregate type, and binder content. It was found that the fracture energy was not sensitive to binder content at low and intermediate temperature ranges and air void content. Dave et al. (2011) reached a similar conclusion. Hill et al. (2013) concluded that mixtures with RAP had lower fracture energy and were more susceptible to cracking. Arnold et al. (2014) also found that RAS material in the mixture could lower the fracture energy. The DCT test and fracture energy are sensitive to recycled materials, i.e., RAP and RAS (Zhou et al., 2016).

2.5.1.1 Correlation of Laboratory Test with Field Performance

Marasteanu et al. (2012) used the DCT test data and field performance data in a national pooled fund study to find a correlation between the DCT fracture energy (tested at PG low temperature plus 10 °C) and the amount of low temperature cracking in the field as shown in Figure 2.12. The data suggested a minimum fracture energy of 400 J/m² (for DCT test at PG low temperature plus 10 °C) for resistance against low temperature cracking. A fracture energy between 350 to 400 J/m² is considered a boundary between acceptable and poor cracking resistance. This range may be acceptable in less important projects where low to moderate levels of low temperature cracking may be acceptable. A minimum fracture energy of 600 J/m² was suggested for more significant projects (Marasteanu et al., 2012).

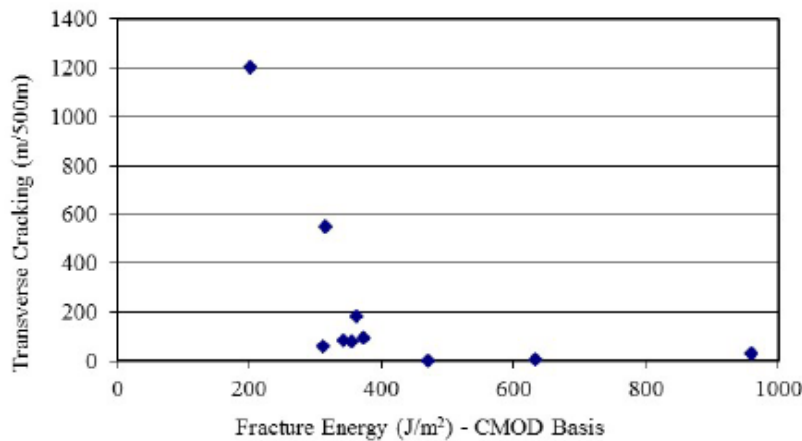


Figure 2.12. Field cracking performance data versus DCT fracture energy for defining a specification limit (Marasteanu et al., 2012)

Furthermore, a specification was suggested for asphalt mixtures based on the data of a correlation between DCT test data and field performance data (Marasteanu et al., 2012). Since the data came from

tests on cores taken from the field of older and aged pavements, a 15% increase in the fracture energy was suggested so that the specification could be used for laboratory mixtures and short-term aged mixtures. The low temperature cracking limits on three types of projects and/or traffic classes are shown in Table 2.2. Higher DCT fracture energies were proposed for the projects with higher traffic levels or significance in order to limit thermal cracking, considering the potential of rapid aging near the surface of these pavements (Marasteanu et al., 2012). In brief, the DCT test results can be used with defined failing/passing criteria for distinguishing low temperature cracking resistance.

Table 2.2. Suggested low temperature cracking specification limits for DCT test results for loose mixtures (Marasteanu et al., 2012)

DCT Test Property	Project Significance/Traffic Level		
	High, >30 M ESALs	Moderate, 10 M to 30 M ESALs	Low, <10 M ESALs
Minimum Fracture Energy (at PG low temperature plus 10°C) (J/m ²)	690	460	400

2.5.2 Semi-Circular Bend (SCB) Test (Low Temperature)

The Semi-Circular Bend (SCB) test for low temperature cracking was developed to characterize cracking resistance of asphalt mixtures (Li and Marasteanu, 2004, Marasteanu et al., 2012). The SCB and DCT tests have some attributes in common. The SCB test is also conducted at a temperature 10°C higher than the PG low temperature. The cracking parameter and outcome of the SCB test for low temperature cracking is fracture energy, similar to the DCT test. The SCB test is performed in a CMOD- controlled mode as is the DCT test. However, this test is conducted at crack opening rate of 0.03 mm/min, 33 times slower rate than that of the DCT test. The specimen thickness in the SCB test is 1 in., which is thinner than the DCT test. This test is conducted according to the AASHTO TP 105-13 Standard. The test setup and specimen are displayed in Figure 2.13. The SCB test setup and sample preparation using cylinders made with Superpave Gyratory Compactor are simple.

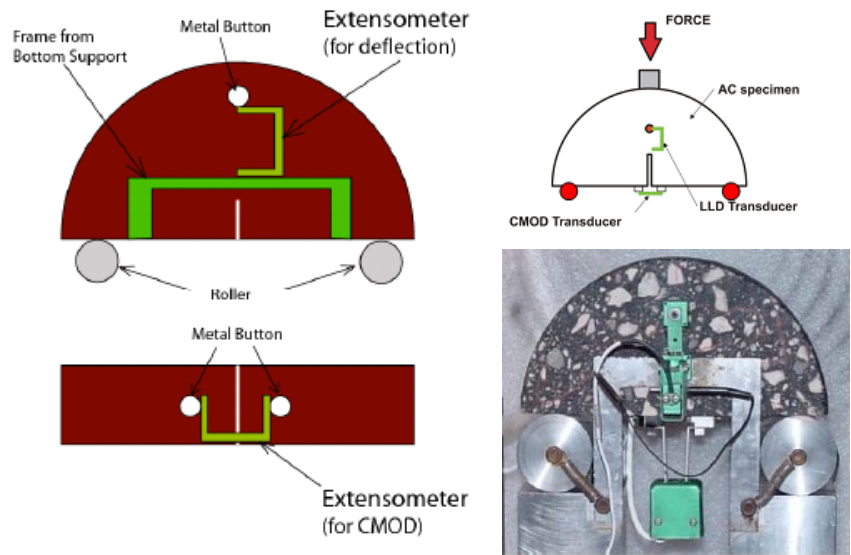


Figure 2.13. SCB test experimental setup and specimen (Li and Marasteanu, 2004, Li et al., 2008a, Marasteanu et al., 2012)

A servo-hydraulic testing machine, with an environmental chamber, can be used for conducting the SCB test. An Epsilon extensometer, mounted vertically with a 38-mm gauge length and ± 1 mm range, measures the Load Line Displacement (LLD). The load versus LLD can be used to calculate the fracture energy and fracture toughness (Li and Marasteanu, 2004, Marasteanu et al., 2012). Fracture energy in the SCB test is obtained by calculation of the area under the load – Load Line Displacement (LLD) curve normalized with initial ligament thickness and length (Marasteanu et al., 2012). The CMOD measurement is not used for the calculation of the fracture energy. The CMOD constant rate is used for keeping the test stable in the post peak regime. Typical Load versus LLD curves are displayed in Figure 2.14. The environmental chamber controls the temperature and an independent thermometer verifies that temperature. The typical COV of the SCB test results is reported around 20% (Marasteanu et al., 2012, Zhou et al., 2016). The SCB test can be conducted on the specimens compacted in the laboratory and the core samples from the field.

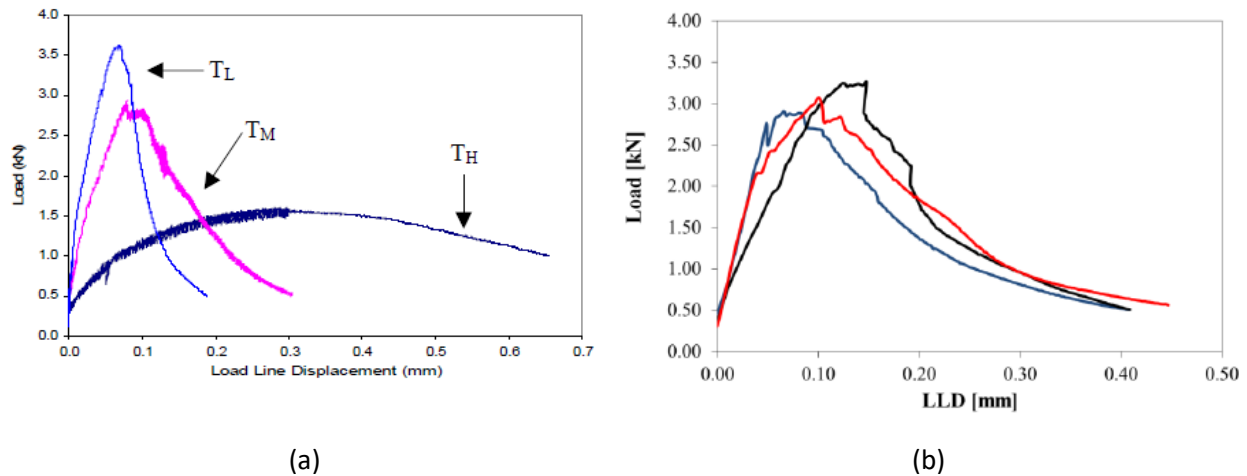


Figure 2.14. Typical load versus LLD curves (a) at different temperatures (Li et al., 2008a), (b) for three replicates (Marasteanu et al., 2012)

Li and Marasteanu (2004) investigated the low temperature resistance of similar mixtures with three different asphalt binders using the SCB test. They found that the SCB fracture energy is sensitive to the binder PG grade. Li et al. (2008b) investigated the effect of asphalt content, air voids, and aggregate type on the SCB fracture energy. It was found that the fracture energy is sensitive to the air void content and aggregate type; however, it is not sensitive to binder content. Li et al. (2008b) also investigated that effect of RAP content on fracture energy. The results showed that a high RAP content of decreased the fracture energy. However, the result of another study (West et al., 2013) indicated that RAP content did not have consistent or significant effect on the SCB fracture energy.

2.5.2.1 Correlation of Laboratory Test with Field Performance

Using the same procedure as used for the DCT test, the SCB test outcomes were evaluated to find a correlation between field transverse cracking and the mixture fracture energy and toughness (Marasteanu et al., 2012). The laboratory fracture energy data versus cracking data from the field are displayed in Figure 2.15. A minimum value of 350 J/m² was suggested as a limiting value for the SCB fracture energy in order to protect the pavement against low temperature cracking based on the data. The value was also adjusted to 350 J/m² in order to consider the effects of aging. It was found that the fracture toughness had a good correlation with field transverse cracking as shown in Figure 2.16. Thus, a minimum value of 800 kPa.m^{0.5} was proposed as a limiting value for the SCB fracture toughness.

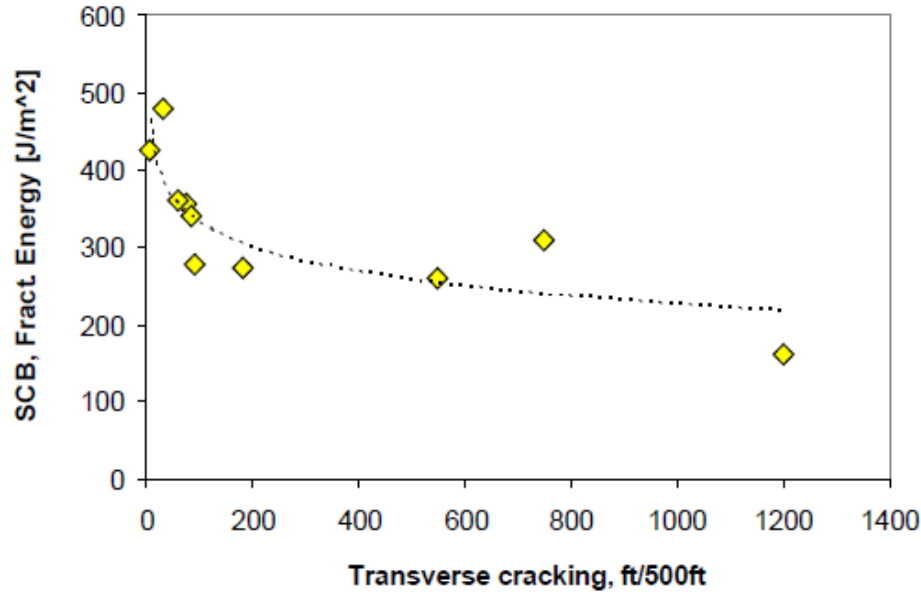


Figure 2.15. Field cracking performance data versus SCB fracture energy for defining a specification limit (Marasteanu et al., 2012)

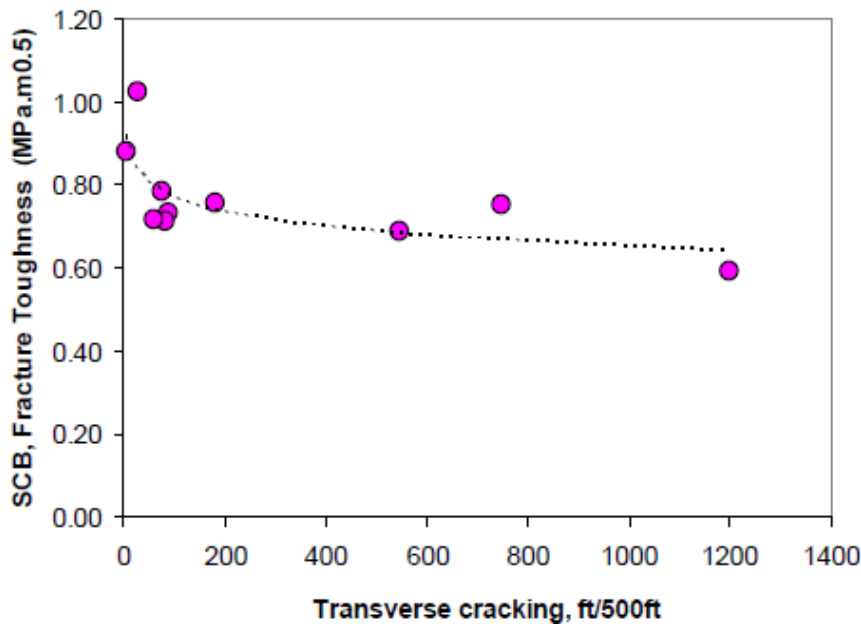


Figure 2.16. Field cracking performance data versus SCB fracture toughness for defining a specification limit (Marasteanu et al., 2012)

2.5.3 Indirect Tensile (IDT) Test

The Indirect Tensile (IDT) test for low temperature cracking was developed during the Strategic Highway Research Program (SHRP) (Roque and Buttlar, 1992, Buttlar and Roque, 1994). This test is conducted according to AASHTO T 322-07. Creep compliance and strength were determined at low temperatures in the IDT test using cylindrical specimens. These two parameters are input data into the AASHTOWare

Pavement ME design for the prediction of low-temperature cracking. The cylindrical specimen has diameter of 6 in. and thickness of 1.5 to 2 in. the test setup and specimen are shown in Figure 2.17. Each asphalt mixture is usually tested at three different temperatures determined based on the PG grade of the asphalt binder.

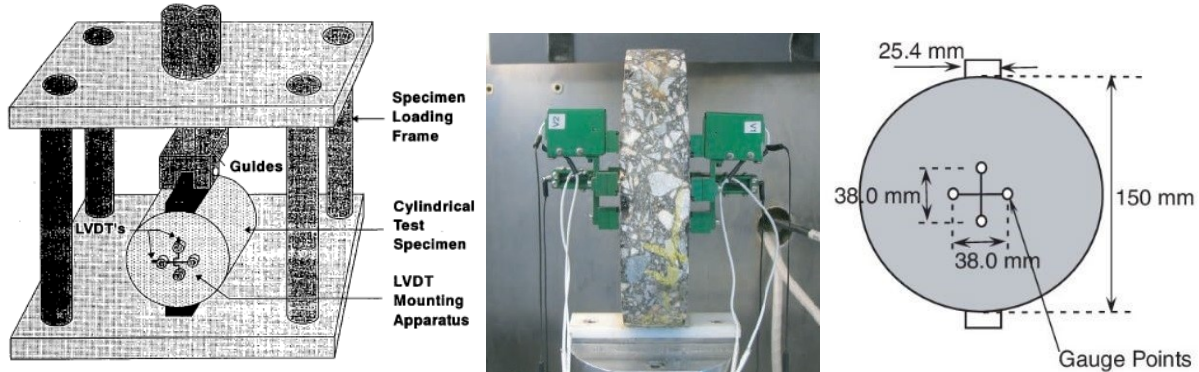


Figure 2.17. IDT test setup and specimen (Buttler and Roque, 1994)

A compressive load is applied across a diameter of the cylindrical specimen which creates a region of uniform tensile stress in the horizontal direction. In the IDT creep test, a constant load that generates horizontal deformation between 0.00125 mm and 0.019 mm is exerted for 1,000 seconds. The LVDTs record the horizontal and vertical deformations during the testing time. This data is used to compute the creep compliance and stiffness as a function of time. In the IDT strength test, the equipment exerts a vertical compressive load at a constant rate of 12.5 mm/minute until failure. The diametral loading creates a region of uniform tensile strain across the vertical plane in the sample. The failure tensile strength is calculated at the peak load using the specimen dimensions and maximum load. Typical IDT creep compliance versus time curves are displayed in Figure 2.18.

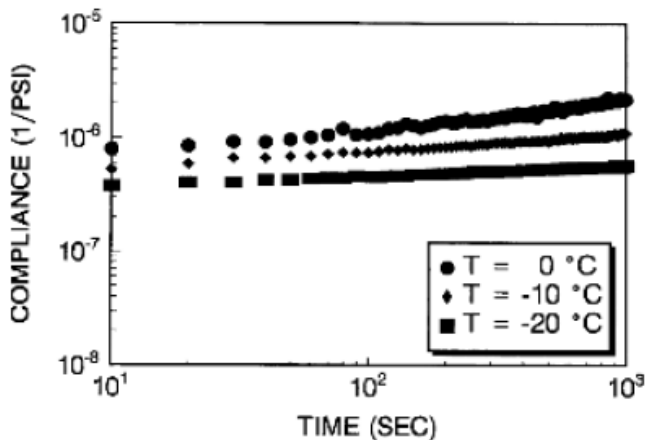


Figure 2.18. Typical creep compliance results from the IDT creep test (Roque and Buttler 1992)

The IDT test can be conducted on specimens made and compacted in the laboratory as well as field cores. The COV of the IDT tensile strength test is reported to be around 7%, and that of the IDT creep test is reported to be around 11% (Christensen and Bonaquist, 2004). The extensive historical data show

that the IDT creep compliance and tensile strength are a function of asphalt binder content, binder type, air voids, recycled materials (RAP), air void, aggregate type, and degree of aging (Zhou et al., 2016).

2.5.3.1 Correlation of Laboratory Test with Field Performance

The IDT test is mostly a mechanistic-oriented test. The IDT creep compliance and tensile strength are usually used as input data in TCMODEL for prediction of the low temperature cracking of the pavement (Zhou et al. 2016). The IDT creep compliance and tensile strength have been used in the development of mechanistic empirical pavement design. These parameters can also be used for simple comparison between mixtures.

2.5.4 Illinois Flexibility Index Test (I-FIT or IL-SCB)

Al-Qadi et al. (2015) developed the Illinois-Semi-Circular Beam (IL-SCB), also known as the Illinois Flexibility Index Test (I-FIT), for fracture testing at an intermediate temperature of 25°C (77°F) at University of Illinois at Urbana-Champaign. They found that low-temperature fracture tests were not reliable for the comparison of different asphalt mixtures. Al-Qadi et al. (2015) conducted intermediate-temperature IL-SCB test at a displacement rate of 50 mm/min. Fracture energy alone was not enough to distinguish between different asphalt mixtures in some cases. For example, although two asphalt mixtures could have very close fracture energy values, they might show different load versus displacement behaviors and cracking response, as shown in Figure 2.19.

Fracture energy is a function of peak load (or strength) and maximum displacement at the end of the test (ductility). An asphalt material with even high strength may have a lower displacement in the post peak regime of the load deflection curve. This explains why some brittle asphalt mixtures with high amounts of recycled materials may have similar or even greater fracture energy than the control mixtures without any recycled materials (Al-Qadi et al., 2015).

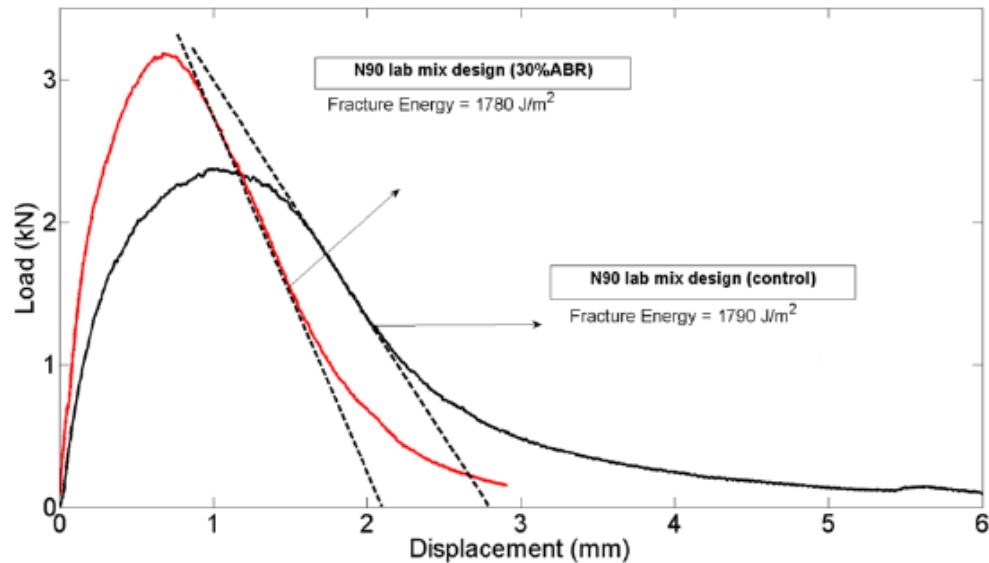


Figure 2.19. Different load-displacement curves of two asphalt mixtures with the same fracture energy obtained from IL-SCB tests (Al-Qadi et al., 2015)

Al-Qadi et al. (2015) developed a parameter that could describe the fracture processes through the use of load-displacement curves and evaluate the cracking potential of asphalt mixtures. The major mechanism that alters the load-displacement behavior of the mixture in a fracture test is related to the size of the fracture process zone, in which void formation or microcracking occurs. The size of the fracture process zone is controlled by inhomogeneous components and inconsistencies in the microstructure of the material and is a function of distribution of aggregates, maximum aggregate size, shape, and matrix volume and properties. It was hypothesized that the fracture process zone and, any parameter derived from it, would influence crack propagation speed. The following parameters from IL-SCB test that might affect formation of the fracture process zone were considered in the development of flexibility index (FI), as shown in Figure 2.20:

- Fracture energy (G_f).
- Peak load (P_{max}).
- Critical displacement (u_1).
- Displacement at the maximum load (u_0).
- Displacement at the end of test (u_{final}).
- Slope at inflection point (m).

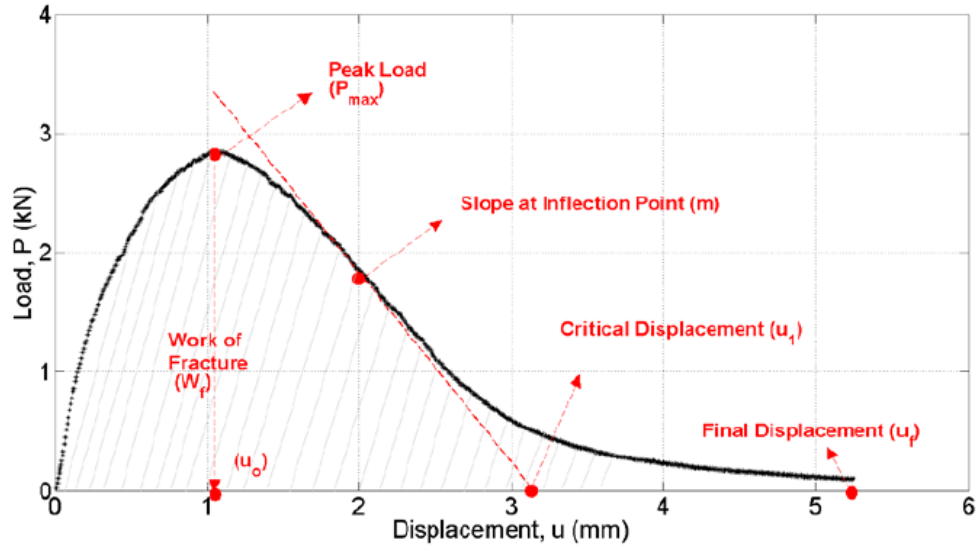


Figure 2.20. Parameters in a typical load displacement curve from IL-SCB test (Al-Qadi et al., 2015)

The flexibility index (FI) accounts for the size of the fracture process zone or other property combinations with good correlations to crack growth speed. The FI was defined as (Al-Qadi et al., 2015):

$$FI = A \times \frac{G_f}{|m|} \quad (5)$$

where A is a calibration coefficient and was assumed equal to 0.01 for laboratory compacted and field samples. This value may vary for the field samples where aging and field compaction can affect the mechanism.

The IL-SCB test is conducted according to AASHTO TP 124-16. The average COV of fracture energy from the IL-SCB test was reported as 4.6% and the COV of the FI was reported to be approximately 10% to 15% for both laboratory-compacted and field asphalt mixtures (Al-Qadi et al., 2015).

2.5.4.1 Correlation of Laboratory Test with Field Performance

The FI obtained from IL-SCB was compared with field performance data including severity of distresses, condition rating score (CRS), and field observations (Al-Qadi et al., 2015). Pavements were divided into three categories based on the pavement conditions: Good, Fair, and Poor. The comparison of FI values to the field pavement performance data is displayed in Figure 2.21. As shown in the figure, the results indicated that pavements with good performance usually had FI values higher than 10, while the ones with worse performance had FI values between 1.3 and 3.9.

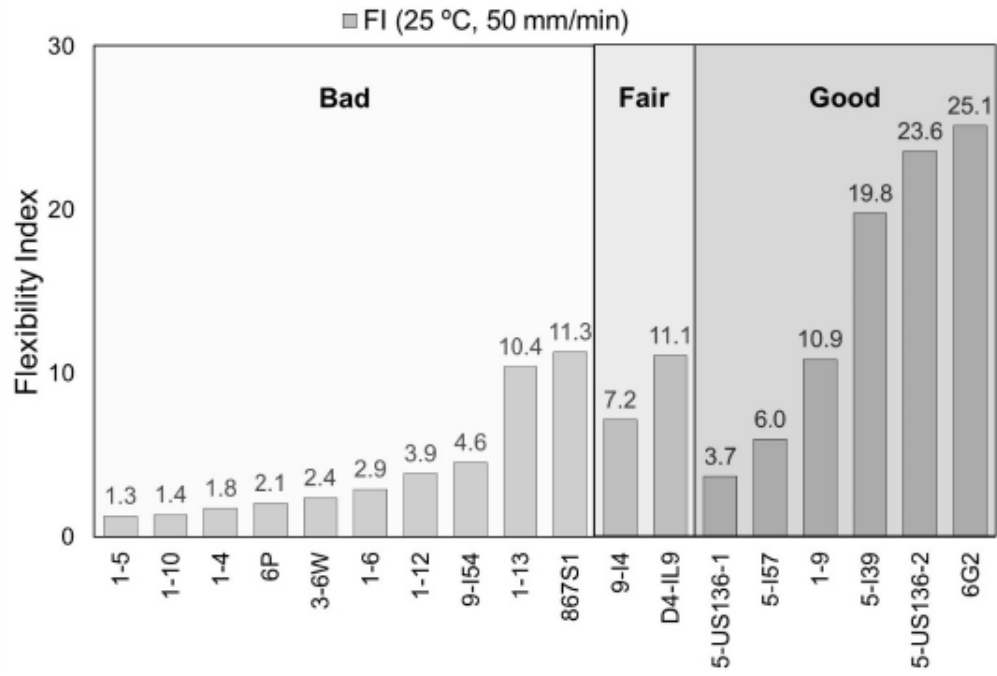


Figure 2.21. Comparison of flexibility index to field performance (Al-Qadi et al., 2015)

2.5.5 Thermal Stress Restrained Specimen Test (TSRST)

Jung and Vinson (1994) developed the Thermal Stress Restrained Specimen Test (TSRST) as a part of SHRP. In this test, the specimen is cooled and the temperature drops, but the specimen is restrained against contraction. Therefore, tensile stresses are generated in the specimen. The experimental setup is displayed in Figure 2.22. Fracture strength and temperature are recorded as shown in Figure 2.23. There was a standard test method, i.e., AASHTO TP 10, for this test; however, this standard was withdrawn and is inactive now. The test specimen is a 2×2×10 in. beam, and cooling rate is usually 10°C/hr. Fracture temperature can be compared with the required fracture temperature for a given location.

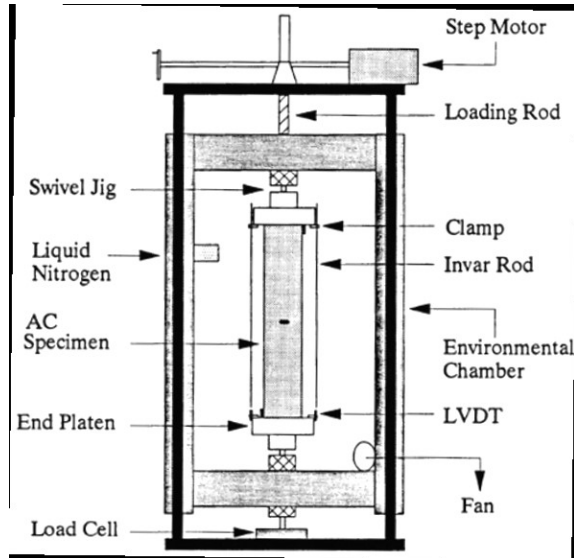


Figure 2.22. TSRST experimental setup (Jung and Vinson, 1994)

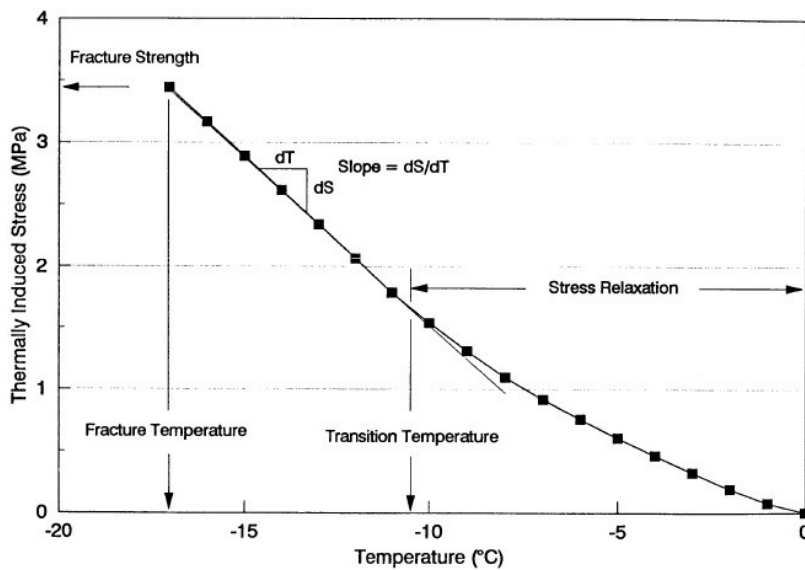


Figure 2.23. Typical results of the TSRST including fracture temperature and fracture strength (Jung and Vinson, 1994)

The COV of fracture temperature and fracture strength are reported to be 10% and 20%, respectively (Jung and Vinson, 1994). Specimen preparation of the TSRST is difficult, since it is a long beam, and must be cut from a larger slab specimen which requires a rolling compactor. Gluing the long beam to the TSRST equipment platen is also difficult. TSRST results are sensitive to mixture properties including asphalt binder content, binder type, air voids, aggregate type, and aging (Zhou et al., 2016).

Hajj et al. (2010) developed a similar test called Uniaxial Thermal Stress and Strain Test (UTSST), which is a modified version of the TSRST. UTSST uses a cylindrical specimen with typical diameter of 2.25 in. and height of 5.5 in.

2.5.5.1 Correlation of Laboratory Test with Field Performance

The TRST has not been used much in practice since it was not included in the Superpave mix design. Therefore, the correlations of the laboratory results to the field performance are limited. Marasteanu et al. (2007) conducted TSRST on the specimens recovered from MnRoad. It was found that TSRST could provide a good indication of the resistance of a mixture to low temperature cracking.

2.5.6 Texas Overlay Test

Germann and Lytton (1979) originally developed the Overlay Test (OT). Zhou and Scullion (2005) updated and standardized the OT. It was then adopted by Texas Department of Transportation (TxDOT) as standard test procedure Tex-248-F and by New Jersey Department of Transportation (NJDOT) as NJDOT B-10 test method. The OT equipment consists of two steel plates, a temperature control chamber, and an oscillating actuator. The trimmed asphalt mixture specimen is glued to the top of the plates. One plate is fixed and the other moves in the horizontal direction. Thus, it simulates the opening and closing of cracks or joints underneath an asphalt layer. The OT specimen typically has a length of 6 in., width of 3 in. and height of 1.5 in. The equipment for the OT is shown in Figure 2.24. The specimen may be prepared from gyratory compactor samples or field cores.

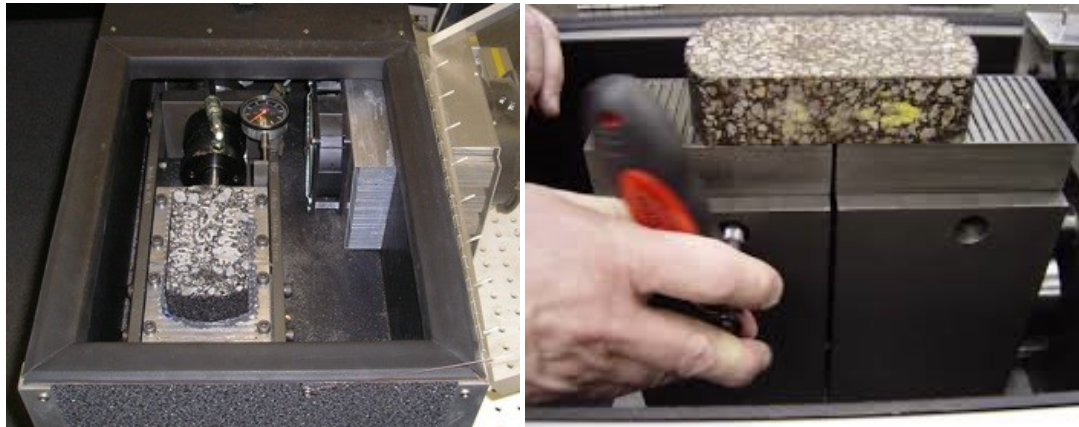


Figure 2.24. Overlay tester

The OT test is run in the displacement control mode with a maximum opening displacement of 0.025 in. This test is cyclic with a frequency of 1 cycle per second with a triangular loading wave function. The specimen temperature is close to room temperature, most often 25 °C (77 °F). The failure is defined as the time when the load decreases as much as 93% of the peak load at the first cycle. Number of load repetitions to the failure is reported at the end of the test. A typical OT results is shown in Figure 2.25. Fracture parameters, A and n , can also be obtained from load versus displacement curve.

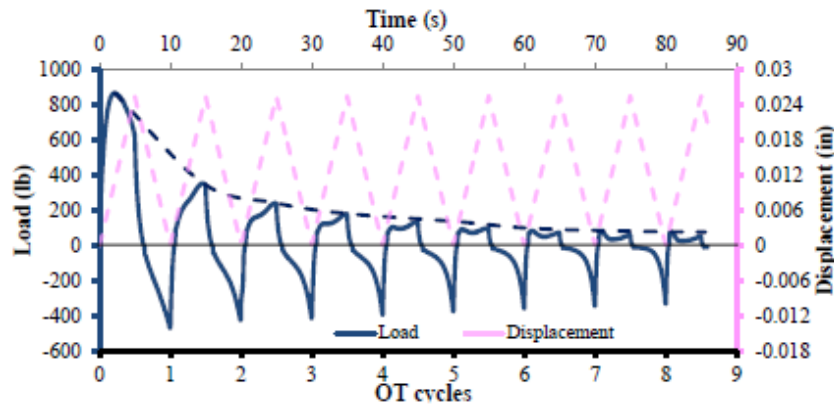


Figure 2.25. Typical results of overly test (Walubita et al., 2012)

Walubita et al. (2012) found that the COV of the OT results was around 30% for most dense-graded mixtures. This COV is higher than the reported COV of most of the monotonic cracking tests. However, they also noted that a higher COV might be the nature of cyclic loading cracking tests.

2.5.6.1 Correlation of Laboratory Test with Field Performance

Many research studies have reported a good correlation between the OT results and field reflection cracking in Texas, New Jersey and Nevada (Zhou and Scullion, 2005, Zhou et al., 2006, Hajj et al., 2010, Walubita et al., 2012, and Zhou et al., 2016). Loria-Salazar (2008) noted that the Texas OT is one of the few laboratory test methods with performance validation. TxDOT has defined a minimum number of load repetitions for different types of mixtures (Zhou et al., 2016):

- Stone-Matrix Asphalt: minimum 200 load cycles.
- Permeable Friction Course, Fine PFC: minimum 200 load cycles.
- Thin Overlay Mixtures: minimum 300 cycles.
- Thin Bonded Friction Courses, Fine PFC: minimum 200 cycles.

2.5.7 IDEAL Cracking Test (IDEAL-CT)

Zhou et al. (2017) developed an indirect tensile asphalt cracking test (IDEAL-CT) as a practical cracking test for routine use in asphalt mix design, quality control, and quality assurance (QA/QC). The IDEAL-CT is typically conducted at the room temperature, i.e., 25 °C (77 °F). The IDEAL-CT is similar to the IDT strength test with a loading rate of 50 mm/min. The cylindrical specimens for this test can have various dimensions, for example a diameter of 100 or 150 mm and variable heights. Typically the samples are the same size as those used for the Hamburg Wheel Tracking Test with a diameter of 150 mm, height of 62 mm with an air void content of $7 \pm 0.5\%$. These dimensions were suggested since this size of specimen is typical for QC/QA. The IDEAL Cracking Test setup and a typical force displacement curve are displayed in Figure 2.26. The test procedure has been standardized in ASTM D-8225.

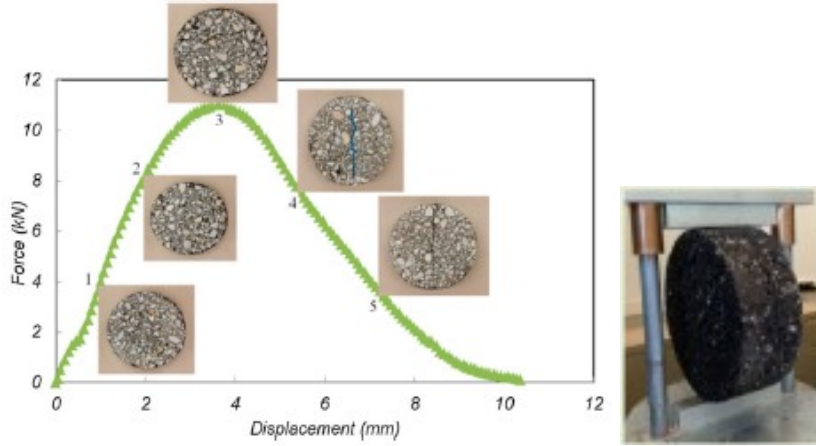


Figure 2.26. IDEAL cracking test setup and typical test results (Zhou et al., 2017)

This test requires no cutting, gluing, instrumentation, or drilling. Testing time is short at about 1 min. The maximum COV of the test results is reported to be approximately 25%. The average COV of IDEAL Cracking Test was reported to be approximately 12.7% for 15 sets of 3 samples (Newcomb and Zhou, 2018). This test is sensitive to asphalt mixture properties such as asphalt binder type and content, and aggregate type, and degree of aging. Zhou et al. (2017) developed a Cracking Test (CT) Index:

$$CT\ Index = \frac{t}{62} \times \frac{G_f}{|m_{75}|} \times \left(\frac{l_{75}}{D}\right) \quad (6)$$

where G_f is the work of fracture calculated by the area under the load versus vertical displacement curve divided by the area of the cracking face, t is the specimen thickness or height (mm), l_{75} is the displacement when the load in the post peak region reduces to 75% of the peak load, $|m_{75}|$ is the absolute value of the slope of the load vs. displacement curve at the point where the load in the post peak region reduces to 75% of the peak load, and D is the specimen diameter. Higher CT Index results indicate higher cracking resistance.

2.5.7.1 Correlation of Laboratory Test with Field Performance

Zhou et al. (2017) investigated the correlation of the IDEAL-CT results to the field cracking performance. They studied the accelerated pavement testing data from the Federal Highway Administration accelerated loading facility (FHWA ALF), in-service roads in Texas, and full-scale test section in Minnesota (MnROAD). All test results indicated that the IDEAL-CT results exhibited good correlation with reflection cracking, thermal cracking, and fatigue cracking in the field. The specification limits have not been defined at this time.

Table 2.3 presents a summary of the mixture tests presented in this report.

Table 2.3. Summary of asphalt mixture tests

Test Method	Cracking Mode	Standard Method	Test Specimen	Testing Measurement and Dominant Testing/ Cracking Parameter	Relationship to Performance	Testing Equipment
DCT Test	Low Temperature Cracking	ASTM D 7313-13	Disk-shaped specimen, D= 6 in. H= 2 in. Notch= 2.46 in. D (holes): 1 in.	Fracture energy	Pass/fail; correlation of field cracking and fracture energy	Commercially available
SCB Test	Low Temperature Cracking	AASHTO TP 105-13	Semi Circular Specimen D= 6 in. H= 1 in. Notch= 0.6 in.	Fracture energy and Fracture toughness	Pass/fail; correlation of field cracking and fracture energy	Commercially available
IDT Test	Low Temperature Cracking	AASHTO T 322-07	Cylindrical specimens D= 6 in. H= 1.5 to 2 in.	Creep compliance and tensile strength	Input data for temperature cracking model	Hydraulic test machines can be used
I-FIT	Cracking	AASHTO TP 124-16	Semi Circular Specimen D= 6 in. H= 1 in.	Flexibility Index (FI) and fracture energy	Correlation of field cracking and FI	
TSRST/ UTSST	Low Temperature Cracking	AASHTO TP 10 (inactive)	TSRST Beam: L=10 in. b=2 in. (50 mm) HW= 2 in. UTSST: D= 2.25 in. H= 5.5 in.	fracture temperature, fracture stress	Limited data	Commercially available

Test Method	Cracking Mode	Standard Method	Test Specimen	Testing Measurement and Dominant Testing/ Cracking Parameter	Relationship to Performance	Testing Equipment
OT	Reflection Cracking	Tex-248-F (cyclic tests) and NJDOT B10	L= 6 in. W = 3 in. H = 1.5 in.	No. of load repetitions to failure (or fracture parameters: A and n)	Defined criteria; Correlation of field cracking and number of cycles	Commercially available
IDEAL CT	Cracking	NA	D= 6 in. H= 2.44 in.	Cracking Test (CT) Index	Criterion; correlation of field cracking and CT Index	Commercially available

2.6 SUMMARY AND RECOMMENDATIONS FOR PERFORMANCE TESTING

Based upon the results of the literature review, the following recommendations were made regarding the selection of binder parameters and tests to be conducted in this research:

1. ΔT_c – This parameter is determined with standard Superpave rheological equipment, i.e., PAV and BBR. The testing is performed at low temperature and it is performed on materials conditioned in the PAV for up to 40 hours. Although it may require up to 40 hours of conditioning, the results have been correlated to pavement performance and to the efficacy of rejuvenators for high RAP mixtures. It should be noted that the Asphalt Institute (2019), in a survey of state DOTs, found that 8 agencies had adopted ΔT_c as a specification and 2 others were scheduled to adopt it in 2020.
2. Glover-Rowe Parameter – This value may be obtained using the DSR during normal binder testing at an unaged state and with up to 40 to 80 hours of PAV conditioning. The results have been correlated to the performance of field-aged asphalt pavements. Rowe (2017) suggested the use of a G-R maximum of less than or equal to 600 kPa for durability cracking or thermal cracking.

For asphalt mixture testing, the following recommendations are made regarding mixture design and QC/QA test development in this research:

1. Mixture Design – In the design of asphalt mixtures, two cracking tests may be practically incorporated. The first is the DCT test because it is a low temperature test, and thermal cracking is the primary distress of interest to Mn/DOT. The IDEAL cracking test should be performed to establish a baseline for QC/QA testing during construction.
2. QC/QA – The DCT test takes a long time to prepare, condition, instrument, and test which precludes its use in providing timely information in the field. Therefore, it is suggested that the IDEAL cracking test should be used as a quality control and quality assurance test. Although it is performed at an intermediate temperature, the baseline established between the DCT and IDEAL cracking test should provide a good target for construction (Newcomb and Zhou, 2018). Recall, the IDEAL cracking test is performed on uncut, laboratory compacted specimens at an easily achievable temperature.

CHAPTER 3: MATERIALS AND METHODS

The asphalt binder and mixture cracking tests used for characterizing the resistance to the low temperature and reflection cracking were described in the Literature Review. In this chapter, the materials, methodology, and test procedures used in this research project are discussed. Selected MnDOT projects, from which asphalt binders and mixtures were sampled for testing in this study, are discussed. The asphalt mixtures and binders received from MnDOT are described as are the experimental test plans for these materials.

The properties of the binder used in hot-mix asphalt (HMA) for pavement projects are of key significance in the short and long-term performance of the pavements. Based on the binder test results, an agency can decide if the selected binder has a good resistance to the common distresses. The research team conducted DSR and BBR testing for binder characterization at high and low temperatures. This plan focuses mostly on the cracking performance tests.

Furthermore, the IDEAL cracking test and the DCT test procedures used for performance testing of mixtures in terms of cracking are described in this chapter. The experimental plan to determine the sensitivity of the IDEAL cracking test to the time between compaction of samples and the crack testing is addressed. The focus of the test plan for mixture testing using the IDEAL cracking test is to develop/suggest realistic methods for QC/QA testing in terms of cracking resistance. The correlation between some IDEAL cracking test and DCT test results from other studies/experiments is also discussed.

3.1 CONSTRUCTION PROJECTS AND STUDIED MATERIALS

Selected projects from MnDOT's 2018 and 2019 construction seasons were identified for cracking test validation. A summary of the projects is shown in Table 3.1. The asphalt binders and loose mixtures were shipped to the TTI laboratory where the research team performed binder testing for these projects, including DSR testing for obtaining the Glover-Rowe (GR) parameter and BBR tests to determine ΔT_c . Moreover, the IDEAL cracking test was conducted to evaluate the mixtures' cracking resistance. DCT test results, conducted on the materials from these projects, were provided by MnDOT. TTI received materials and/or data for six MnDOT projects in 2018, as shown in Table 3.1. TTI received materials for six asphalt mixtures from five projects in 2018, with one project having two mixtures. No mixture was provided for one of the projects in 2018. TTI received asphalt binders and mixtures from three more projects from MnDOT 2019 construction season, as presented in Table 3.1.

Table 3.1. Summary description of MnDOT construction projects and the asphalt materials used in this study

Project	District	County/Aggregate Source	TTI ID	Location	Project Plan	Description	Mix Type	Binder
0304-037	Detroit Lakes	Otter Tail County Line	P3	T.H. 59	Grading, Full Depth Reclamation (FDR), Mill & Overlay	2018 pilot	SPWEB340C	58H-34
0704-100	Mankato	Blue Earth	P6	T.H. 22	Reconstruction-Grading, Mill & Overlay, Bituminous Surfacing	2017 pilot (carryover)	SPWEB440C	58H-34
1118-021	Baxter	Cass	P4	T.H. 371	Milling, FDR, & Overlay	2018 pilot	SPWEA340C	58H-34
6904-046	Duluth	St. Louis	P5A P5B	T.H. 1	Reconstruction-Grading, Bituminous Surfacing	2017 pilot (carryover)	SPWEA340C SPWEB340C	58-34
8607-063	Baxter	Wright	P2	T.H. 55	Grading, FDR, Milling, and Bituminous Surfacing	2018 pilot	SPWEA440C	58H-34
3109-041	Bemidji	Itasca	P1	T.H. 46	FDR- Grading, Milling, Bituminous Surfacing	2018 pilot	*	58H-34
7301-38	-	Stearns	P7	T.H. 4	-	2019 Season	SPWEA340C	58H-34

Project	District	County/Aggregate Source	TTI ID	Location	Project Plan	Description	Mix Type	Binder
7303-50	-	Sommers Pit	P8	T.H. 15	-	2019 Season	SPWEA440C	58V-34
8606-60	-	Naaktgeboren	P9	T.H. 55	-	2019 Season	SPWEA340C	58H-34

* No mixture received.

The MnDOT Standard Specifications for Construction (2018) has detailed information on the mixture designations in Table 3.1. According to the specification, the first two letters indicate the mixture design type. SP at the beginning of the mix type indicates the Superpave gyratory mixture design. The third and fourth letters indicate the pavement layer. For example, WE stands for wearing and shoulder wearing course, and NW indicates Non-wearing course. The fifth letter in the mix type indicates the maximum aggregates size: A refers to ½ in., B is ¾ in., C is 1 in., and D is 3/8 in. The sixth digit is the level of traffic according to the MnDOT Standard Specifications for Construction (2018) Table 2360-1. The seventh and eighth letters indicate the air void requirement. Designation 40 is for 4.0% air voids in wear mixtures, and 30 indicates 3.0% air voids for non-wear mixtures and shoulder. The last letter stands for the asphalt binder grade in accordance with Table 2360-2 in the 2018 MnDOT specification book.

3.2 ASPHALT MIXTURES CRACKING TESTS

The IDEAL-CT is well-suited to fit into a quality control/quality assurance framework. First, the raw materials, including aggregates and asphalt binder, and asphalt mixture properties should be controlled and tested according to MnDOT Standard Specifications for Construction (2018) and the Schedule of Materials Control for the 2018 Standard Specifications. Item 2360 for mixtures, Item 3139 for aggregates and Item 3151 for binders are applicable. The sample size and the number of tests per day are determined in the MnDOT Schedule of Materials Control 2018.

The DCT and IDEAL cracking tests are suggested performance tests for cracking performance of asphalt mixtures. As discussed, the DCT is a time-consuming procedure requiring extensive sample preparation and temperature conditioning. The amount of time involved in performing the DCT would inhibit its use in production testing. Thus, it is proposed that the DCT be used in the mixture design evaluation, and that the IDEAL cracking test be conducted during mix design at the optimum asphalt content to establish a target value to be used for QC/QA practices. This defined target value should be achieved in the IDEAL CT in the QC/QA checks and in the construction process.

Another approach for the application of the IDEAL cracking test in QC/QA process is to perform this test and use its performance criteria directly for acceptance. The determination of specification limits for the CT Index is ongoing in order to tie the criteria to pavement structure, climate and traffic.

The performance criteria for DCT test will be ultimately defined for application in the mix design process by specifications developed by MnDOT. The performance criteria suggested for the results of the DCT and IDEAL cracking tests (Newcomb and Zhou, 2018) are presented in Table 3.2. These criteria are suggested based upon previous work by researchers of the tests or applied by MnDOT (Newcomb and Zhou, 2018).

Table 3.2. Criteria suggested for cracking performance tests (Newcomb and Zhou, 2018)

Test	Test Temperature (°C)	Loading Rate (mm/min)	Test Parameter	Test Criteria	Reference
DCT (Low Volume Roads)	PG Low Temperature + 10 °C (LTPPBind site specific, 98% reliability)	1	Fracture Energy (J/m ²)	Minimum 450 (J/m ²)	Wagoner et al. 2006
DCT (High Volume Roads)				Minimum 500 (J/m ²)	
IDEAL Cracking Test	25	50	CT Index	80	Zhou et al. 2017

A specification was suggested for asphalt mixtures based on the available data on a correlation between DCT test results and field performance data (Marasteanu et al., 2012). Since the data came from tests on cores taken from the field of older and aged pavements, a 15% increase in the fracture energy was suggested so that the specification could be used for laboratory mixtures and short-term aged mixtures. The low temperature cracking limits on three types of projects and/or traffic classes are shown in Table 3.3. Higher DCT fracture energies were proposed for projects with higher levels of traffic or significance in order to limit thermal cracking, considering the potential of rapid aging near the surface of these pavements (Marasteanu et al., 2012).

Table 3.3. Suggested low temperature cracking performance criteria for DCT Test (Marasteanu et al., 2012)

DCT Test Parameter	Test Temperature (°C)	Project Significance/Traffic Level		
		High, >30 M ESALs	Moderate, 10 M to 30 M ESALs	Low, <10 M ESALs
Minimum Fracture Energy (J/m ²)	PG low temperature + 10 °C (LTPPBind site specific)	690	460	400

3.2.1 IDEAL Cracking Test Procedure

The IDEAL cracking test was conducted at room temperature, i.e., 25 °C (77 °F) in this study. The IDEAL cracking test is an Indirect Tensile (IDT) strength test with a loading rate of 50 mm/min. However, the loading for the IDEAL test is continued after the peak load to capture the material fracture properties. A more detailed discussion and a standard test procedure for performing this test is presented in ASTM D 8225.

3.2.2 DCT Test Procedure for MnDOT Mixtures

The standard test procedure for performing the DCT test is ASTM D 7313-13. MnDOT has developed an alternative test procedure which changes the conditioning of specimens (Newcomb and Zhou, 2018; Hanson, 2015). In the DCT test, a disk-shaped asphalt mixture specimen is pulled apart by a direct tensile force. The test continues until the post peak load decreases to 0.02 lb (0.1 kN). The specimen has a diameter of 6-in. (150-mm), thickness of 2-in. (50-mm) with two 1-in. (25 mm) holes on either side of a 2.46-in. (62.5 mm) notch. The notch is cut into a flattened surface of the circumference.

MnDOT uses a modified version of the ASTM test procedure for the DCT test (Newcomb and Zhou, 2018; Hanson, 2015). The objective of the modifications was to improve the repeatability and practicality of the test. Modifications made to the ASTM test method for temperature conditioning of the specimens are as follow (Hanson, 2015):

- Specimens need to reach the test temperature no sooner than 0.75 hours, but within 1.5 hours.
- Specimens should remain in the conditioning chamber for a minimum of 2 hours before testing.
- All testing should end within 5 hours of initial placement of the sample into conditioning chamber.

Because of the extensive changes to, and familiarity with the DCT procedure, MnDOT performed this testing.

3.3 ASPHALT MIXTURES TESTING PLAN

The IDEAL cracking test has been used to evaluate the cracking resistance of the asphalt mixtures during mix design and QC/QA phases. Before performing the IDEAL cracking test, the MnDOT loose mixtures were reheated, compacted, and tested to produce the test specimens within the desired range of air void content ($7 \pm 0.5\%$). First, the mixtures were tested to measure the theoretical maximum specific gravity (G_{mm}) based on AASHTO T 209. Then, cylindrical samples were compacted and tested to measure the air void content and to determine the bulk specific gravity based on AASHTO T 166. These samples were used to find the required weight and dimensions of the test specimens to be used for the IDEAL cracking test to achieve $7 \pm 0.5\%$ air void content. The experimental plan for conducting the IDEAL cracking tests on the specimens from MnDOT 2018 mixtures is as follows.

3.3.1 Designed Experimental Plan for Application of IDEAL Cracking Test

3.3.1.1 MnDOT 2018 Mixtures

After heating the loose mixture samples from MnDOT to the compaction temperature, the specimens for the IDEAL cracking tests were molded in the gyratory compactor with a target air void content of $7 \pm 0.5\%$. The air void content and G_{mb} of the compacted specimens were measured after the specimens were cooled to ambient temperature. The cracking test was conducted on the specimens after conditioning in an air chamber or water bath for 1 to 2 hours to assure that the specimens reached the testing temperature.

Since the application of the IDEAL cracking test in QC/QA was investigated in this project, the testing was performed as soon as possible after molding and measuring the SSD weights to obtain the air void contents and G_{mb} . Thus, the first series of the IDEAL cracking tests were performed about 3.5 ± 0.5 hours after compaction, as shown in Table 3.4. Different times between molding and testing were used in this project to investigate the effect of the timing on the test results and QC/QA practices. The testing plan for the IDEAL cracking test is presented in Table 3.4. The specimens remained at the room temperature or in a chamber with a temperature of $25\text{ }^{\circ}\text{C}$ ($77\text{ }^{\circ}\text{F}$) during the proposed time between compaction and crack testing.

Table 3.4. Timing matrix for IDEAL cracking test

Testing Time after Compaction	Testing Temperature ($^{\circ}\text{F}$)	No. of Replicates
$3\text{ }1/2 \pm 1/2$ hrs.	77	3 to 4
22 ± 2 hrs.	77	3 to 4
$3 \pm 1/4$ days	77	3 to 4
$14 \pm 1/2$ days	77	3 to 4

3.3.1.2 MnDOT 2019 Mixtures

The IDEAL cracking test was also performed on the mixtures from the MnDOT 2019 construction season. The IDEAL cracking test was conducted on the lab mixed, lab compacted (LMLC) samples and the plant mixed- lab compacted (PMLC) samples. The LMLC mixtures were fabricated with three different binder contents, i.e., optimum binder content (OBC), OBC + 0.5 percent, and OBC - 0.5 percent. The sensitivity of the IDEAL cracking test to binder content could be evaluated through comparing the CT Index for mixtures with binder contents of OBC and OBC \pm 0.5 percent. The results of the CT Index were compared between plant mixed, lab compacted (PMLC) and lab compacted (LMLC) specimens with different binder contents.

3.3.2 Correlation between DCT Test and IDEAL Cracking Test Results

IDEAL and DCT tests were performed on four MnDOT mixtures (Newcomb and Zhou, 2018). The experimental data are shown in Table 3.5. Five replicates were tested for each of the DCT test and IDEAL cracking test for each mixture and asphalt content, as presented in Table 3.5 (Newcomb and Zhou, 2018). A correlation between the DCT test and IDEAL cracking test results was found using these experimental data for four mixtures with different asphalt contents as presented in Figure 3.1.

Table 3.5. IDEAL and DCT tests experimental data (after Newcomb and Zhou, 2018)

Mix No.	CT Index (IDEAL CT)				Fracture Energy (J/m ²) (DCT)			
	AC (%)	Mean	Std. Dev.	COV (%)	AC (%)	Mean	Std. Dev.	COV (%)
1	4.9	53.9	9.28	17	4.9	385.0	38.12	10
	5.4	64.2	8.11	13	5.4	446.0	59.00	13
	5.9	105.0	12.44	12	5.9	511.8	110.94	22
2	4.9	79.4	8.32	10	4.9	545.4	64.91	12
	5.4	115.3	10.83	9	5.4	676.0	164.38	24
	5.9	151.9	13.30	9	5.9	779.2	198.05	25
3	5.3	38.8	2.05	5	5.3	429.8	28.42	7
	5.8	85.3	13.24	16	5.8	518.4	24.86	5
	6.3	105.5	13.53	13	6.3	577.6	21.88	4
4	5.5	76.0	6.47	9	5.5	580.2	75.98	13
	6.0	125.4	17.82	14	6.0	700.0	62.66	9
	6.5	156.3	16.52	11	6.5	664.6	73.41	11

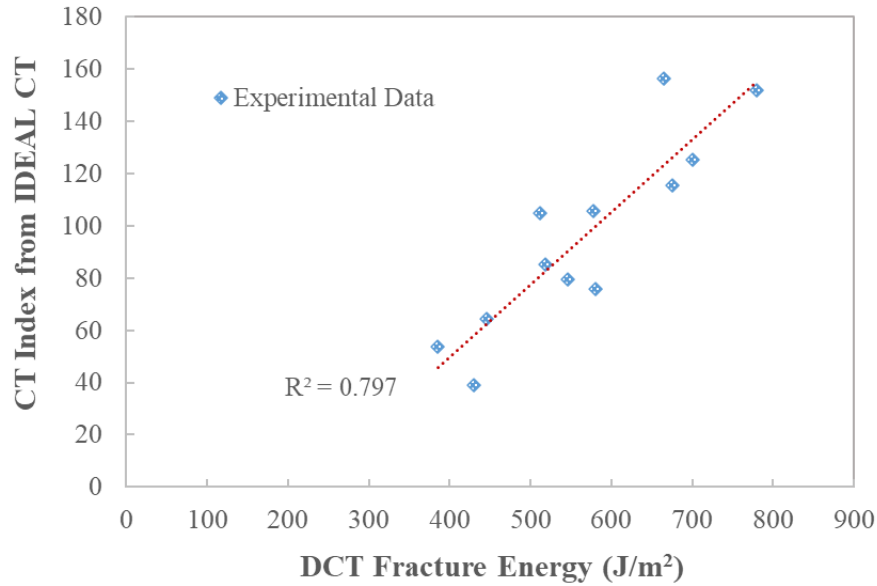


Figure 3.1. Correlation between the DCT and IDEAL cracking test results

The equations which correlate CT Index obtained from IDEAL cracking test and DCT fracture energy in this series of data are as follows:

$$CT\ Index = 0.2762 (G_f) - 60.443 \quad (7)$$

$$CT\ Index = 15.628 e^{(0.0031 G_f)} \quad (8)$$

where G_f is the DCT fracture energy (J/m^2). The CT Index generally increases with increasing the DCT fracture energy as demonstrated in Figure 3.1. The first equation is a linear correlation with an R^2 of 80%, while the second one has an exponential form with an R^2 of 77%. Both equations show an acceptable coefficient of determination.

Furthermore, the experimental data collected from MnROAD and the National Center for Asphalt Technology (NCAT) were used to investigate whether a correlation between the DCT test and IDEAL cracking test results existed. The IDEAL cracking test was conducted on eight Minnesota mixtures at NCAT through the NCAT and MnROAD partnership. The DCT test was performed on the eight mixtures in Minnesota under MnDOT supervision. The tests were performed on plant mixed, lab compacted (PMLC) mixtures, which included two general categories of mixtures: Reheated Plant Mixed, Lab Compacted (RH PMLC) and Critically Aged Plant Mixed, Lab Compacted (CA PMLC) mixtures. The CA PMLC mixtures were subjected to loose mix aging with the mix spread in thin layers for 6 hours at 135°C. The data are presented in Table 3.6.

Table 3.6. IDEAL cracking and DCT tests results from NCAT/MnROAD partnership (Taylor, 2018)

Mix Type	Reheated Plant Produced Mix (RH PMLC)					Critically Aged Plant Produced Mix (CA PMLC)				
Test	IDEAL Cracking Test		DCT Test			IDEAL Cracking Test		DCT Test		
Mix No.	Avg CT Index	COV (%)	Avg Fracture Energy (J/m ²)	COV (%)	No. of Replicates	Avg CT Index	COV (%)	Avg Fracture Energy (J/m ²)	COV (%)	No. of Replicates
C16	29.4	14	455	10.6	15	19.7	7	407	15.6	12
C17	53.2	5	425	14	15	30.3	19	381	10.1	11
C18	52.3	15	419	10.2	13	30.6	28	395	13.4	11
C19	106.6	26	444	14.5	16	39.6	21	413	10.8	10
C20	63.8	11	507	14.3	15	31.6	26	474	14.2	12
C21	28.8	17	573	11.1	16	20.4	19	444	13.8	12
C22	22.4	13	340	9.1	14	7.6	7	301	9.7	11
C23	48.3	27	675	13.8	14	16.3	13	509	13.4	12

No specific correlation was found between the CT Index and DCT fracture energy in this data, as shown in Figure 3.2 and Figure 3.3. One reason for this difference could be that the mixtures used for DCT test and IDEAL cracking test were aged, compacted and tested in different laboratories. Therefore, the mixture properties may have differed in the mixtures tested for the DCT test and IDEAL cracking tests. In addition, different conditions of storing the materials (e.g. temperature, time) in different locations where the DCT test and IDEAL cracking tests were performed might have affected the results. Moreover, the time span between the production and testing might affect the aging and explain different test results in the two laboratories. Currently, the between-laboratory variability for these tests has not been well defined.

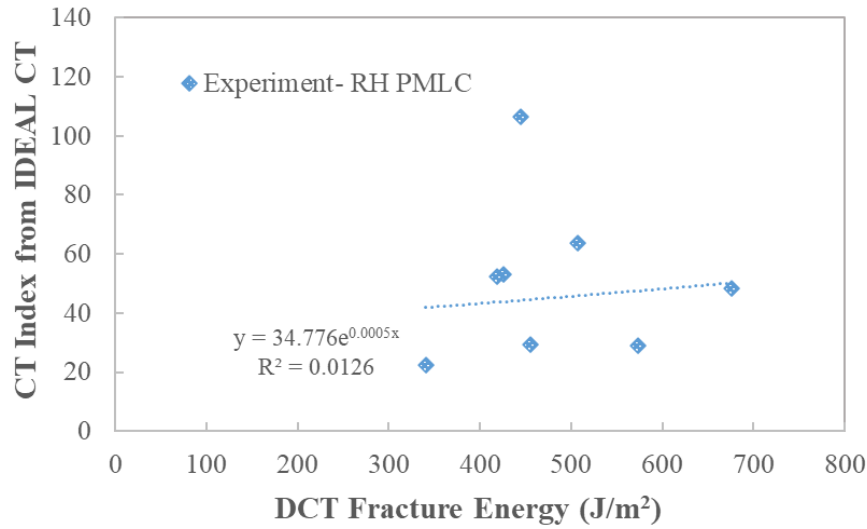


Figure 3.2. DCT test vs. IDEAL cracking test results for RH PMLC mixtures conducted by NCAT/MnROAD

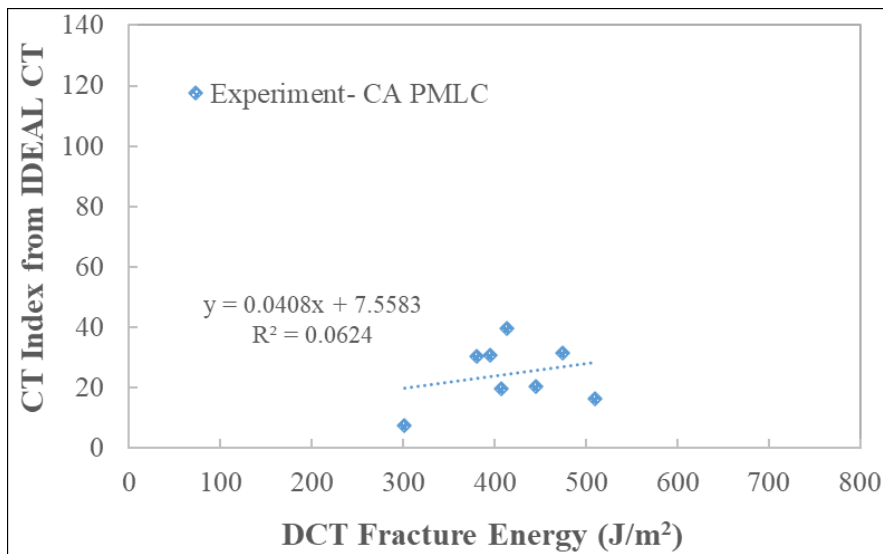


Figure 3.3. DCT test vs. IDEAL cracking test results for CA PMLC mixtures conducted by NCAT/MnROAD

TTI also conducted IDEAL cracking tests on RH PMLC mixtures. Table 3.7 shows the average CT Index results for NCAT/MnROAD 2016 cracking experiment mixtures, conducted by TTI and NCAT. Figure 3.4 shows the average CT Index results for the MnROAD/NCAT partnership 2016 cracking experiment mixtures, and compares the CT index values between the TTI and NCAT/MnROAD results. The fact that all the TTI CT index results are greater than the corresponding NCAT/MnROAD results suggests that the difference between the two data sets is most likely partially systematic.

Table 3.7. IDEAL cracking test results for RH PMLC mixtures conducted by TTI and NCAT/MnROAD

Mix No.	CT index (TTI)	CT index (NCAT)	Difference (%)
16	71.8	29.4	59.1
17	84.6	53.2	37.1
18	65.5	52.3	20.2
19	125.5	106.6	15.1
20	67.0	63.8	4.7
21	78.2	28.8	63.2
22	64.2	22.4	65.1
23	90.4	48.3	46.6

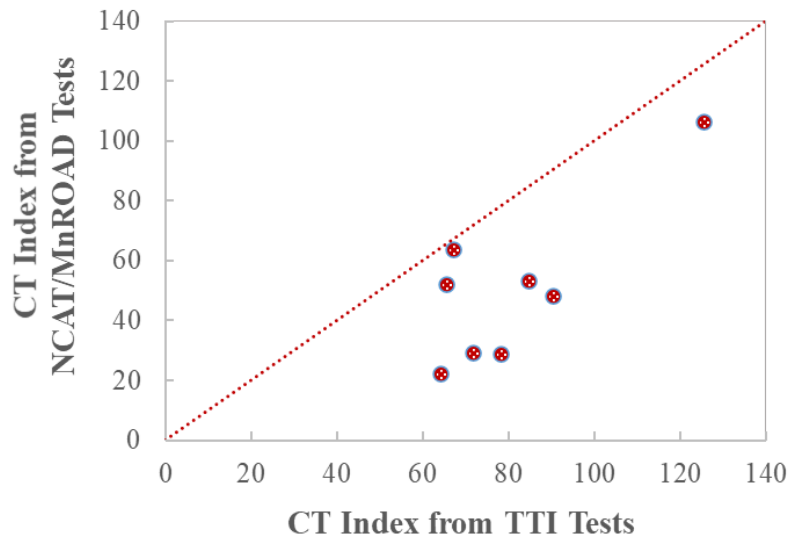


Figure 3.4. Comparison of CT Index from IDEAL cracking tests performed by TTI and NCAT/MnROAD

Additionally, the DCT fracture energies obtained by the NCAT/MnROAD partnership versus CT Index from TTI Ideal cracking tests are plotted in Figure 3.5 for RH PMLC mixtures. No specific correlation was found between the CT index and DCT fracture energy in this data, as shown in Figure 3.5. Likewise, there were different storage conditions for the materials (e.g. temperature, time) in the different laboratories where the DCT and IDEAL cracking tests were performed as well as different aging conditions might have affected the results. These factors along with the possible differences between properties of the mixtures might explain the different test results between the laboratories.

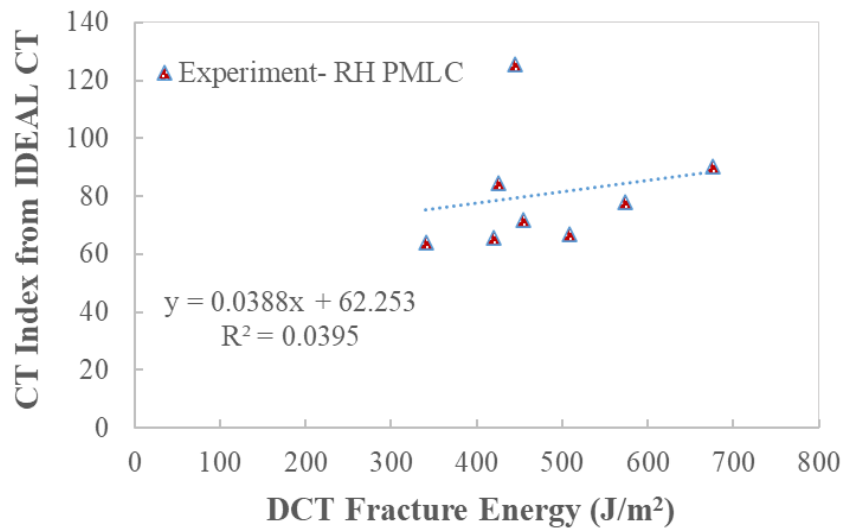


Figure 3.5. Relation between NCAT/MnDOT DCT test results vs. TTI IDEAL cracking test results for RH PMLC mixtures

3.4 ASPHALT BINDERS TESTING PLAN

The asphalt binder experimental plan is presented in this section. The testing plan was performed on all nine projects from 2018 and 2019 construction season, as presented in Table 3.1. The plan included performance grade (PG) tests for the original binder (OB) (unaged binder) and short-term aged binder (rolling thin-film oven (RTFO)) to verify the high temperature binder grade. The BBR tests were conducted on the PAV20 aged binders to obtain the PG low temperatures. The BBR tests were performed to measure the low temperature stiffness (S-value), relaxation (m-value), and the ΔT_c parameter to determine the low temperature binder PG grade and cracking performance parameters. The BBR tests were run at two temperatures to find the low temperatures which satisfy the conditions where the S-value < 300 MPa (maximum stiffness threshold) and the m-value > 0.300 (minimum m threshold). Continuous grading of these binders was also obtained and reported for high and low temperatures.

Furthermore, the tests to determine the Glover-Rowe (G-R) parameter were conducted to gain an understanding of the effect of aging on the binders. The G-R parameter was obtained and calculated for all binders at different aging stages including (OB, RTFO, pressure aging vessel 20 (PAV20), PAV40, and PAV80) using the DSR device. The G-R parameter is used to evaluate the cracking resistance of binders with aging. The PAV process was used to simulate long-term aging of asphalt binder during the pavement life. The PAV samples were used for BBR and DSR testing to obtain the G-R and ΔT_c parameters. The multiple-stress creep recovery (MSCR) tests were also conducted on RTFO-aged binder to determine the non-recoverable creep compliance (J_{nr}) and percent recovery to establish if the required MnDOT specifications were met. The MSCR test is used to evaluate the rutting performance and the behavior of binders and modified binders at high temperatures. Figure 3.6 shows a summary of the asphalt binder testing plan in this study.

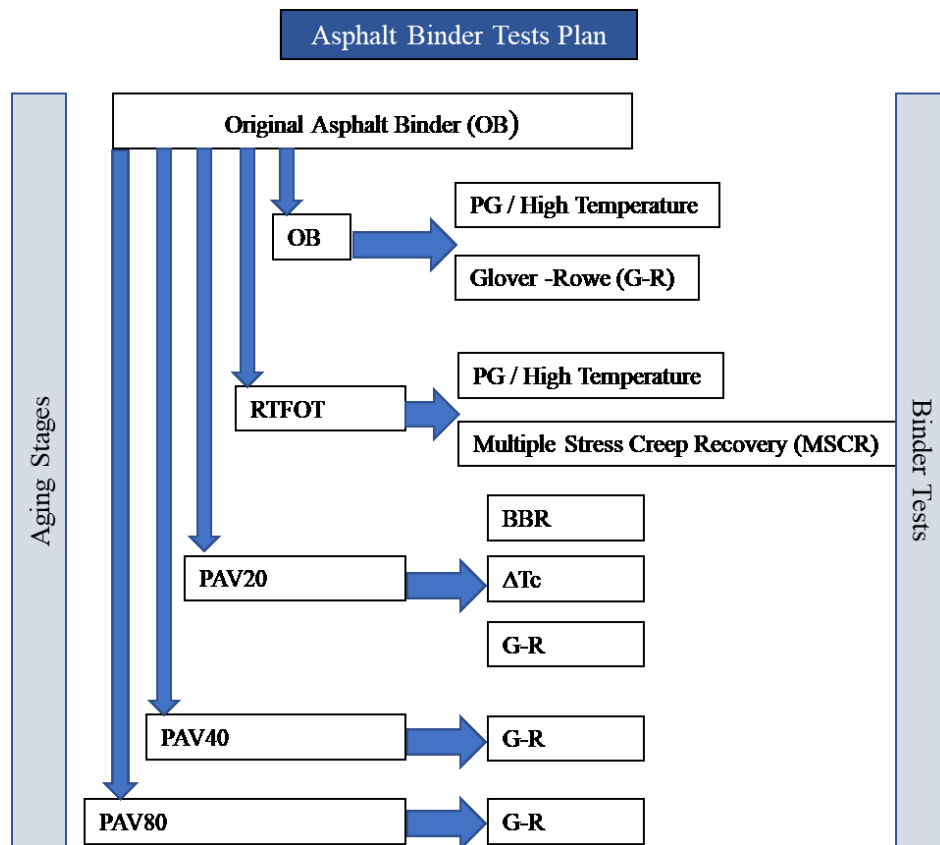


Figure 3.6. Asphalt binder testing plan

CHAPTER 4: RESULTS AND DISCUSSIONS OF ASPHALT BINDERS AND MIXTURES TESTING

4.1 INTRODUCTION

This chapter presents the results of the experimental plan performed on the MnDOT asphalt mixtures and binders from selected construction projects received in 2018 and 2019. The Ideal Cracking Test was conducted on all mixtures received from MnDOT. The CT Index determined from the IDEAL Cracking Test is a composite representation of the fracture energy and post-peak ductility of the material, and a greater CT index value indicates better cracking resistance.

One of the key problems in QC/QA testing is the time between sampling and compacting the material and testing at the plant for QC and testing the sample at a DOT laboratory for QA. Often this time interval results in mixtures changes, especially in volumetric properties, that show significant differences between QC and QA test results. For the 2018 mixtures, an experiment was developed to examine the differences in results between freshly molded samples and samples tested at different time intervals (up to 14 days). For the 2019 mixtures, this research focused on the differences between the IDEAL Cracking Test results of the lab-mixed and plant-mixed materials. The effect of different binder contents was also studied.

4.2 SAMPLE PREPARATION AND TESTING OF MNDOT PROJECT MATERIALS

The IDEAL cracking test was used to evaluate the cracking resistance of the MnDOT asphalt mixtures both in mix design and in QC/QA. After heating the loose mixtures received from MnDOT at the compaction temperature, the specimens for the IDEAL cracking tests were molded in the gyratory compactor with a target air void content of 7 ± 0.5 percent. Then, the bulk specific gravity (G_{mb}) of the compacted specimens was measured after the specimens had been cooled to ambient temperature. The IDEAL cracking test was performed on the specimens having acceptable air void contents after conditioning for 1 to 2 hours at the testing temperature.

4.2.1 Asphalt Mixture Volumetric Properties

The MnDOT mixtures used for the cracking test evaluation in this project are listed in Table 4.1. The 2018 G_{mm} measurements by MnDOT and the TTI research team are shown in in this table and they are very close. Although the 2019 MnDOT results for G_{mm} values were not available it is reasonable to expect that the TTI results also would have been relatively close to those from MnDOT.

Table 4.1. MnDOT and TTI maximum specific gravity (G_{mm}) results

Project ID	Project	MnDOT G_{mm}	TTI G_{mm}
P2	8607-63	2.500	2.488
P3	0304-37	2.471	2.481
P4	1118-21	2.467	2.487
P5-A	6904-46	2.474	2.475
P5-B	6904-46	2.475	2.461
P6	0704-100	2.433	2.463
P7 (TH4)	NA	NA	2.489
P8 9 (TH15)	NA	NA	2.491
P9 (TH 55)	NA	NA	2.525

NA: Not available.

4.3 ASPHALT MIXTURE TESTING RESULTS

4.3.1 MnDOT 2018 Mixtures

In order to be useful as a tool for QC/QA, a test needs to give meaningful and repeatable results for both QC and QA. The usefulness of the IDEAL cracking test was established in an earlier project for MnDOT (Newcomb and Zhou, 2018). However, the question remained regarding the repeatability over time because QC testing is done shortly after the production of the material at the plant by the contractor's testing laboratory, and QA testing is normally done at a DOT laboratory days or even weeks later. The question that needed to be answered was whether the CT index would change significantly over time for intervals up to two weeks after production and compaction.

Since the application of the IDEAL cracking test in QC/QA was being investigated in this project, the testing was performed as soon as practical after molding and measuring the SSD weights. Thus, the first series of the IDEAL cracking tests were performed in 3.5 ± 0.5 hours after compaction as presented in Table 4.2. Groups of samples were then tested for cracking resistance at 22 hours, 3 days, and 14 days after compaction. The testing plan for the IDEAL cracking test conducted on 2018 mixtures is presented in Table 4.2. The specimens remained at a chamber with a temperature of 25 °C (77 °F) during the proposed time periods between compaction and crack testing.

Table 4.2. Timing for performing IDEAL cracking test conducted on MnDOT mixtures received in 2018

Testing Time after Compaction	Testing Temperature (°F)	No. of Replicates
3 1/2 ± 1/2 hrs.	77	3 to 4
22 ± 2 hrs.	77	3 to 4
3 ± 1/4 days	77	3 to 4
14 ± 1/2 days	77	3 to 4

The results of the IDEAL-CT tests conducted at different times after compaction were compared to investigate if the time interval after compaction would have a significant effect on the CT index. The average CT index values are presented in Figure 4.1 to Figure 4.6 for each 2018 project for the different time intervals between compaction and testing. The standard errors are also plotted in these graphs for each mixture and time. As can be seen in the graphs, there are no clear trends with respect to the time interval between compaction and testing. This is a meaningful result as it indicates that QA testing can take place up to two weeks after compaction and still be compared with the QC results so long as care is taken to protect the sample from damage.

The average IDEAL cracking test results at the different testing time intervals in the experimental test plan and coefficient of variation (COV) are presented in Table 4.3 to Table 4.8 for the 2018 MnDOT mixtures. The air void contents of the specimens were within the target air void content of $7 \pm 0.5\%$, as shown in the tables. Achieving this range of air void with this accuracy may be challenging at times. The air void contents may be affected by the change of Superpave gyratory compactors, change of standard molds, and repeated calibration of compactors.

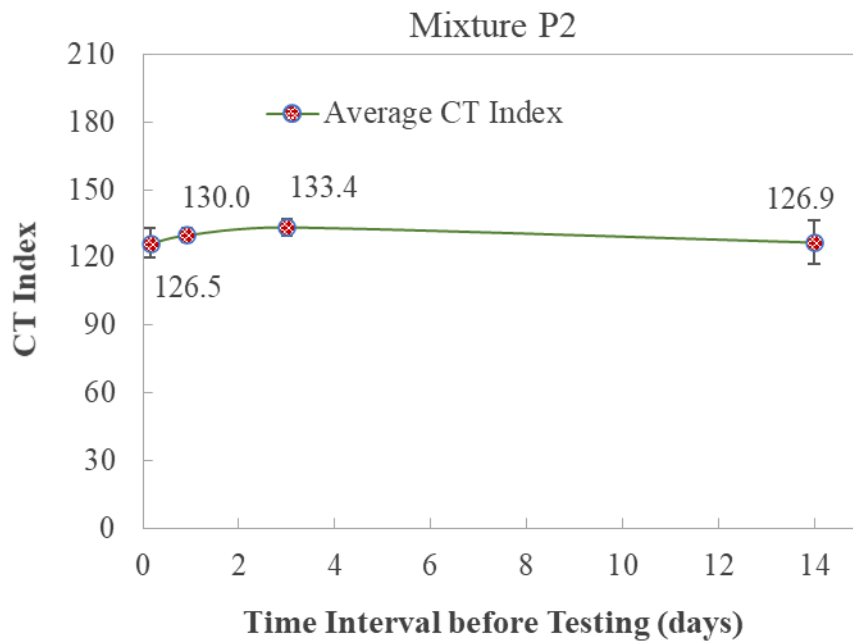


Figure 4.1. Comparison of IDEAL cracking test results at different testing time intervals after compaction for Mixture P2

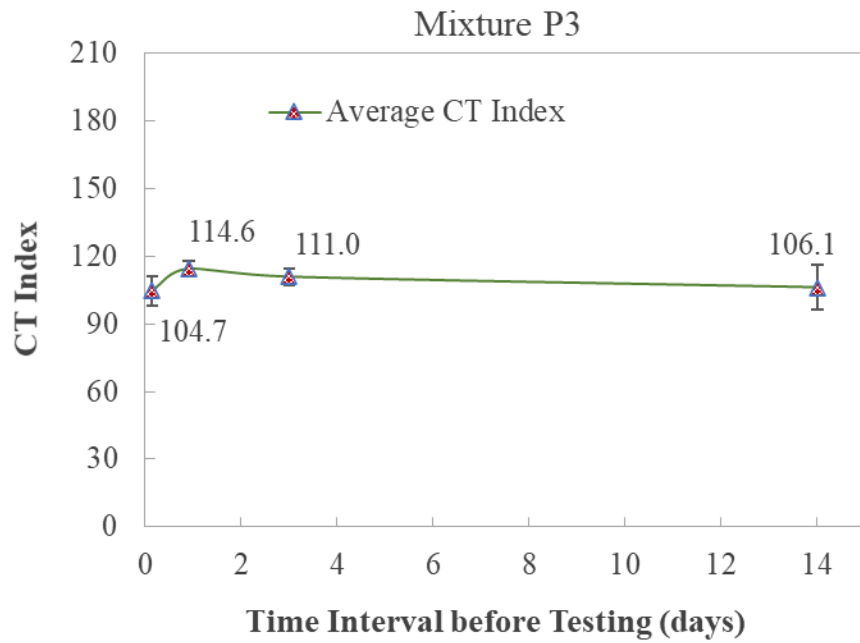


Figure 4.2. Comparison of IDEAL cracking test results at different testing time intervals for Mixture P3

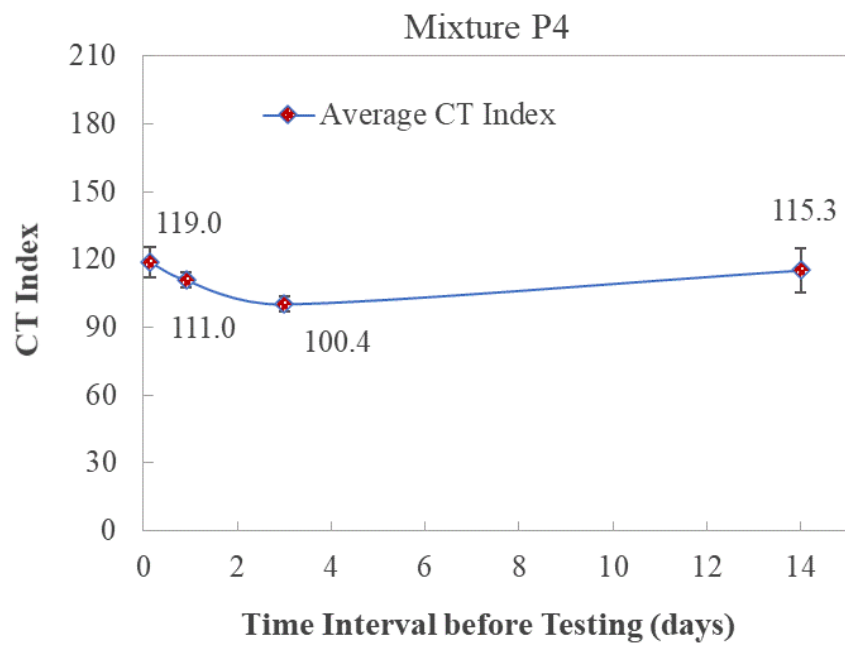


Figure 4.3. Comparison of IDEAL cracking test results at different testing time intervals for Mixture P4

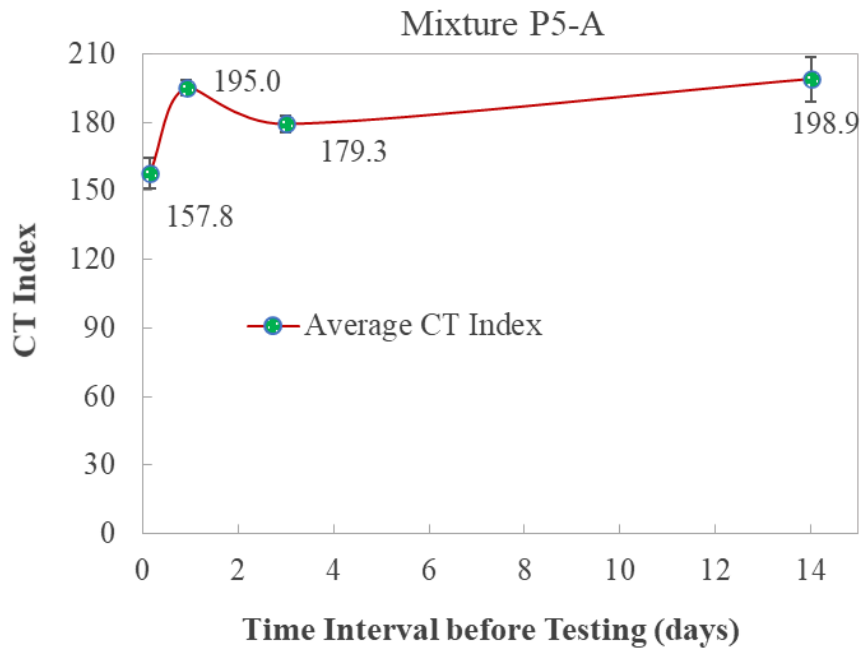


Figure 4.4. Comparison of IDEAL cracking test results at different testing time intervals for Mixture P5-A

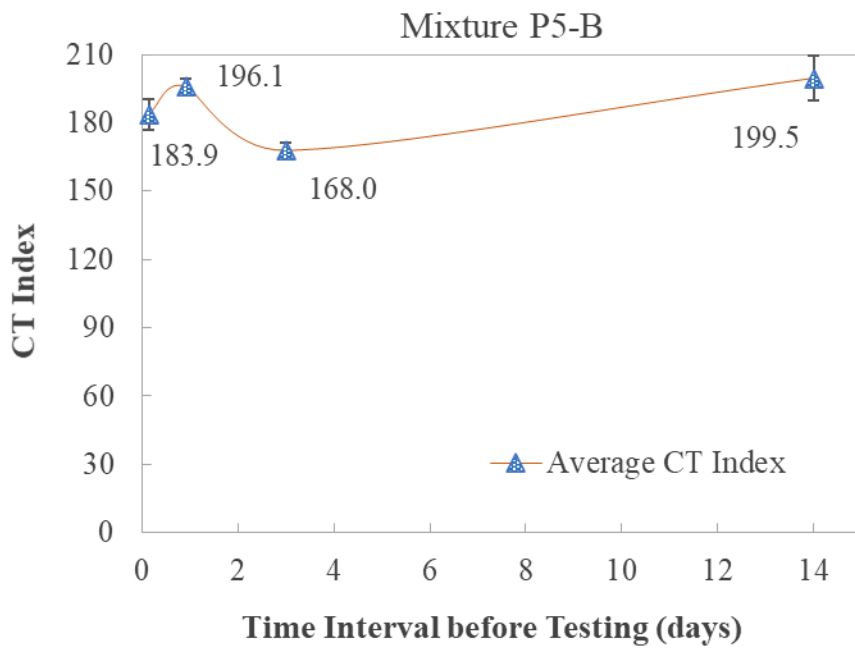


Figure 4.5. Comparison of IDEAL cracking test results at different testing time intervals for Mixture P5-B

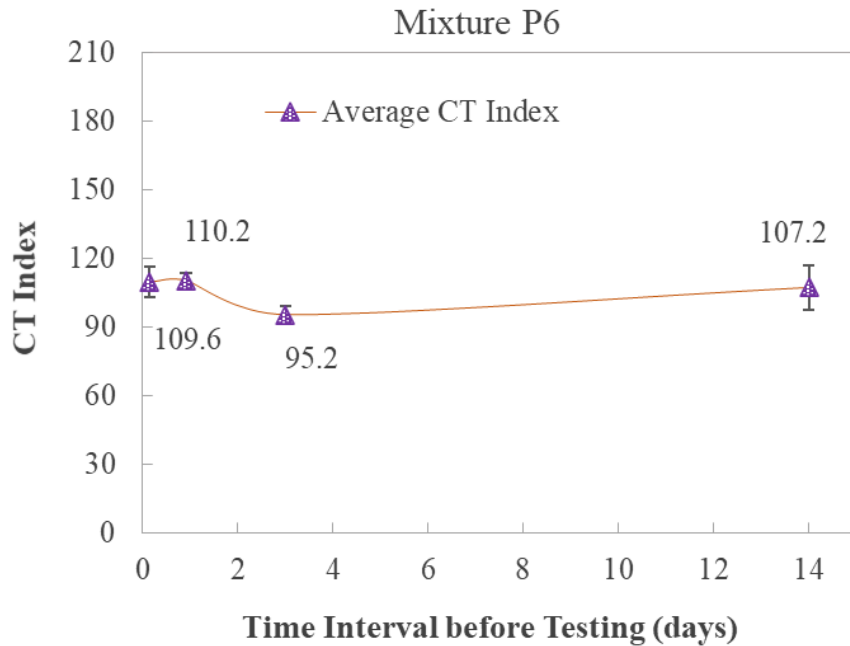


Figure 4.6. Comparison of IDEAL cracking test results at different times for Mixture P6

Table 4.3. IDEAL cracking test results for 2019 Mixtures P2 in Project 8607-63

Testing Time after Compaction	No. of Replicates	Avg. Air Void Content (%)	Avg. CT Index	St. Dev. CT Index	COV. CT Index (%)
3 1/2 hrs.	4	7.1	126.5	13.5	10.7
22 hrs.	4	7.1	130.0	6.7	5.1
3 days	4	6.8	133.4	7.2	5.4
14 days	4	6.8	126.9	19.6	15.5

Table 4.4. IDEAL cracking test results for Mixture P3 in Project 0304-37

Testing Time after Compaction	No. of Replicates	Avg. Air Void Content (%)	Avg. CT Index	St. Dev. CT Index	COV. CT Index (%)
3 1/2 hrs.	4	6.7	104.7	9.6	9.2
22 hrs.	4	7.1	114.6	23.2	20.3
3 days	4	6.7	111.0	8.3	7.5
14 days	4	6.6	106.1	5.3	5.0

Table 4.5. IDEAL cracking test results for Mixture P4 in Project 1118-21

Testing Time after Compaction	No. of Replicates	Avg. Air Void Content (%)	Avg. CT Index	St. Dev. CT Index	COV. CT Index (%)
3 1/2 hrs.	4	6.8	119.0	14.6	12.2
22 hrs.	4	7.0	111.0	10.5	9.5
3 days	4	6.8	100.4	11.6	11.6
14 days	4	6.8	115.3	5.9	5.1

Table 4.6. IDEAL cracking test results for Mixture P5-A in Project 6904-46

Testing Time after Compaction	No. of Replicates	Avg. Air Void Content (%)	Avg. CT Index	St. Dev. CT Index	COV. CT Index (%)
3 1/2 hrs.	4	6.9	157.8	8.3	5.3
22 hrs.	4	7.2	195.0	8.4	4.3
3 days	5	6.9	179.3	21.6	12.1
14 days	4	6.9	175.9	9.7	4.8

Table 4.7. IDEAL cracking test results for Mixture P5-B in Project 6904-46

Testing Time after Compaction	No. of Replicates	Avg. Air Void Content (%)	Avg. CT Index	St. Dev. CT Index	COV. CT Index (%)
3 1/2 hrs.	4	6.5	183.9	31.4	17.1
22 hrs.	4	6.8	196.1	37.6	19.2
3 days	4	6.8	168.0	17.6	10.5
14 days	6	7.0	199.5	16.5	8.3

Table 4.8. IDEAL cracking test results for Mixture P6 in Project 0704-100

Testing Time after Compaction	No. of Replicates	Avg. Air Void Content (%)	Avg. CT Index	St. Dev. CT Index	COV. CT Index (%)
3 1/2 hrs.	3	7.2	109.6	23.3	21.3
22 hrs.	4	7.3	110.2	5.6	5.1
3 days	5	7.1	95.2	4.7	4.9
14 days	4	7.2	107.2	9.8	9.2

The mean CT Indices of all the tests conducted at the different times after molding for the different 2018 MnDOT projects are presented and compared, as shown in Figure 4.7. The mean CT Index of all the tests conducted for these projects at 22 ± 2 hours after compaction is presented and compared, as shown in Figure 4.8. The standard errors for the test results are also plotted in these figures.

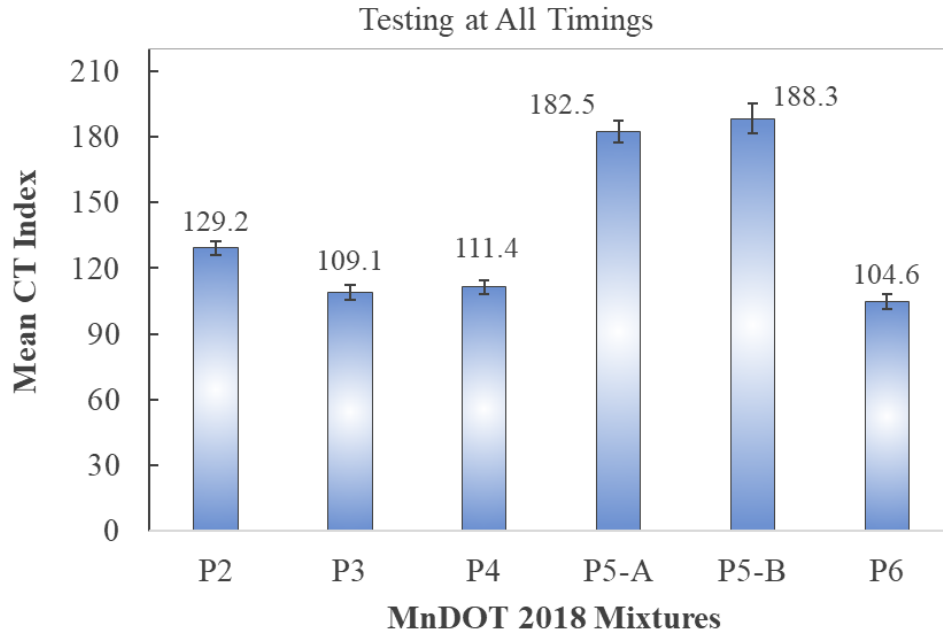


Figure 4.7. Mean CT Index from IDEAL cracking test conducted at different time intervals from compaction for the 2018 MnDOT mixtures

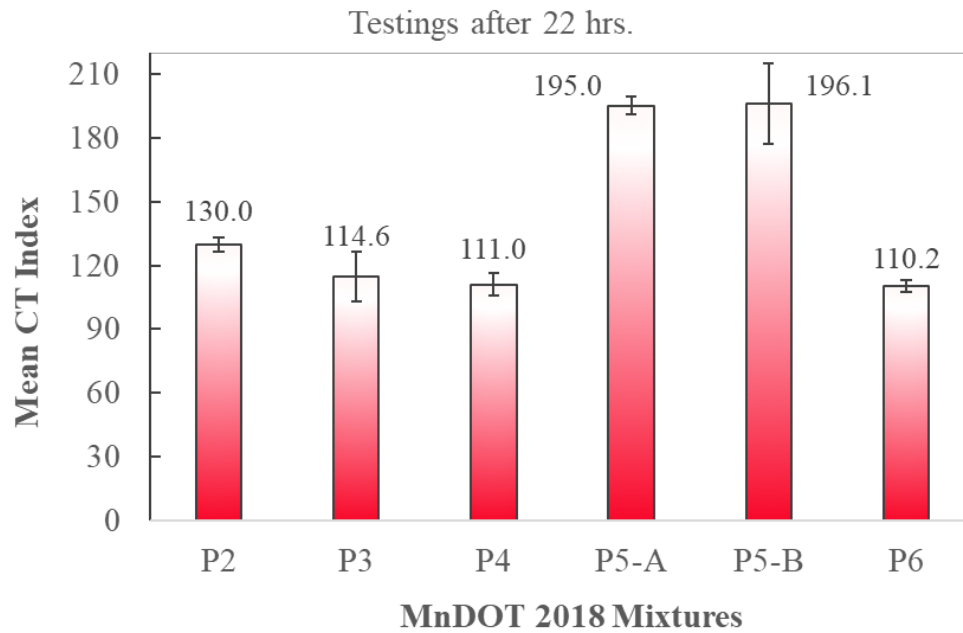


Figure 4.8. Mean CT Index from IDEAL cracking test conducted at 22 hours after molding for the 2018 MnDOT mixtures

The highest CT Index in 2018 were for mixtures P5-B (SPWEB340C) and P5-A (SPWEA340C). After the mixtures from project P5, the ranking of CT Index from the high to low was P2 (SPWEA440C), P4 (SPWEA340C), P3 (SPWEB340C), and P6 (SPWEB440C), respectively. All the CT Index results from the 2018 mixtures were higher than the threshold of 80 recommended by Zhou et al. (2017) for all mixtures.

The COV of the CT Index results was calculated to evaluate the variability of the test results. The COVs of the CT Index results for the MnDOT 2018 mixtures for the different testing times after compaction are shown in Figure 4.9. The COV was below 12.5 percent for approximately 80 percent of the tests and was as low as 4 percent and as high as 22 percent.

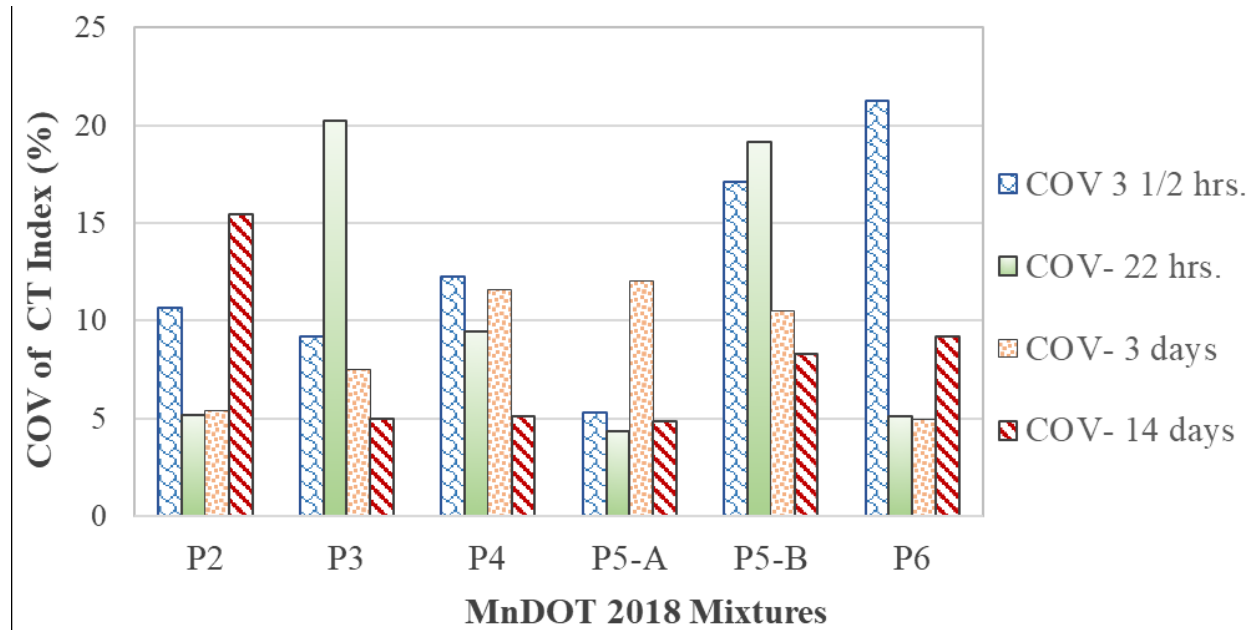


Figure 4.9. COV of CT Index results for the MnDOT 2018 mixtures at different timings

The sensitivity of the IDEAL Cracking Test to the asphalt binder contents was also evaluated for MnDOT 2018 mixtures. The CT Index determined from the testing 22 hrs. after compaction has been plotted versus the asphalt binder content of each of these mixtures in Figure 4.10. Generally, The CT Index increases with higher amounts of asphalt in the mixtures, as demonstrated in this figure. Mixtures P5-B and P5-A which showed the highest CT Index had the highest asphalt binder contents.

Moreover, the MnDOT team performed some DCT tests on the 2018 mixtures. The results of DCT test fracture energy is presented in Table 4.9. The DCT Fracture Energy was plotted versus the CT Index from IDEAL cracking, as demonstrated in Figure 4.11, to see if a correlation between these parameters exists. The DCT test was conducted by the MnDOT team, while the IDEAL cracking test was performed by the TTI team. The CT Index determined from the testing after 22 hrs. of compaction, and the average of CT Index of the results from all time intervals were used in these graphs. The R-squared was low for these data points. This may be due to the fact that these two tests were performed at two different laboratories. This can cause differences in volumetric properties, storage conditions, storage time, and aging conditions. The air void contents of the samples might have been different as well.

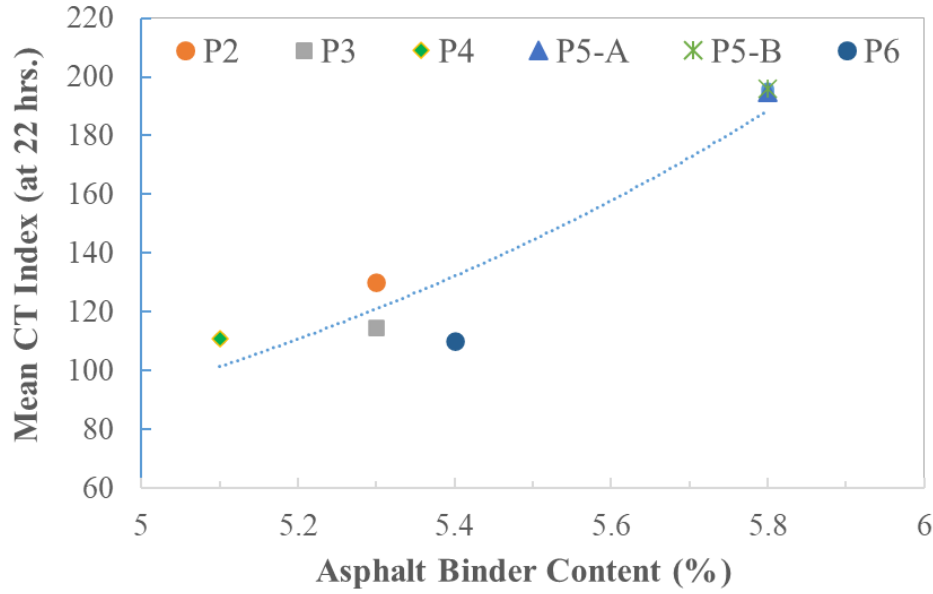


Figure 4.10. Asphalt binder content vs. CT Index for 2018 mixtures

Table 4.9. Results of DCT test and IDEAL cracking test for 2018 mixtures

Mixture	DCT Fracture Energy (J/m ²) (by MnDOT)	CT Index (IDEAL CT) (by TTI)	
		After 22 hrs.	Average of All Times
P2	601.1	130.0	129.2
P3	366.4	114.6	109.1
P4	474.2	111.0	111.4
P5-A	559.0	195.0	182.5
P5-B	536.8	196.1	188.3
P6	553.7	110.2	104.5
P7	442.4	179.9	
P8	504.4	86.6	
P9	449.1	147.4	

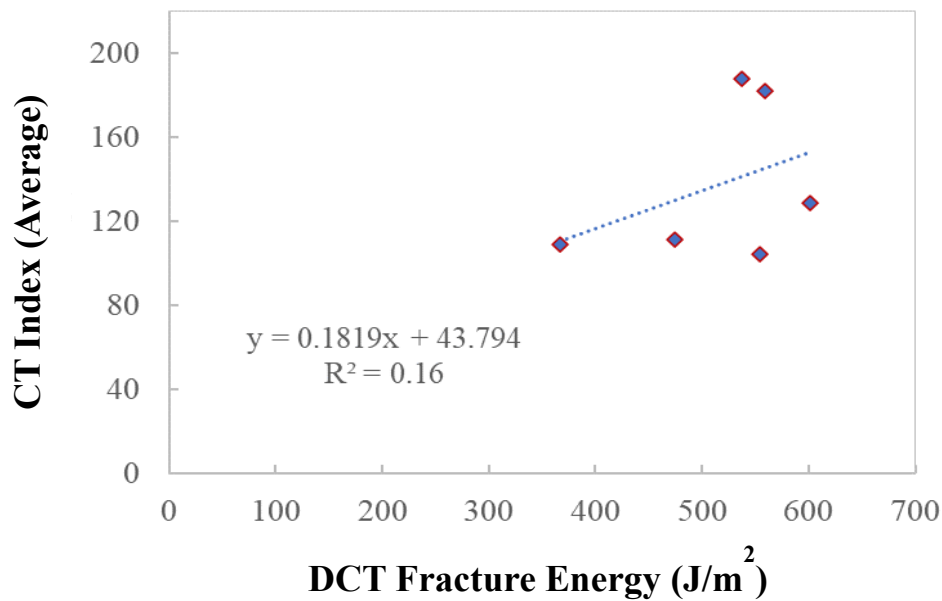


Figure 4.11. DCT fracture energy vs. CT Index from IDEAL cracking test

4.3.1.1 Statistical Analysis of CT Index Results

A One-way Analysis of Variance (ANOVA) test, F-tests, Welch’s Test, and Tukey HSD tests were performed on the CT Index results of the mixtures from 2018 construction season. These analyses were performed to investigate if the CT index at different times from compaction were different and if the variance of the CT Index obtained different time intervals were equal.

The one-way ANOVA indicated that the mean of the CT Index at four different testing conditions was not different for mixtures P2, P3, P4, P5-B, and P6. The statistical analysis (F-tests) indicated that the variance of the CT Index at four different testing conditions was not different for mixtures P2, P3, P4, P5-A, and P5-B. The Tukey HSD test also indicated that the mean of the CT Index at four different testing conditions was not different for mixtures P2, P3, P4, P5-B, and P6. In general, the effect of the time interval was consistent across the mixtures.

The statistical analysis (F-tests) indicated that the variance of the CT Index at four different testing conditions was not equal for mixture P6. Based on the statistical test (Welch’s test) results, the mean of the CT Index at the four different testing times was not different for mixture P6, assuming the variance of the CT Index at four different testing conditions was not equal. Again, the statistical analysis showed that, for the most part, the time interval had no statistically significant effect on the CT index.

The ANOVA test indicated that the mean of the CT Index at four different testing conditions was different for mixture P5-A. The statistical analysis (F-tests) suggested that the variance of the CT Index at four different testing conditions was equal for mixture P5-A. The Tukey HSD test indicated that the mean of the CT Index at four different testing conditions was different for mixture P5-A. The CT Index

obtained at 3 ½ hours after sample fabrication was different from the others, except for the 3-day testing. Again, the results were, for the most part, consistent.

4.3.2 MnDOT 2019 Mixtures

The results of the IDEAL cracking tests performed on the mixtures from the MnDOT 2019 construction season are presented in Figure 4.12. The IDEAL cracking test was conducted on the lab mixed, lab compacted samples (LMLC) and the plant mixed, lab compacted (PMLC) samples. The LMLC mixtures were fabricated with three different binder contents, i.e., optimum binder content (OBC), OBC + 0.5 percent, and OBC - 0.5 percent. The sensitivity of the IDEAL cracking test to binder content is very evident in comparing the CT Index for mixtures with OBC and OBC ± 0.5 percent. The COV of PMLC specimens were 14 percent, 16 percent, and 13 percent for TH4, TH15, and TH55 mixtures, respectively. The range of COV was between 3 and 22 percent for LMLC mixtures which compares well with the 2018 mixtures. The average of the CT Index and the COV for these mixtures are presented in Table 4.10.

The CT Index for all the 2019 mixtures were higher than the threshold of 80 suggested by Zhou et al. (2017), except for the TH 15 (P8) and TH 55 (P9) lab compacted mixtures with binder content 0.5 percent less than OBC. This demonstrates the effect of binder content on the cracking resistance and how the IDEAL cracking test captured it. In the 2018 mixtures, it distinguished between mixtures with higher asphalt content with different ranges of the CT Index. In the 2019 mixtures, it distinguished between different binder contents of the same mixture.

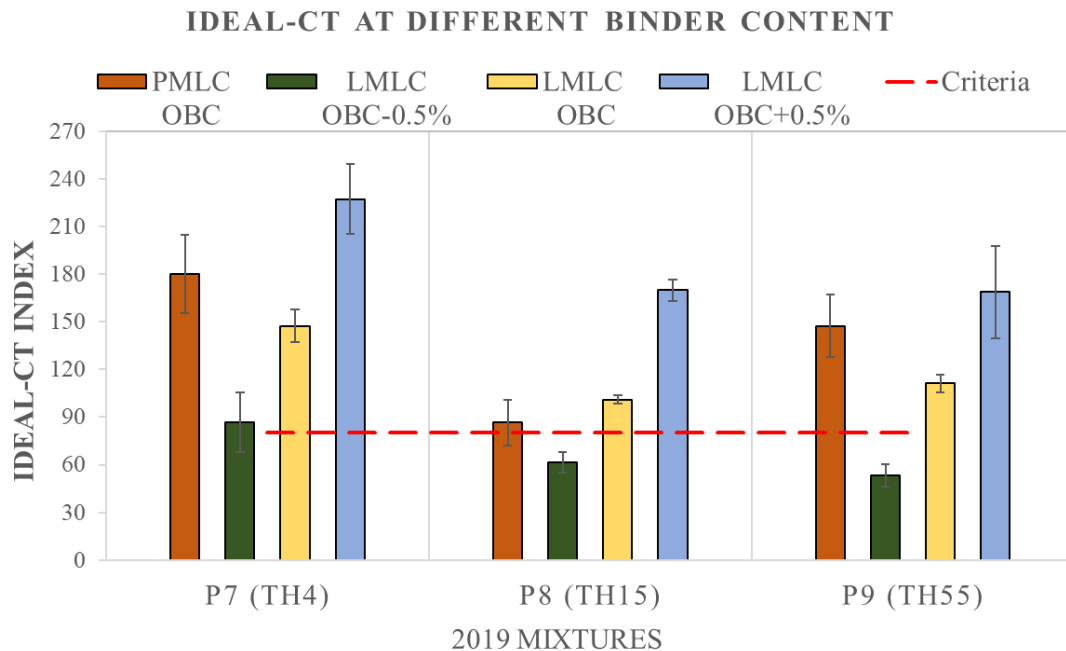


Figure 4.12. IDEAL cracking test results for 2019 mixtures with different binder contents

Table 4.10. Results of IDEAL cracking on 2019 projects

Mixture	Binder Content	Asphalt Content (%)	Average CT Index	St. Dev.	COV, %
P7 (TH4)	OB-0.5%	4.8	86.7	18.79	22
	OB	5.3	147.4	10.33	7
	OB + 0.5%	5.8	227.3	21.98	10
P8 (TH15)	OB- 0.5%	4.8	61.3	6.50	11
	OB	5.3	100.9	2.71	3
	OB+ 0.5%	5.8	170.0	6.78	4
P9 (TH55)	OB- 0.5%	4.8	53.3	6.93	13
	OB%	5.3	111.1	5.64	5
	OB+0.5%	5.8	168.8	29.09	17

4.4 ASPHALT BINDER TESTING RESULTS

Asphalt binders oxidize with time becoming increasingly stiff and brittle. They become more susceptible to fracture at cold temperatures as they age, which leads to thermal cracking, the primary mode of failure for asphalt pavements constructed in colder climates. Low temperature behavior, aging, and the elasticity of binder are important to the field performance of pavements.

The binder testing plan was performed according to the binder testing plan on six pilot projects from the MnDOT 2018 construction season and three 2019 projects. The plan included PG testing for unaged or original binder (OB) and short-term aged binder, conditioned in a RTFO, to verify the high temperature grade of the binders. The BBR test was used to measure the low temperature stiffness (S-value) and low temperature relaxation (m-value). The difference between the critical temperatures for the S-value and m-value (ΔT_c) was used to identify the low temperature behavior of the binders. The Glover-Rowe (G-R) parameter was used to investigate the change of physical properties of asphalt binders with aging. The G-R parameter was calculated for different aging stages including OB, RTFO, PAV20, PAV40, and PAV80 to study the potential of rate of crack initiation. In addition, the multiple-stress creep recovery (MSCR) test was performed on RTFO short-term aged binder to determine the non-recoverable creep compliance (J_{nr}) and percent recovery.

4.4.1 Bending Beam Rheometer

Two replicates for each project were prepared and tested at -24°C (10°C warmer than low-temperature grade of the asphalt binder PG XX-34) and -30°C . The stiffness and the m-value were determined according to AASHTO M 320. All asphalt binders failed when they were tested at -30°C and passed at -24°C . Thus, all the binders met the requirements of PG XX-34. Table 4.11 shows the BBR test results of MnDOT asphalt binders from the 2018 and 2019 projects. Figure 4.13 shows the continuous PG grading at low temperature for PAV20 aged binders.

Table 4.11. BBR test results of MnDOT asphalt binder from 2018 and 2019 projects

Project	Aging	Test Temp.	m-value	S value (MPa)	Results
P1	PAV 20	-30	0.243	572	Failed
		-24	0.303	280	Passed
P2	PAV 20	-30	0.258	455	Failed
		-24	0.341	259	Passed
P3	PAV 20	-30	0.260	513	Failed
		-24	0.300	219	Passed
P4	PAV 20	-30	0.276	462	Failed
		-24	0.327	245	Passed
P5	PAV 20	-30	0.255	549	Failed
		-24	0.313	258	Passed
P6	PAV 20	-30	0.263	508	Failed
		-24	0.329	250	Passed
P7 (TH4)	PAV 20	-30	0.264	456	Failed
		-24	0.325	209	Passed
P8 (TH15)	PAV 20	-30	0.279	434	Failed
		-24	0.340	205	Passed
P9 (TH55)	PAV 20	-30	0.273	515	Failed
		-24	0.324	233	Passed

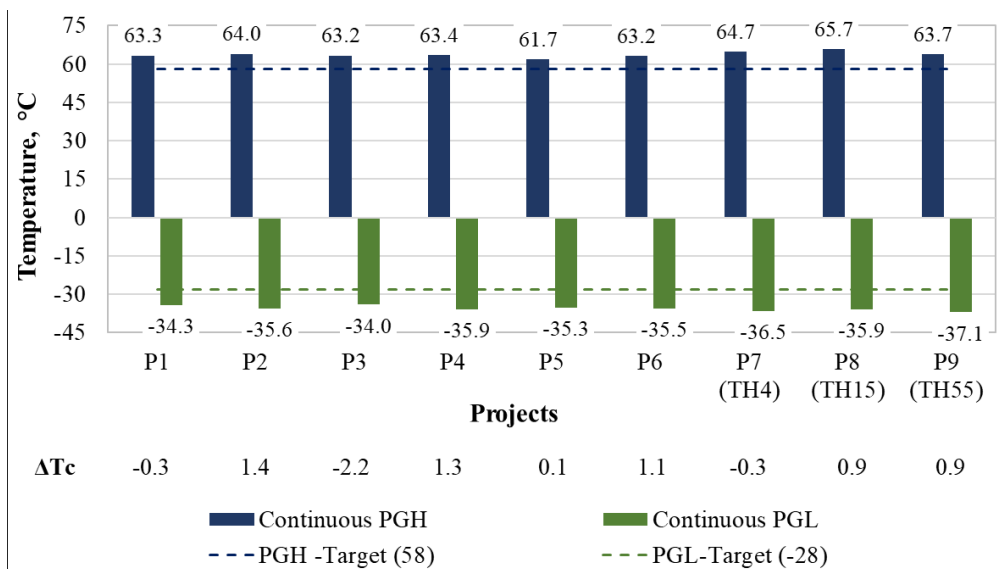


Figure 4.13. High temperature and low temperature PG grading results for binders of 2018 and 2019 projects

The relaxation (m-value) measured by BBR testing may deteriorate significantly with aging at a faster rate than the stiffness (S-value). Since ΔT_c is the difference in the critical temperatures for stiffness and relaxation, it can provide a metric for the potential loss of relaxation at cold temperatures (Reinke,

2018). When ΔT_c becomes more negative, cracking is more likely to occur at low temperature. Although there are currently no standards, if the ΔT_c value of a binder falls below -5 degrees it is generally considered to be prone to low temperature cracking.

Using the BBR test results presented in Table 4.12, the ΔT_c values were calculated and presented in Table 4.13. along with the continuous grading results for these binders. Binders from P2, P4, P5, P6, TH 15 (P8), and TH 55 (P9) projects showed positive values of ΔT_c . Binders from P1 and TH 4 (P7) have slightly negative values of -0.3, while the binder from P3 has a value of -2.2 degrees. Figure 4.13 presents the ΔT_c values as well as the continuous grading results for all the asphalt binders tested in this study. All binders from the 2018 and 2019 projects seem to have good to very good resistance to cold temperature cracking as measured by ΔT_c .

Table 4.12. Continuous PG low grading and the ΔT_c of the tested binders

Construction Season	Project ID	Continuous PG High Temperature (°C)	Continuous PG Low Temperature (°C)	ΔT_c (°C)
2018	P1	63.3	-34.3	-0.3
	P2	64.0	-35.6	1.4
	P3	63.2	-34.0	-2.2
	P4	63.4	-35.9	1.3
	P5	61.7	-35.3	0.1
	P6	63.2	-35.5	1.1
2019	P7 (TH4)	64.7	-36.5	-0.3
	P8 (TH 15)	65.7	-35.9	0.9
	P9 (TH 55)	63.7	-37.1	0.9

Table 4.13. PG high temperature testing results for original binders using DSR

Project	Aging	Sample	T (°C)	G*/ Sin(δ) (kPa)	PG High Temp.	Avg. PG High Temp
P1	OB	A	64	0.97	63.7	63.3
			58	1.73		
		B	64	0.88	62.8	
			58	1.52		
P2	OB	A	64	1.00	64.0	64.0
			58	0.57		
		B	64	0.99	63.9	
			58	1.77		
P3	OB	A	64	0.98	63.9	64.2
			58	1.73		
		B	64	1.03	64.5	
			58	0.60		
P4	OB	A	64	1.74	63.4	63.4
			58	0.92		
		B	64	1.74	63.4	
			58	0.92		
P5	OB	A	64	1.43	61.7	61.7
			58	0.73		
		B	64	1.44	61.7	
			58	0.73		
P6	OB	A	64	1.63	63.2	63.2
			58	0.90		
		B	64	1.67	63.2	
			58	0.90		
P7 (TH4)	OB	A	64	1.08	64.9	64.7
			58	0.60		
		B	64	1.03	64.4	
			58	0.58		
P8 (TH15)	OB	A	64	1.15	65.7	65.7
			58	0.63		
		B	64	1.14	65.6	
			58	0.64		
P9 (Th55)	OB	A	64	1.80	63.8	63.7
			58	0.97		
		B	64	1.79	63.7	
			58	0.96		

4.4.2 High Temperature Performance Grade (PG)

Two replicates were prepared for each aging condition for each binder from each project to determine the PG high temperature of OB and RTFO aged binders. Some asphalt binders were classified as 58H-34 modified binder from different sources. One of the asphalt binders was a 58-34 unmodified binder, and one was 58V-34. The samples were tested according to AASHTO T 315 using Dynamic Shear Rheometer (DSR).

presents the PG grading testing results at high temperature for Original Binders. Table 4.14 presents the results of PG testing at high temperature for RTFO aged binders.

Table 4.14. PG high temperature testing results for RTFO aged binders using DSR

Project	Aging	Sample	T (°C)	G*/Sin(δ) (kPa)	PG High Temp.	Avg. PG High Temp.
P1	RTFO	A	64	2.06	63.5	63.7
			58	3.82		
		B	58	4.18	64.0	
			64	2.18		
P2	RTFO	A	64	2.53	65.7	65.8
			70	1.38		
		B	64	2.55	65.8	
			70	1.39		
P3	RTFO	A	64	2.01	63.3	63.2
			58	3.63		
		B	64	1.99	63.2	
			58	3.59		
P4	RTFO	A	64	2.33	64.7	64.8
			70	1.28		
		B	64	2.37	65.0	
			70	1.31		
P5	RTFO	A	58	4.02	63.5	63.5
			64	2.05		
		B	58	3.92	63.4	
			64	2.00		
P6	RTFO	A	64	2.54	65.8	65.5
			70	1.40		
		B	64	2.43	65.3	
			70	1.34		

Project	Aging	Sample	T (°C)	G*/Sin(δ) (kPa)	PG High Temp.	Avg. PG High Temp.
P7 (TH4)	RTFO	1	64	3.54	68.8	69.1
			70	1.95		
		2	64	3.72	69.4	
			70	2.07		
P8 (TH15)	RTFO	1	70	2.40	70.9	70.9
			76	1.38		
		2	70	2.40	70.9	
			76	1.38		
P9 (TH55)	RTFO	1	64	3.31	68.6	68.3
			70	1.87		
		2	64	3.25	68.0	
			70	1.81		

4.4.3 Glover-Rowe Parameter

The Glover-Rowe (G-R) parameter is becoming widely recognized as an indicator of long-term cracking performance. The G-R parameter can be studied on a Black Space diagram (Figure 4.14), which represents the log G* versus phase angle, determined by the DSR testing. The quality of different binders can be compared, and the effect of aging on the binder performance in terms of cracking resistance can be evaluated. Soft binders and those that have a high ductility will tend to be at the lower right side of the diagram. As binders start to lose ductility with aging and become more brittle (poor cracking resistance), the phase angle decreases and G* increases. This aging extends the binder location on the diagram from the lower right to the upper left side until it reaches the transition zone (cracking damage zone). Once it passes through the transition zone, it crosses into the block cracking zone. Thus, it is a way to tie binder hardening to performance.

Results of the DSR testing to obtain the G-R parameter at 15 °C and 0.005 rad/sec are presented on the black space diagram for all pilot project asphalt binders in Figure 4.14. Transition zone curves have been plotted on the diagram using the Glover-Rowe equation with limits of 180 kPa (damage onset) and 600 kPa (visible cracking). Original binder, RTFO, PAV20, PAV40, and PAV80 aged binders were tested with two to three replicates for each condition. Table 4.15 presents all the results of frequency sweep test for all the projects to determine the G-R parameter.

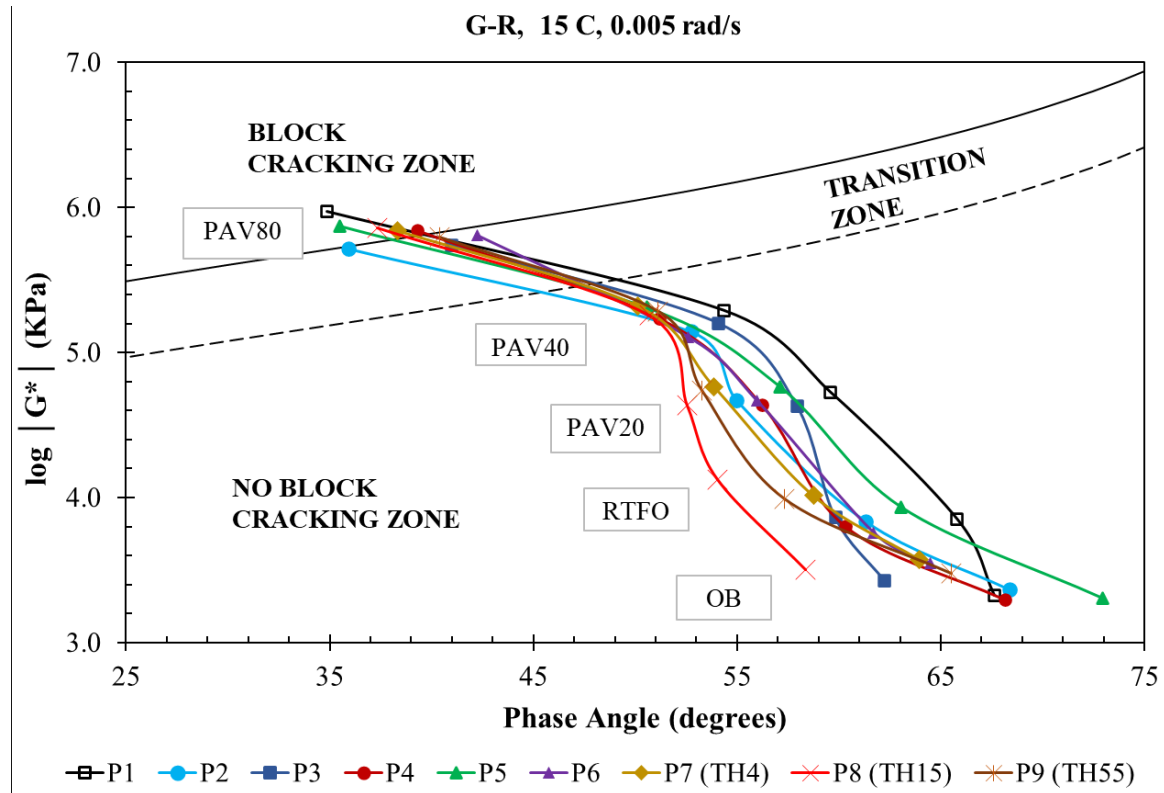


Figure 4.14. Black space diagram and the Glover-Rowe parameter testing results

Table 4.15. Frequency sweep test results for G-R parameter conducted at 15 C and 0.005 rad/s

Sample Year	Blends	Aging	G* (kPa)	δ	G-R (kPa)	Log G*
2018	P1	OB	2.12	67.63	0.33	3.3
		RTFO	7.11	65.80	1.31	3.9
		PAV 20	53.47	59.57	15.91	4.7
		PAV 40	195.15	54.35	81.61	5.3
		PAV 80	937.18	34.85	1104.80	6.0
	P2	OB	2.29	68.39	0.33	3.4
		RTFO	6.77	61.34	1.77	3.8
		PAV20	46.66	54.99	18.76	4.7
		PAV40	138.30	52.79	63.51	5.1
		PAV 80	519.81	35.97	579.81	5.7
	P3	OB	2.68	62.25	0.66	3.4
		RTFO	7.31	59.83	2.14	3.9
		PAV 20	42.82	57.95	14.23	4.6
		PAV 40	159.67	54.08	67.86	5.2
		PAV 80	546.70	40.99	475.00	5.7
	P4	OB	1.98	68.17	0.30	3.3
		RTFOT	6.32	60.32	1.78	3.8
		PAV 20	43.04	56.23	16.00	4.6
		PAV 40	170.73	51.19	86.09	5.2
		PAV 80	687.91	39.30	650.38	5.8
	P5	OB	2.03	72.96	0.18	3.3
		RTFO	8.64	63.05	1.99	3.9
		PAV 20	58.13	57.12	20.40	4.8
		PAV 40	204.85	50.56	107.08	5.3
		PAV 80	746.68	35.48	853.06	5.9
	P6	OB	3.52	64.46	0.72	3.5
		RTFO	5.71	61.71	1.46	3.8
		PAV 20	46.40	55.99	17.52	4.7
		PAV 40	127.96	52.62	59.37	5.1
		PAV 80	645.31	42.25	525.88	5.8

Sample Year	Blends	Aging	G* (kPa)	δ	G-R (kPa)	Log G*
2019	P7 (TH4)	OB	3.75	63.94	0.80	3.6
		RTFO	10.30	58.75	3.25	4.0
		PAV 20	58.08	53.87	25.00	4.8
		PAV 40	209.43	50.12	112.56	5.3
		PAV 80	690.59	38.34	688.71	5.8
	P8 (TH15)	OB	3.17	58.38	1.03	3.5
		RTFO	13.34	54.05	5.75	4.1
		PAV 20	43.35	52.56	20.18	4.6
		PAV 40	180.85	50.69	93.81	5.3
		PAV 80	726.14	37.36	757.65	5.9
	P9 (TH55)	OB	3.75	63.94	0.80	3.6
		RTFO	10.30	58.75	3.25	4.0
		PAV 20	58.08	53.87	25.00	4.8
		PAV 40	209.43	50.12	112.56	5.3
		PAV 80	690.59	38.34	688.71	5.8

The average of two or three values have been used and plotted in the diagram. As expected, all OB asphalt binders are located at the lower right side of the diagram. The G* and the G-R parameter increase with aging level, while the phase angle decreases. All the asphalt binders fall within the no block cracking zone for aging levels up to PAV40. Comparatively speaking, this indicates good behavior for all the project binders. At PAV80, all the binders except three cross into the block cracking zone. Binders from projects P2, P3, and P6 remained in the transition zone after 80 hrs. of conditioning in the PAV.

4.4.4 Multiple Stress Creep Recovery (MSCR) Test

The Multiple Stress Creep Recovery (MSCR) test is a supplement to the Superpave PG asphalt binder high temperature specification. AASHTO TP70 and AASHTO MP19 provide the protocol and specification for the MSCR test. This test can assist with the evaluation of the permanent deformation susceptibility due to the correlation between the MSCR value and rutting of asphalt pavements. Furthermore, the MSCR test provides information about the effectiveness of polymers for improving binder cracking resistance and durability. The MSCR test can replace other tests used to indicate the polymer modification of asphalt binders, such as elastic recovery and force ductility.

The MSCR test can be performed using the DSR device using a creep and recovery concept to determine the percentage of recoverable and non-recoverable creep compliance (J_{nr}) at the 3.2 kPa stress level. The MSCR percent recovery can be used to identify how a polymer performs in the binder and J_{nr} can assist in evaluating the rutting resistance. This test is performed on RTFO aged binder samples at high temperatures. It includes ten cycles per stress level with a one-second loading and a nine-second rest

period, at shear stress levels of 0.1 kPa and 3.2 kPa. Figure 4.15 shows the MSCR cycles and the calculation of the J_{nr} value.

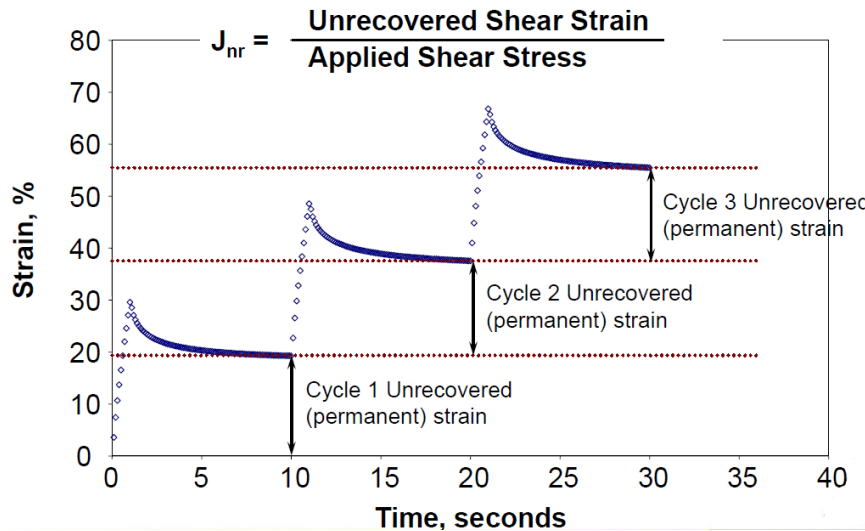


Figure 4.15. MSCR cycle and determination of the J_{nr} value

In this study, the MSCR test was performed on samples of asphalt binders from the 2018 and 2019 projects to determine the J_{nr} value and percentage of elastic recovery at 3.2 kPa. Results of the MSCR test performed at 58°C are presented in Table 4.16 and Figure 4.16 for all the projects. A minimum 30 percent recovery and a maximum J_{nr} value of 2.00 (1/kPa) are required for the 58H-34 binder according to the MnDOT implementation of the multi-stress creep asphalt binder specification. These requirements were met for the 58H-34 binders tested in this study. Moreover, the minimum 55 percent recovery and maximum J_{nr} value of 1.00 (1/kPa) required for the 58V-34 binder (P8, TH 15) were also met. Although the PG 58-34 (P5) binder appears to be marginal in Figure 4.16, it passes the requirements for that grade. Figure 4.16 shows that all the binders, except P5, all fall in the region of high elasticity, indicating that they should perform well in rutting resistance at high temperatures.

Table 4.16. MSCR test results conducted at 58°C

Construction Season	Project ID	Binder	%Rec @ 3.2 kPa	J _{nr} @ 3.2 kPa (kPa ⁻¹)
2018	P1	58H-34	49	0.889
	P2	58H-34	48.3	0.748
	P3	58H-34	65.3	0.607
	P4	58H-34	43.1	0.886
	P5	58-34	25.2	1.459
	P6	58H-34	47	0.806
2019	P7 (TH 4)	58H-34	51.7	0.553
	P8 (TH 15)	58V-34	72.6	
	P9 (TH 55)	58H-34	60.4	0.445

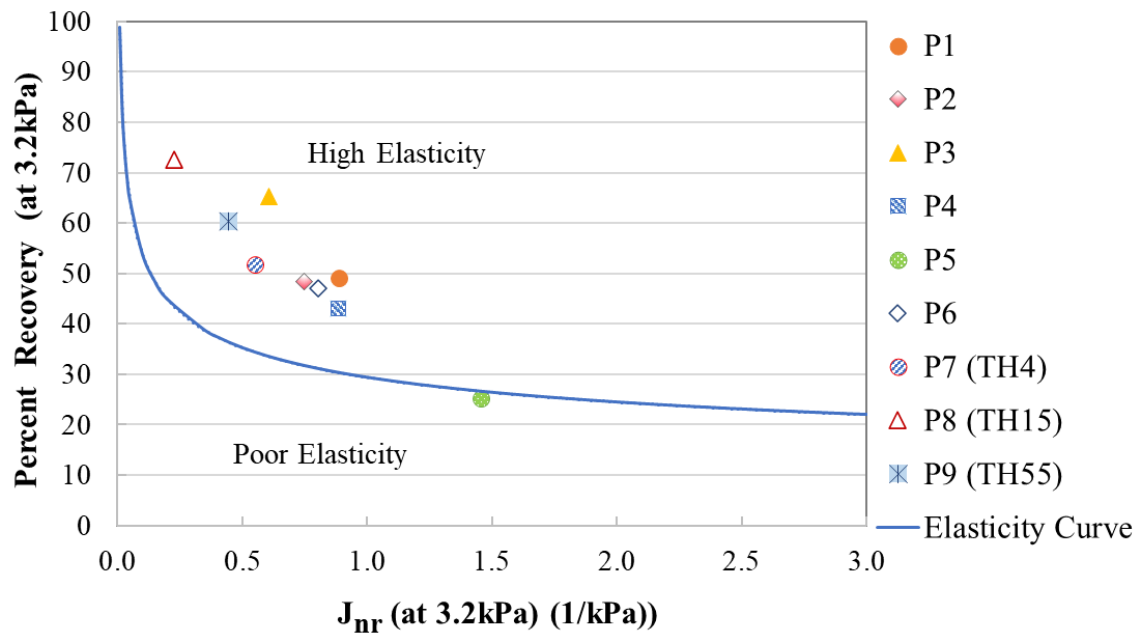


Figure 4.16. MSCR elastic recovery curve and asphalt binder test results

CHAPTER 5: RESEARCH BENEFITS AND IMPLEMENTATION

5.1 BACKGROUND

The current approach to asphalt mixture design uses only minimal performance testing in determination of the best combination of ingredients. The implementation of cracking tests will help ensure the quality and resistance to low-temperature or reflection cracking. This will lessen the number of premature failures in asphalt pavements, resulting in longer service lives.

Considering the vital role of the pavement network in the nation's economy and its social benefits such as access to schools and services and general mobility (Van Dam et al., 2015; FHWA Website), there is an opportunity to improve the sustainability of the pavement infrastructure. Generally, improved pavement performance in terms of cracking resistance results in higher degrees of sustainability encompassing positive economic, environmental and social effects (including safety). Enhanced performance of pavements leads to lower-cost maintenance and rehabilitation (M&R), lower number and length of work zones, higher levels of roadway safety, fewer adverse environmental effects, and lower consumption of materials and resources.

The implementation of cracking performance tests could ultimately reduce the amount of funding required for rehabilitation and/or reconstruction and help maintain pavements in acceptable condition. The consequences of implementation will be: 1) lower life cycle costs, 2) savings in material costs, 3) lower user costs, 4) greater safety due to fewer work zones, and 5) an overall reduction in pollution.

This project was intended to refine of asphalt binder and mixture tests capable of addressing low temperature and reflection cracking in Minnesota asphalt pavements. By implementation of defined cracking criteria, refined or improved test methods, proposed frequency of testing in the laboratory and QC/QA, it could promote and bring about more sustainable pavements. Some examples of the impact of improvements in the quality of paving materials and pavement cracking performance on sustainability with regard to the three aspects previously mentioned are (Van Dam et al., 2015; FHWA Website):

- Economic: Construction, maintenance, and rehabilitation costs; vehicle operating costs; and crash costs.
- Environmental component: Energy consumption, Greenhouse Gas (GHG) emissions, air quality, and noise.
- Social component: Safety (fatalities, injuries, property damage), smoothness, access, mobility, vehicle operating costs, and GHG emissions; aesthetics.

5.2 ECONOMIC ASPECTS

This research can benefit taxpayers with reduced construction expenditures required for rehabilitation projects. Asphalt pavements are subject to deterioration due to factors such as climate and environmental conditions, traffic loading, and aging. Adequate planning in design and construction, and preservation of the infrastructure contribute to make the pavement system perform efficiently against

adverse conditions, and thus avoid or delay the costs of future maintenance and rehabilitation (M&R) (Peshkin et al., 2011; Arabali et al., 2017). If these practices are carried out on a system-wide basis, they can lead to a more sustainable pavement network. Enhancing the resistance of asphalt materials to cracking improves pavement performance and delays major and minor rehabilitation (Geiger, 2005; Peshkin et al., 2011) and/or reconstruction, as shown in Figure 5.1. Therefore, greater cracking resistance of paving materials brings about a significant cost savings for the public over the life cycle, and a more sustainable pavement network.

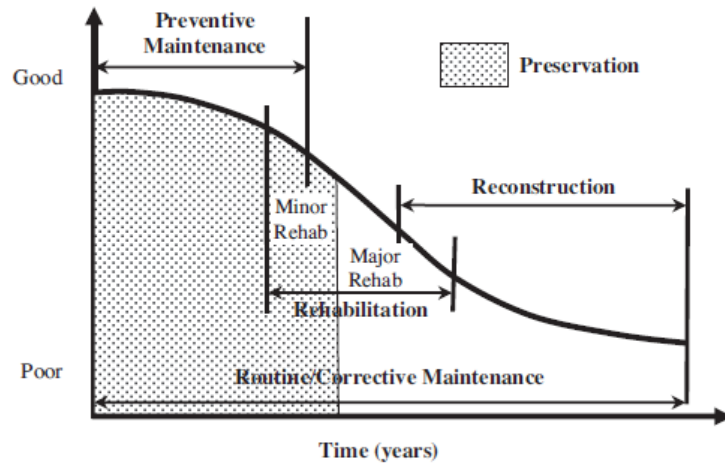


Figure 5.1. Pavement performance curve and different M&R treatments (Peshkin et al., 2011)

Life-Cycle Cost Analysis (LCCA) (Walls and Smith, 1998) is a tool for measuring the economic aspect of sustainability. LCCA can be used to evaluate and quantify the long-term economic efficiency of materials selection and timing of M&R treatments over the pavement life cycle. Since one outcome of this project is to promote higher quality of asphalt materials with enhanced resistance to cracking, the LCCA should show lower net present values (NPV) for construction projects using an improved cracking test procedure in materials specifications and design compared to the current, purely volumetric methods. Implementation of any approach leading to enhanced service life and increased timing between M&R treatments, as intended in this project, reduces agency costs and user costs. Therefore, it saves financial resources for other public activities and interests. User costs include a combination of vehicle operating, crash and delay costs, and include work zone user costs (Walls and Smith, 1998). A benefit-to-cost-ratio analysis and equivalent annual cost along with LCCA are the methods for evaluating the cost-effectiveness of different materials selection, design and M&R strategies (Peshkin et al., 2011; Arabali et al., 2017).

5.3 ENVIRONMENTAL ASPECTS

Any improvement in the pavement service life and the use of better performing materials reduces the need for excess materials production as it delays and decreases the M&R and reconstruction. Enhanced pavement cracking performance has environmental benefits, since it saves resources and materials and lessens the need for raw materials production, e.g., asphalt binders and aggregates, and production of

asphalt mixtures. Materials production affects sustainability factors such as air quality, water quality, ecosystem health, human health and safety, and depletion of non-renewable resources (Van Dam et al., 2015; FHWA Website). Furthermore, the lower levels of M&R activities result in fewer work zones and less traffic congestion. Thus, the air pollution from vehicle emissions caused by the traffic congestion in the construction zones diminish (Zhang et al., 2018).

Asphalt binders and mixtures have various impacts on the environment. The production of different types of asphalt binders (asphalt cement, cutbacks, emulsions) from the crude source to refinement processes and transport has adverse environmental effects, such as energy consumption, GHG emission, and air pollution. The procedures for production of and inclusion of polymers, rubber, emulsifying agents, solvents, and other binder modifying agents also alter the impacts. They generally increase the environmental effects per unit mass in the material production phase of the life cycle (FHWA 2015). The type of asphalt mixture, e.g., HMA, WMA, dense graded, or open graded, and the type of placement, either placed with a paver or as a surface treatment, also influence the environmental impacts. Additionally, the type and amount of recycled materials, whether RAP, RAS or any other material, may beneficially influence the environmental impacts. One significant factor is how changes in the mixtures influence the pavement performance, since a reduction in pavement performance may nullify the environmental benefits (FHWA 2015).

Paving materials with greater cracking resistance will reduce usage of petroleum resources. Sustainability is considered in the asphalt mixture design which includes the specifications for materials that meet the performance thresholds of the individual layers as well as the whole pavement system (Van Dam et al., 2015; FHWA Website).

5.4 SOCIAL ASPECTS

It is important to find effective solutions to enhance roadway safety to decrease crashes and save lives (Tighe et al., 2000). Traffic accidents, injuries, and fatalities are primary issues for transportation agencies and the public, which come with considerable property damage and economic losses (Noyce et al., 2007; Tighe et al., 2000). They also disrupt the traffic flow, and waste time in the delivery of services or goods. Researchers have indicated that pavement condition could significantly affect the crash frequencies (Al-Masaeid, 1997, Tighe et al., 2000). For example, roads with defects such as potholes and severe cracking might increase the probability of multiple-vehicle accidents on rural roads (Al-Masaeid, 1997, Tighe et al., 2000).

Work zones are hazardous roadway environments in terms of the number of public and worker fatalities (Khattak et al., 2002; Behm, 2005). The number of fatalities in work zones is more than 1,100 each year (Bureau of Labor Statistics, 2004; Mitropoulos et al., 2005; Behm, 2005). A longer duration of work zones significantly increased both injury and non-injury crash rates (Khattak et al. 2002).

One of the outcomes of this project would be diminished exposures of the public to work zones and, thus, a decreased frequency of work zone crashes. This improvement in roadway safety could be achieved through enhancing pavement performance. This may be done by improving asphalt mixture

resistance to cracking. This will reduce the frequency of M&R, and consequently lessen the number and length of required work zones. It could provide improved ride quality and reduced risk to workers and road users over time.

CHAPTER 6: ECONOMIC POTENTIAL OF CRACKING PERFORMANCE TESTS

6.1 LIFE CYCLE COST ANALYSIS

A life cycle cost analysis (LCCA) was conducted in order to investigate the possible economic effects of the application of cracking performance tests. Different scenarios with and without the application of cracking tests in mixture design and QC/QA have been considered. The life cycle cost analysis was performed for an analysis period of 40 years. Pavements with 6 in. HMA thickness and 12 in. HMA thickness for a typical trunk highway and a perpetual pavement, respectively, were considered as different scenarios. Thus, four different scenarios were considered in the economic analysis in terms of the LCCA and the corresponding Present Worth Value (PWV). An overall 2-year increase between overlay treatments seemed reasonably conservative to account for improved cracking performance due to the application of cracking tests during mixture design and construction. Thus, for the 6-in. HMA scenarios, the overlay interval was increased from 12 to 14 years, and for the 12-in. HMA scenarios the overlay interval was increased from 14 to 16 years. The description of each scenario is provided below:

- **Scenario 1:** 6 in. pavement without application of the cracking tests, with 2 in. mill and overlay at 12 and 24 years, and remove and replace 6 in. HMA at 36 years.
- **Scenario 2:** 6 in. pavement with application of the cracking tests, with 2 in. mill and overlay at 14 and 28 years, and remove and replace 6 in. HMA at 42 years.
- **Scenario 3:** 12 in. pavement without application of the cracking tests, with a 2 in. mill and overlay at year 14, year 28, and year 42.
- **Scenario 4:** For the 12 in. pavement with application of the cracking tests, with a 2 in. mill and fill at year 16, year 32, and year 48.

The parameters used in the LCCA are presented in Table 6.1. Historically, the discount rate has been assumed to be between three and four percent. The current long-term rate is about two percent which would favor more expensive, longer lasting solutions such as perpetual pavements. For this study, a discount rate of three percent was assumed. Moreover, the statistical analysis results on the data provided by the MnDOT technical advisory panel for the HMA awarded prices and annual HMA quantities used in the LCCA are presented in Table 6.2. Three different prices were used in the LCCA, the 25% quartile, the average, and the 75% quartile for each scenario. Furthermore, the average value and the 75% quartile of annual HMA quantities were used in this analysis.

Table 6.1. Parameter used in the life cycle cost analysis

Interest Rate	4.0 %
Inflation Rate	1.0 %
Discount Rate	3 %
Analysis Period (Year)	40

Table 6.2. Statistical analysis of the HMA quantity and price on the provided data

Statistical Analysis Data	HMA Awarded Price (by Tons)	HMA Annual Quantity (Tons)
Average	\$60.67	17,535.6
Standard Deviation	\$15.08	17,713.5
25% Quartile	\$49.16	5,498.0
Median	\$59.18	13,251.8
75% Quartile	\$68.81	28,756.7

6.2 POTENTIAL PROJECT LEVEL SAVINGS

The results of the LCCA and the PWV of the different scenarios are given and compared in Figure 6.1 and Figure 6.2. Figure 6.1 presented the PWV of the scenario using the average annual HMA quantity, and Figure 6.2 shows the PWV of the scenario using the 75% quartile annual HMA quantity.

The results of the LCCA indicate that the application of cracking performance tests may decrease the agency costs and the PWV for both pavements with 6 in and 12 in. of HMA, as shown in these figures. Scenario 2 shows that with the application of the cracking tests there is a lower PWV than in Scenario 1 without the cracking tests for the 6-in pavement. Scenario 4 with application of the cracking tests showed a lower PWV than Scenario 3 without application of the cracking tests in the 12 in pavement. The difference in estimated costs with and without the application of the cracking tests and the effect of cracking tests is more pronounced for the 6 in. pavement configuration compared to the 12 in. pavement, and the LCCA has a greater relative difference in the long-term agency costs for 6 the in.

pavement design. This is logical, since the 12 in. pavement, being in the category of perpetual pavements, has higher initial cracking resistance due to a greater structural capacity.

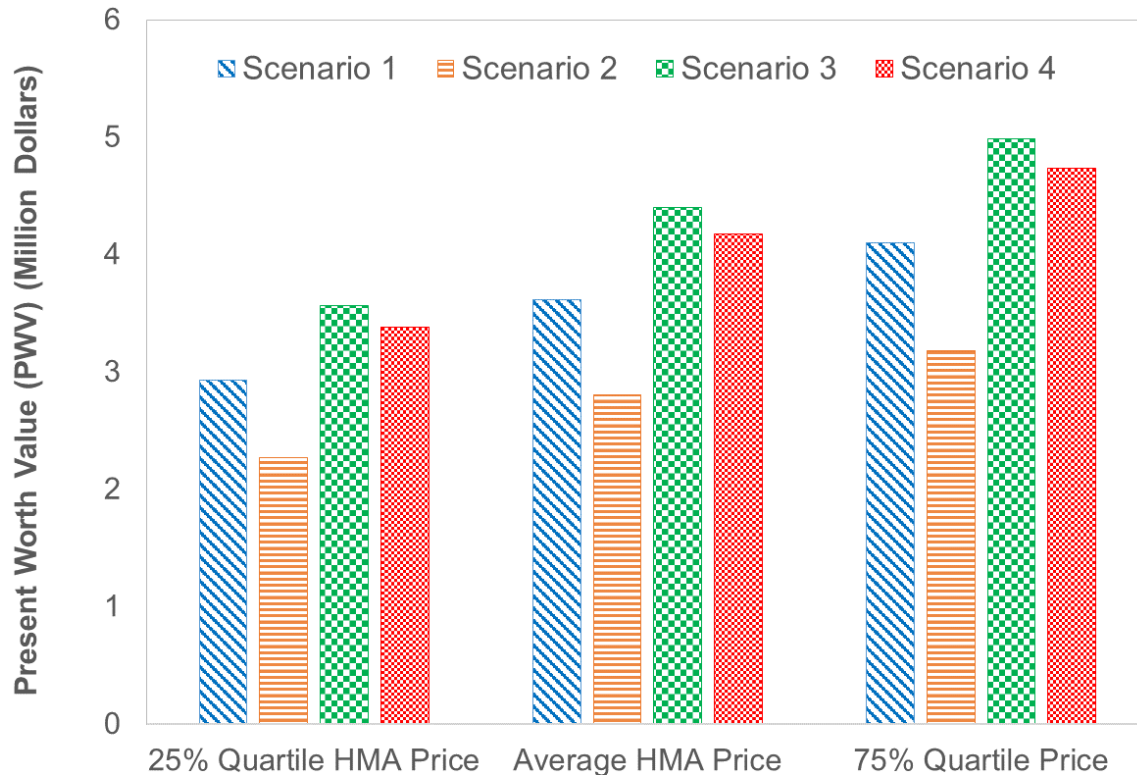


Figure 6.1. Life cycle cost analysis results and present worth value for different scenarios using the average annual HMA quantity on a project level basis.

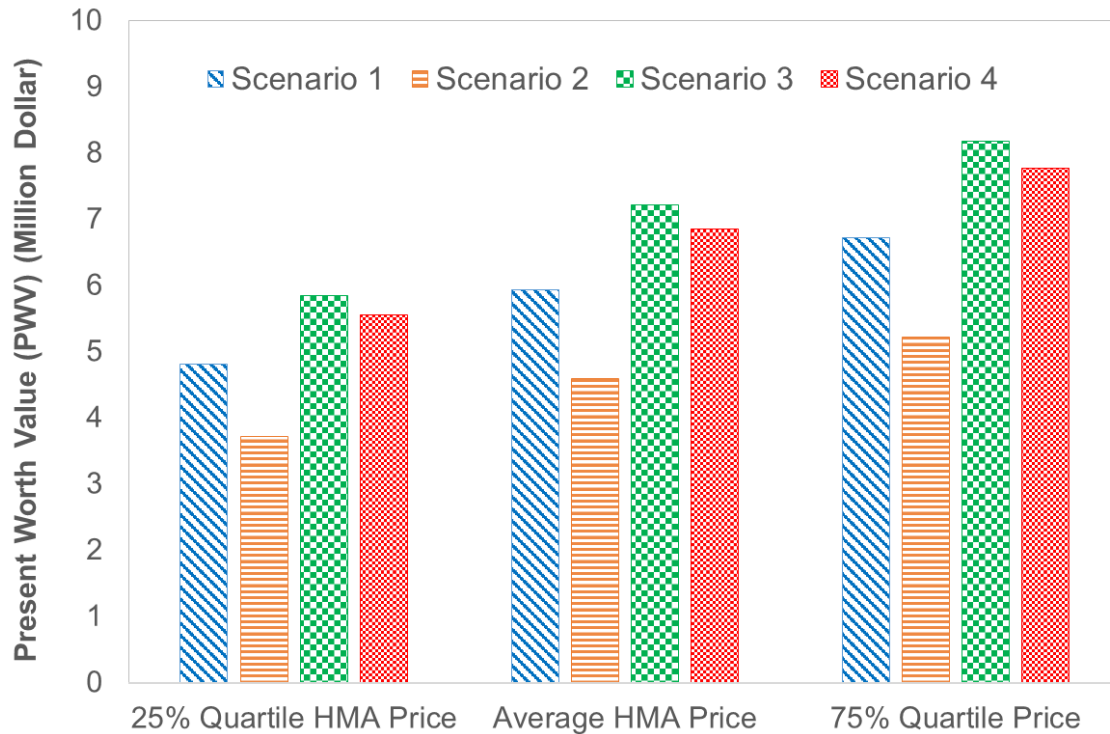


Figure 6.2. Life cycle cost analysis results and present worth value for different scenarios using the 75% quartile annual HMA quantity on a project level basis

6.3 POTENTIAL STATEWIDE SAVINGS

The total estimated cost savings with application of the cracking performance tests statewide are demonstrated in Figure 6.3 and Figure 6.4, using the average and 75% Quartile Annual HMA Quantity, respectively. In order to obtain an order-of-magnitude estimate, the estimated life cycle costs along with the average annual number of projects were considered in the cost saving estimations in the state. For this purpose, the average annual number of projects over a 4.5-year period from 2016 to the summer of 2020 was obtained using the data received from MnDOT and used in LCCA calculations. The annual average number of projects is presented in Table 6.3. Although it is a crude estimate, the addition of 2 years to the interval between overlays, can have an appreciable impact on the PWV of asphalt pavements over a 40-year analysis period.

The discrepancy of cost savings with and without application of the cracking tests and the effect of cracking tests is more recognized in the 6 in. pavement configuration compared to the 12 in pavement, as mentioned before. The results indicated higher long-term agency cost savings for 6 the in. pavement design compared to the 12 in. pavement with application of cracking tests.

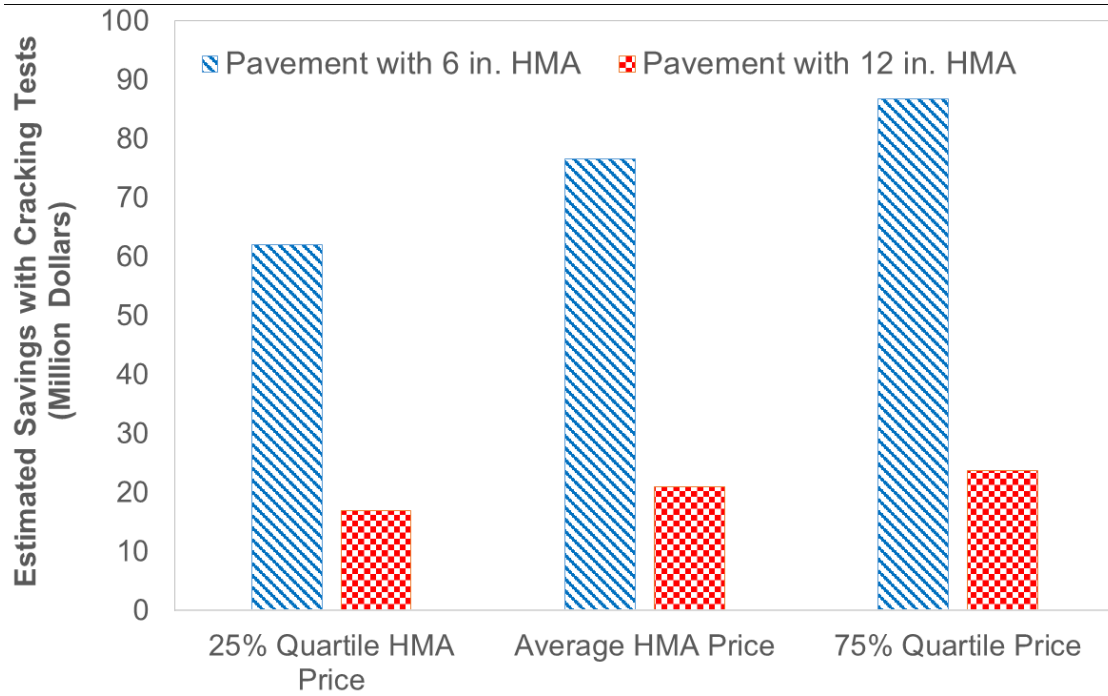


Figure 6.3. Estimated cost savings with the application of cracking tests statewide using the average annual HMA quantity.

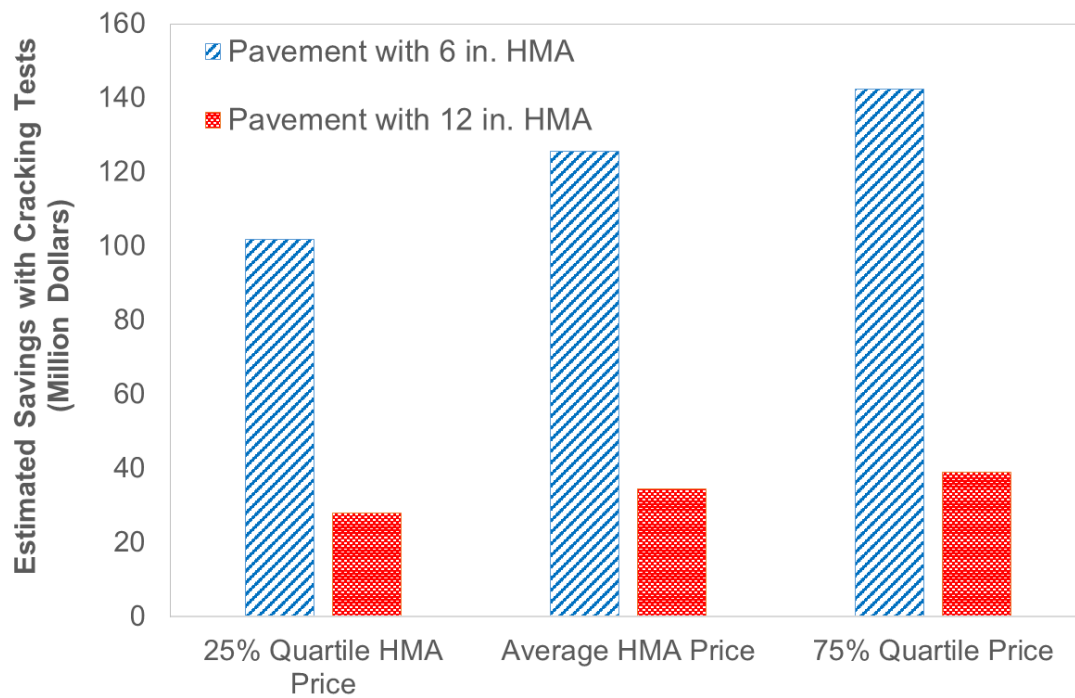


Figure 6.4. Estimated cost savings with the application of cracking tests statewide using the 75% quartile annual HMA quantity

Table 6.3. Estimate of the annual number of projects in the state

Year	No. of Projects
2016	72
2017	120
2018	98
2019	81
2020	100
Average	94

CHAPTER 7: FIELD VALIDATION PLAN

7.1 INTRODUCTION

In order to validate the use of binder and mixture cracking tests in assessing the ability of asphalt mixtures to resist failures, a plan is needed to build and monitor field test sections over a period of years. In general, several sections would be designed and constructed throughout the state using the binder and mixture cracking tests recommended in this study within the framework of the current MnDOT 2360 specifications. There are two approaches that could be taken in the design and construction of test sites. The first would be to use a factorial experiment design and the second would be a demonstration project with shadow specifications.

The objectives of building and monitoring these test sections include:

- To assess the practicality of incorporating ΔT_c and G-R in the binder selection process.
- To establish limits for ΔT_c and G-R which meaningfully differentiate cracking performance in the field.
- To assess the practicality of incorporating IDEAL CT and DCT testing in the design of asphalt mixtures.
- To assess the practicality of monitoring IDEAL CT cracking resistance during production.
- To establish limits for IDEAL CT and DCT which meaningfully differentiate cracking performance in the field.

In Minnesota, most asphalt pavement cracking is either reflection cracking or thermal cracking. Although the mechanisms for crack initiation and propagation differ, these distresses are strongly related to asphalt binder aging and asphalt mixture ductility. Thermal cracking initiates at the top or near the top of the pavement and propagates downward whereas reflection cracking begins at the interface between a cracked or jointed surface and propagates upward to the surface.

7.2 FACTORIAL DESIGN

The factorial experiment design would be the more thorough scientific approach, although it would be costlier. Binder selection would be controlled by the type of anticipated cracking, i.e., binders to be evaluated for thermal cracking would be selected based upon ΔT_c , and binders to be evaluated for reflection cracking would be based upon G-R. The parameter ΔT_c could be used for thermal cracking since it is determined from low-temperature testing, and G-R could be used for the intermediate temperature evaluation of reflection cracking which may occur over a broader range of temperatures.

Mixtures should be designed at two levels of asphalt content, one at the optimum asphalt content and one at the optimum minus 0.4% using the current MnDOT 2360 specification to differentiate cracking resistance. During mix design, both IDEAL CT and DCT testing would be done at the two levels of asphalt content with the mixture having the optimum asphalt content demonstrating the higher cracking resistance. After establishing a baseline value for IDEAL CT during mix design, the cracking test would be

used as a QC/QA tool to ensure that the plant produced mixture maintains a desirable level of cracking resistance.

The minimum individual test section lengths should be at least 750 ft with transitions between sections being no less than 100 ft. The locations of the test sections should be well marked with long metal pins as should areas for distress mapping. The distress mapping areas should generally be no less than 0.1-mile long (528 ft) in the driving lane, since this is the minimum pavement evaluation length required by FHWA and would leave a minimum of 222 ft for periodic materials sampling. If materials sampling is done for research purposes during the monitoring of the test sections, the sampling areas should be separate from the distress mapping areas. In other words, the sampling should be done only in the 222-ft materials sampling area.

The condition of the pavements prior to overlay construction should be thoroughly documented to include distress mapping, falling weight deflectometer (FWD), and ground penetrating radar (GPR) before construction. These measurements will be useful in explaining the performance of the test sections. It is especially important to accurately map the cracking in the reflection cracking experiment. Follow-up distress surveys should be conducted at 6-month intervals for no less than 4 years after construction and preferably until cracking appears.

The experimental matrices for thermal and reflection cracking are shown in Table 7.1 and Table 7.7.2 . Each field test site would have four sections distinguished by asphalt binder and asphalt mixture cracking susceptibility. The field test sites will likely have different asphalt sources, aggregate sources, contractors, climates, etc. and these will need to be treated as co-variables in the analysis. Also, as ΔT_c for the asphalt binders will be design variables for thermal cracking, the G-R values will need to be treated as co-variables. Likewise, for the reflection cracking sections, G-R will be the design variable and ΔT_c will be a co-variable.

Table 7.1. Experimental matrix for thermal cracking test sites

Binder Cracking Resistance Level	$\Delta T_c \leq -5.0$		$\Delta T_c \geq -5.0$	
	Mixture AC Level	Opt.-0.4%	Opt.	Opt.-0.4%

Table 7.7.2. Experimental matrix for reflection cracking test sites

Binder Cracking Resistance Level	$G-R \leq 450 \text{ kPa (PAV40)}$		$G-R \geq 450 \text{ kPa (PAV40)}$	
	Mixture AC Level	Opt.-0.4%	Opt.	Opt.-0.4%

Although RAP content will have a profound impact on the cracking resistance of mixtures, the DCT and IDEAL CT tests have shown good sensitivities to the presence of RAP. Thus, it could be handled in the analysis as a co-variable. In other words, in addition to holding to the same gradations at each of the four test sites, the RAP could be held constant as well provided that the RAP is well blended and subject to minimal variability in the construction of the test sections.

7.2.1 Thermal Cracking

Thermal cracking occurs when cooling ambient temperatures result in a restrained contraction of an asphalt mixture, and the induced tensile stress exceeds the strength of the mixture. This may happen due to an onset of cold weather where there is a continual drop in temperature, through a process of temperature cycling inducing fatigue in the mixture, or a combination of these. Depending upon the rate of cooling, thermal cracking can occur earlier or later in a pavement's life. The onset of thermal cracking is also very dependent upon the rate of aging of the asphalt binder and whether physical hardening occurs. Many state DOTs, including Minnesota, report that the implementation of Superpave binder specifications has resulted in less thermal cracking.

The potential delay or complete lack of thermal cracking could make the construction and monitoring of test sections ineffectual, unless two significantly differing sources of the same asphalt binder grade can be found. These differences would need to be reflected in the results of ΔT_c testing since this parameter represents cold temperature behavior. Most states that have implemented this parameter in specifications have selected a minimum value of -5.0°C after 40 hours of PAV aging (Asphalt Institute, 2019). Utah has set a minimum value of -2.0°C while Texas and Oklahoma set their minimum values at -6.0°C . It also should be noted that five out of the 10 states using ΔT_c set their PAV requirement at 20 hrs. while the other five set theirs at 40 hours. For validation of ΔT_c , each test section should have one asphalt with a value greater than -5.0°C and another with a value of less than -5.0°C . The farther apart these values are from one another in the test sections, the better the chance is of distinguishing performance. Except for the PAV aging of 40 hrs., this metric does not require an extraordinary amount of testing.

The mixture crack susceptibility will be largely influenced by the asphalt content and RAP content in the mixtures. The mixtures should have identical gradations and RAP contents for all four sections of each test site, but their asphalt contents should be separated by at least 0.4% (current allowable variability from the optimum) which should provide adequate separation of mixture cracking resistance. It is suggested that a minimum of four test sites in each test section be used in this experiment.

7.2.2 Reflection Cracking

The reflection cracking test sections should have the G-R parameter as the binder cracking resistance variable. As suggested by Rowe (2011), a G-R differentiation of one asphalt having a value less than 450 kPa (significant cracking) and another with a value of more than 450 kPa after PAV aging of 40 hrs. should be used. The greater the separation of G-R values, the more likely it is that a difference in performance will be noticed.

Zhou et al. (2010) identified the following variables that most affect the occurrence and rate of reflection cracking: 1) traffic loading level, 2) climate, 3) asphalt overlay thickness, 4) overlay mix type, 5) asphalt binder type, and 6) load transfer efficiency (LTE). Research on reflection cracking conducted at TTI and the Center for Transportation Infrastructure Systems (CTIS) have shown that there is a clear relationship between mixture ductility as measured by the overlay test and the time to cracking in the field (Zhou and Scullion, 2005) (Barros et al. 2019). Reflection cracking is generally more severe in overlays of jointed concrete pavement than in overlays of asphalt surfaces. It is recommended that, if possible, the test sections for the validation of the cracking tests be sites where jointed concrete pavement is to be overlaid with asphalt mixtures.

Mixture testing for the reflection cracking test sites should follow the same process as for the thermal cracking test sites. The mixtures for all four test sections at each test site should have identical gradations and RAP contents with asphalt contents differing by at least 0.4%. As with the thermal cracking experiment, there should be at least four test sites in different locations around the state. It is strongly recommended that the substrate for the reflection cracking test sections be jointed plain concrete pavement (JPCP) with only grinding of the joints allowed to reduce the initial faulting.

The asphalt mix design should be done according to MnDOT specification 2360 with the addition of DCT and IDEAL CT testing. DCT testing can provide the cracking resistance target for mix design and the IDEAL CT may be used to establish a cracking resistance target for QC/QA. The results of the cracking tests should show sensitivity to binder aging and asphalt content. During mixture production, IDEAL CT testing should be conducted to track cracking resistance at the subplot level. As distresses appear in the test sections, the appropriate crack resistance levels for the DCT and IDEAL CT should become apparent.

7.3 DEMONSTRATION PROJECTS

A less expensive and less rigorous approach to implementation would be the construction of demonstration projects with shadow specifications. Demonstration projects have been conducted to introduce new materials and construction technology to industry and agency personnel. They are used to build confidence in new processes and procedures for participants and spectators, and they normally include an educational component. Successful past demonstration projects have included:

- Warm Mix Asphalt (NAPA, State Asphalt Pavement Associations (SAPAs), FHWA)
- Superpave Mix Design and Evaluation (FHWA)
- Rubblization of Concrete Pavements (SAPAs, NAPA)
- Perpetual Pavements (NAPA, SAPAs)

Successful demonstration projects are sponsored jointly between contractors and DOTs highlighting the need for the new technology, the benefits for public, the advantages to the industry, and the plan for implementation. Incorporation of shadow specifications provides an opportunity for the industry to learn about the testing involved and the application of specifications to materials typically used in the state.

The need for better asphalt binder characterization is due to past observations that the Superpave fatigue cracking parameter $G^*\sin \delta$ does not adequately differentiate cracking and non-cracking susceptible binders (Hajj and Bhasin, 2017). The ΔT_c and the G-R parameters have been directly tied to ductility and field cracking. Using one or both of these parameters in place of the $G^*\sin \delta$ will provide a more meaningful binder cracking specification for the industry. The only drawback is the need for 40-hr PAV aging which could result in some shipping delays for binder suppliers.

The use of cracking tests during mixture design and QC/QA could be used as a springboard for contractor innovation. Performance testing could be used as a means of determining asphalt content on cracking resistance criteria rather than typical volumetric approaches. Some elements of volumetric requirements would need to remain to ensure that pavements do not rut or flush. For instance, it may be desirable to maintain a minimum air void requirement, e.g. two percent, at the maximum number of gyrations (N_{max}). Also, a minimum voids in mineral aggregate (VMA) or asphalt film thickness requirement could help to ensure that mixtures do not become “choked.”

CHAPTER 8: SUMMARY AND CONCLUSIONS

The objective of this research was to review and propose asphalt mixture and binder testing that could be used to assess the potential for cracking of in-service pavements. A review of existing test methods and past MnDOT research was used to focus the effort on two mixture cracking tests and three binder tests. The mixture tests selected included the DCT and the IDEAL CT tests. MnDOT had already identified a modified DCT test for use in evaluating the cold-temperature cracking potential of asphalt mixtures. Based on a previous MnDOT research project, the IDEAL Cracking Test showed promise in terms of the speed of testing and a good correlation to the DCT.

For binder testing, the ΔT_c parameter, G-R parameter, and MSCR test were selected. ΔT_c has been used to describe the cracking potential of asphalt mixtures at low temperatures and appears to be a promising metric. The G-R parameter shows a continuum in damage development across various stages of aging. The MSCR test is a method to evaluate the presence of polymer modifiers in binders and is related to the rutting potential of the binder. These tests were used in evaluating binders and mixtures from MnDOT field sites from the 2018 and 2019 construction seasons.

The asphalt mixtures and binders used in this project are described in this report. The MnDOT projects from which asphalt binders and mixtures were sampled were identified for cracking test validation. The experimental plan for testing the asphalt mixtures and binders from MnDOT 2018 and 2019 construction season were discussed. The asphalt materials for nine projects were received in 2018 and 2019.

The test procedures used for performing the IDEAL cracking test and DCT test characterizing the mixtures' resistance to cracking were discussed. Procedures for the application of IDEAL cracking test in QC/QA practices and determination of target values for the IDEAL cracking CT Index during the design process were discussed. The effects of storage time and time intervals between the compaction of specimens and testing were also investigated for a group of mixtures. Statistical analyses were provided to evaluate the effect of time intervals between molding and cracking tests. Inconsistencies in the time interval between molding and testing happen often in practice especially in quality assurance procedures. For another series of mixtures, the effect of asphalt binder content on the cracking test results was studied in the lab mixed samples.

The research team performed binder testing to characterize the PG high temperature and PG low temperature using DSR and BBR devices. Continuous grading of the binders at low and high temperatures were also provided. The research group conducted DSR testing to determine the Glover-Rowe (G-R) parameter. The G-R parameter was determined for original binders, RTFO aged binders, as well as PAV 20, PAV 40, and PAV 80 aged binders. The results were plotted in the Black Space Diagram. The effect of aging on the cracking resistance of the studied binders was evaluated.

The ΔT_c parameter was determined and investigated for each binder using the m-value and S-values obtained from BBR testing to study the low temperature behavior of binders. This was used to evaluate the resistance of asphalt binders to low temperature cracking with aging. The Multiple Creep and

Recovery (MSCR) test was also performed to study the behavior of binders at high temperatures, as a more recent test to evaluate the rutting performance. The percent recovery and Jnr were evaluated based on the MnDOT specifications for implementation of MSCR.

The information in this report provides a baseline to compare the in-place behavior of these materials as well as a guide for designing field validation projects. There are two approaches that could be taken in the design and construction of validation test sites. One would be a factorial experiment design and the other would be a demonstration project with shadow specifications.

For the factorial approach, mixtures should be designed at two levels of asphalt content, one at the optimum asphalt content and one at the optimum minus 0.4% using the current MnDOT 2360 specification to differentiate cracking resistance. During mix design, both IDEAL CT and DCT testing should be done at the two levels of asphalt content with the mixture having the optimum asphalt content demonstrating the higher cracking resistance. After establishing a baseline value for IDEAL CT during mix design, the cracking test would be used as a QC/QA tool to ensure that the plant produced mixture maintains a desirable level of cracking resistance.

A less expensive and less rigorous approach to implementation would be the construction of demonstration projects with shadow specifications. Demonstration projects have been conducted to introduce new materials and construction technology to industry and agency personnel. They are used to build confidence in new processes and procedures for participants and spectators, and they normally include an educational component. This approach would serve as an educational experience but would not provide the same level of validation as the factorial approach discussed above.

Based on the testing results and the information provided in this report, the following conclusions may be drawn:

1. The IDEAL cracking tests for all of the 2018 and 2019 pilot projects showed that all of the mixtures at the optimum asphalt content demonstrated good to excellent cracking resistance at their optimum binder contents with CT indices greater than 80.
2. For the 2018 asphalt mixtures, it was shown that the time between sample molding and testing could vary as long as two weeks without affecting the IDEAL cracking test results. This could be important for future comparisons of QC and QA testing.
3. The COV was below 12.5 percent for about 75 percent of the IDEAL cracking tests. The COV ranged between 3 percent to 22 percent.
4. It was observed that the CT index failed to make a value of 80 for the 2019 mixtures with asphalt contents less than the optimum --0.5 percent but passed for the asphalt contents that were at the optimum and higher. The three plant-produced mixtures also showed passing results.
5. The IDEAL cracking test also could distinguish between the mixtures with different asphalt contents in 2018 mixtures. Generally, a higher binder content could result in a higher CT Index of the mixtures, which indicated a higher cracking resistance.

6. All of the binders in both the 2018 and 2019 construction seasons showed good to very good resistance to cracking. They all showed good resistance to aging as well. The durability of these binders was further validated by the fact that the ΔT_c values were all greater than -2.5 C. The MSCR testing showed that the binders maintained good elasticity after RTFO aging.

The efforts made to find a correlation between DCT test and IDEAL cracking test results were also described. A linear correlation was found between the DCT fracture energy and IDEAL cracking Index for the test results from a previous MnDOT research project, while no correlation was found for the test results conducted through MNROAD/NCAT partnership. The possible reasons for not finding a correlation were presented.

The implementation of the performance testing may lead to the use of higher-quality materials than are now used and help construct and preserve a more sustainable pavement network. Application of performance testing can bring about substantial economic, environmental, and social benefits. It can lead to higher service lives of pavements, reduce the costs of maintenance and rehabilitation, and save raw materials and resources. It can enhance the safety and reduce the costs of the work zones through a lower need to repair work and work zones. It also lowers the adverse environmental effects of materials production.

REFERENCES

- Al-Masaeid, H. R. (1997). Impact of pavement condition on rural road accidents. *Canadian Journal of Civil Engineering*, 24 (4), pp. 523–532.
- Al-Qadi, I., H. Ozer, J. Lambros, A. E. Khatib, P. Singhvi, T. Khan, J. Rivera-Perez, & B. Doll. (2015). *Testing protocols to ensure performance of high asphalt binder replacement mixes using RAP and RAS* (Final Report FHWA-ICT-15-017). Illinois Department of Transportation, Springfield, IL.
- Anderson, D. A., & R. Bonaquist, (2012). *Investigation of short-term laboratory aging of neat and modified asphalt binders* (NCHRP Report No. 709). Transportation Research Board, National Cooperative Highway Research Program, Washington, DC.
- Anderson, D. A., & T. Kennedy. (1993). Development of SHRP binder specification. *Journal of the Association of Asphalt Pavement Technologies*, 62, 481–507.
- Anderson, D. A., et al. (2001). Evaluation of fatigue criteria for asphalt binders. *Transportation Research Record*, 1766, 48–56. doi:10.3141/1766-07
- Anderson, R. M., G. N. King, D. I. Hanson, & P. B., Blankenship. (2011). Evaluation of the Relationship between Asphalt Binder Properties and Non-Load Related Cracking. *Journal of the Association of Asphalt Pavement Technologies*, 80, 615–649.
- Anderson, T. L. (2005). *Fracture mechanics, fundamentals and application*. Boca Raton, FL: CRC Press.
- Arabali, P., M. S. Sakhaeifar, T. J. Freeman, B. T. Wilson, & J. D. Borowiec. (2017). Decision-Making Guideline for Preservation of Flexible Pavements in General Aviation Airport Management. *Journal of Transportation Engineering: Part B, Pavements*, 143 (2), 04017006-104017006-11.
- Arnold, J. W., B. Behnia, M. E. McGovern, B. Hill, W. G. Buttlar, & H. Reis. (2014). Quantitative Evaluation of Low-Temperature Performance of Sustainable Asphalt Pavements Containing Recycled Asphalt Shingles (RAS). *Construction and Building Materials*, 58, 1–8.
- Asphalt Institute. (2003). *Performance Graded Asphalt Binder Specification and Testing*. Superpave Series No. 1 (SP-1). Asphalt Institute, Lexington, KY.
- Asphalt Institute. (2019). *Use of the ΔT_c Parameter to Characterize Asphalt Binder Behavior*. Asphalt Institute Technical Advisory Committee, Lexington, KY.
- Bahia, H., & D. A. Anderson. (1995). *The Pressure Aging Vessel (PAV): A test to simulate rheological changes due to field aging* (ASTM Special Technical Publication 1241). West Conshohocken, PA.
- Bahia, H. U. (1991). Low-temperature isothermal physical hardening of asphalt cements. (PhD dissertation). Pennsylvania State University, State College, PA

- Barros, L., V. Garcia, J. Garibay, I. Abdallah, & S. Nazarian. (2019). Implications of Including Reclaimed Asphalt Pavement Materials to Performance of Balanced Asphalt Concrete Mixes. *Transportation Research Record*, 2673, 670-678.
- Bažant, Z. P., & J. Planas. (1998). *Fracture and size effect in concrete and other quasibrittle materials*. Boca Raton, FL: CRC Press.
- Behm, M. (2005). Linking construction fatalities to the design for construction safety concept. *Journal of Safety Science*, 43, 589-611.
- Braham, A. F., W. G. Buttlar, & M. O. Marasteanu. (2007). Effect of Binder Type, Aggregate, and Mixture Composition on Fracture Energy of Hot-Mix Asphalt in Cold Climates. *Transportation Research Record*, 2001, 102–109.
- Bureau of Labor Statistics. (2004). National census of fatal occupational injuries in 2003. U.S. Department of Labor, Washington, D.C.
- Buttlar, W. G., & R. Roque (1994). Development and Evaluation of the Strategic Highway Research Program Measurement and Analysis System for Indirect Tensile Testing at Low Temperature. *Transportation Research Record*, 1454, 163-171.
- Carpenter, S. H. (1983). *Thermal Cracking in Asphalt Pavements: An Examination of Models and Input Parameters*. USA CRREL, Hanover, NH.
- Christensen, D., & R. Bonaquist. (2005). *Evaluation of Indirect Tensile Test (IDT) Procedures for Low-Temperature Performance of Hot Mix Asphalt* (NCHRP Report 530, p. 62). NCHRP, Washington, DC.
- Dave, E. V., B. Behnia, S. Ahmed, W. Buttlar, & H. Reis. (2011). Low Temperature Fracture Evaluation of Asphalt Mixtures Using Mechanical Testing and Acoustic Emissions Techniques. *Journal of Asphalt Paving Technologists*, 80, 193-226.
- Dongre, J., M. G. Sharma, & D. A. Anderson. (1989). Development of fracture criterion for asphalt mixes at low temperatures. *Transportation Research Record*, 1228, 94–105.
- Epps, A. (1997). *Thermal Behavior of Crumb-Rubber Modified Asphalt Concrete Mixtures* (UCB-ITS-DS-97-2). Institute of Transportation Studies Dissertation Series, University of California, Berkeley, CA.
- Federal Highway Administration. (FHWA). Website. Retrieved from <https://www.fhwa.dot.gov/pavement/sustainability/>
- Gauthier, G .G., & D. A. Anderson. (2006). Fracture mechanics and asphalt binders. *Road Materials and Pavement Design*, 7 (Special Issue EATA), 9–35. doi:10.1080/14680629.2006.9690056
- Geiger, D. (2005). Pavement preservation definitions. Memorandum. Federal Highway Administration, Washington, DC.

- Germann, F. P., & R. L. Lytton. (1979). *Methodology for predicting the reflection cracking life of asphalt concrete overlays*. Report No. FHWA-TX-79-09, Federal Highway Administration, Washington, DC.
- Glover, C. J., R. R. Davison, C. H. Domke, Y. Ruan, P. Juristyarini, D. B. Knorr, & S. H. Jung. (2005). *Development of a New Method for Assessing Asphalt Binder Durability with Field Evaluation* (FHWA/TX-05/1872-2). Federal Highway Administration and Texas Department of Transportation, Washington D.C.
- Hajj, E., P. Sebaaly, J. Porras, & J. Azofeifa. (2010). *Reflection Cracking of Flexible Pavements Phase III: Field Verification* (Research Report No. 13KJ-1). Nevada Department of Transportation, Research Division, University of Nevada, Reno.
- Hajj, R. & A. Bhasin. (2017). The Search for a Measure of Fatigue Cracking in Asphalt Binders – A Review of Different Approaches. *International Journal of Pavement Engineering*, 19 (3), 205-219.
- Hanson, C. (2015). *Minnesota Disk-shaped Compact Tension Testing (DCT)*. Presented at the Swedish Transport Administration Meeting, Sep. 2015, Stockholm.
- Harmelink, D., & Aschenbrener, T. (2003). *Extent of Top-Down Cracking in Colorado* (Report No. CDOT-DTD-R-2003-7). Colorado Department of Transportation, Denver, CO.
- Hass, R., F. Meyer, G. Assaf, & H. Lee. (1987). A Comprehensive Study of Cold Climate Airport Pavement Cracking. *Proceedings of Association of Asphalt Paving Technologists*, 56, 198–245.
- Hill, B., B. Behnia, W. B. Buttlar, & H. Reis. (2013). Evaluation of Warm Mix Asphalt Mixtures Containing Reclaimed Asphalt Pavement through Mechanical Performance Tests and an Acoustic Emission Approach. *ASCE Journal of Materials in Civil Engineering*, 25 (12), 1887–1897.
- Hills, J. F., & D. Brien. (1966). The Fracture of Bitumens and Asphalt Mixes by Temperature Induced Stresses. *Proceedings of Association of Asphalt Paving Technologists*, 35, 292–309.
- Hoare, T. & S. Hesp. (2000). Low-temperature fracture testing of asphalt binders: Regular and modified systems. *Transportation Research Record*, 1728, 36–42. doi:10.3141/1728-06
- Howell, G. A, G. Ballard, T. S. Abdelhamid, & P. Mitropoulos. (2002). Working near the edge: A new approach to construction safety. Paper presented at the 10th Annual Conference of the International Group for Lean Construction, Gramado, Brazil.
- Jung, D. H., & T. S. Vinson. (1994). *Low-Temperature Cracking: Test Selection* (SHRP A-400). Strategic Highway Research Program, Washington, D.C.
- Kandhal, P.S. (1977). *Low-Temperature Ductility in Relation to Pavement Performance*. ASTM STP 628: *Low-Temperature Properties of Bituminous Materials and Compacted Bituminous Paving Mixtures*. American Society for Testing and Materials, Philadelphia, PA.
- Khattak, A. J., A. J. Khattak, & F.M. Council. (2002). Effects of work zone presence on injury and non-injury crashes. *Journal of Accident Analysis and Prevention*, 34, 19-29.

- Lee, N. K., & S. A. M. Hesp. (1994). Low-temperature fracture toughness of polyethylene-modified asphalt binders. *Transportation Research Record*, 1436, 54–59.
- Lee, N. K., G. R. Morrison, & S. A. M. Hesp. (1995). Low temperature fracture of polyethylene-modified asphalt binders and asphalt concrete mixes. *Journal of the Association of Asphalt Paving Technologists*, 64, 534–574.
- Li, X., A. F. Braham, M. O. Marasteanu, W. G. Buttlar, & R. C. Williams. (2008a). Effect of Factors Affecting Fracture Energy of Asphalt Concrete at Low Temperature. *International Journal of Road Materials and Pavement Design*, 9, 397–416.
- Li, X., & M. O. Marasteanu. (2004). Evaluation of the Low Temperature Fracture Resistance of Asphalt Mixtures Using the Semi-Circular Bend Test. *Journal of Association of Asphalt Paving Technologists*, 73, 401–426.
- Li, X., M. O. Marasteanu, R. C. Williams, & T. R. Clyne. (2008b). Effect of Reclaimed Asphalt Pavement (Proportion and Type) and Binder Grade on Asphalt Mixtures. *Journal of Transportation Research Record*, 2051, 90–97.
- Loria-Salazar, L. (2008). Reflection Cracking of Flexible Pavements: Literature Review, Analysis Models, and Testing Methods (Master's thesis). University of Nevada, Reno, NV.
- Lytton, R., X. Luo, & R. Luo. (2013). *Interim Report of Project NCHRP 1-52: A Mechanistic-Empirical Model for Top-Down Cracking of Asphalt Pavement Layers*. Texas A&M Transportation Institute, College Station, TX.
- Marasteanu, M. O., A. Zofka, M. Turos, X. Li, R. Velasquez, X., Li, W. Buttlar, G. Paulino, ... J. McGraw. (2007). *Investigation of Low Temperature Cracking in Asphalt Pavements: National Pooled Fund Study 776*. Minnesota Department of Transportation, St. Paul, MN.
- Marasteanu, M. O., W. Buttlar, H. Bahia, & C. Williams. (2012). *Investigation of Low Temperature Cracking in Asphalt Pavements: National Pooled Fund Study Phase II*. Minnesota Department of Transportation, St. Paul, MN.
- Marasteanu, M. O., & A. C. Falchetto. (2018). *Review of experimental characterization and modelling of asphalt binders at low temperature*. *International Journal of Pavement Engineering*, 19 (3), 279-291, doi. 10.1080/10298436.2017.1347436
- Masad, E., C. Huang, & J. D'Angelo. (2009). *Characterization of Asphalt Binder Resistance to Permanent Deformation Based on Nonlinear Viscoelastic Analysis of Multiple Stress Creep Recovery (MSCR), Vol. 78*. Association of Asphalt Paving Technologists, St. Paul, MN.
- McDaniel, R., R. Leahy, G. Huber, J. Moulthrop, & T. Ferragut. (2011). *The Superpave Mix Design System: Anatomy of a Research Program* (Web-only document 186). Transportation Research Board, Washington, DC.

- Mitropoulos, P., T. S. Abdelhamid, & G. A. Howell. (2005). Systems Model of Construction Accident Causation. *Journal of Construction Engineering and Management*, 131 (7), 816-825.
- Newcomb, D., & F., Zhou. (2018). *Balanced Design of Asphalt Mixtures* (Final Report MN/RC 2018-22) Minnesota Department of Transportation. St. Paul, MN.
- Noyce, D. A., H. U. Bahia, J. Yambo, J. Chapman, & A. Bill. (2007). *Incorporating Road Safety into Pavement Management: Maximizing Surface Friction for Road Safety Improvements* (MRUTC 04-04). Wisconsin Department of Transportation, Madison, WI.
- Pavement Interactive. Retrieved from <https://www.pavementinteractive.org/>
- Peshkin, D., L. K. Smith, A. Wolters, J. Krstluovich, J. Moulthrop, & C. Alvarado. (2011). *Guidelines for the preservation of high volume-traffic roadways* (S2-R26-RR-2). Transportation Research Board, Washington, DC.
- Readshaw, E .E. (1972). Asphalt specifications in British Columbia for low temperature performance. *Journal of the Association of Asphalt Paving Technologists*, 41, 562–581.
- Reinke, G. (2018) The Relationship of Binder Delta Tc (ΔT_c) & Other Binder Properties to Mixture Fatigue and Relaxation. Presentation given at the FHWA Binder ETG Meeting, Fall River, MA.
- Roque, R., & W. G. Buttlar. (1992). The Development of a Measurement and Analysis System to Accurately Determine Asphalt Concrete Properties Using the Indirect Tensile Mode. *Journal of the Association of Asphalt Paving Technologists*, 61, 304–332
- Rowe, G. (2011). Discussion to “Evaluation of the Relationship between Asphalt Binder Properties and Non-Load Related Cracking.” *Journal of the Association of Asphalt Pavement Technologies*, 2011, 649–663.
- Rowe, G. (2017). Binder specifications with a focus on cracking. Presentation given at the North East Asphalt User/Producer Group, Hartford, CT.
- Rowe, G., G. King, & M. Anderson. (2014). The Influence of Binder Rheology on the Cracking of Asphalt Mixes in Airport and Highway Projects. *Journal of Test and Evaluation*, 42, (5), 1063-1072.
- Sugawara, T., & A. Moriyoshi. (1984). Thermal Fracture of Bituminous Mixtures. *Proceedings of Paving in Cold Areas Mini-Workshop*, 291–320.
- Svasdisant, T., M. Schorsch, G. Y. Baladi, & S. Pinyosunun. (2002). Mechanistic Analysis of Top-Down Cracks in Asphalt Pavements. *Transportation Research Record*, 1809, 126-136.
- Taylor, A. J. (2018). Northern Cracking Group – Laboratory Testing Update. Slide presentation 2018 Fall Sponsor Meeting. National Center for Asphalt Technology, Auburn University, Auburn, AL.

- Tighe, S., N. Li, L. Cowe Falls, & R. Haas. (2000). Incorporating Road Safety into Pavement Management. *Transportation Research Record*, 1699, 1-10.
- Uhlmeier, J. S., Willoughby, K., Pierce, L. M., & Mahoney J. P. (2000). Top-down Cracking in Washington State Asphalt Concrete Wearing Courses. *Transportation Research Record*, 1730(1), 110-116.
- Van Dam, T. J., J. T. Harvey, S. T. Muench, K. D. Smith, M. B. Snyder, I. L. Al-Qadi, A. Kendall. (2015). *Towards Sustainable Pavement Systems: A Reference Document* (FHWA-HIF15-002). Federal Highway Administration (FHWA), Washington, DC.
- Wagoner, M. P., W. G. Buttlar, & G. H. Paulino. (2005). Disk-Shaped Compact Tension Test for Asphalt Concrete Fracture. *Experimental Mechanics*, 45, 270–277.
- Wagoner, M., W. Buttlar, G. Paulino, & P. Blankenship. (2006). Laboratory Testing Suite for Characterization of Asphalt Concrete Mixtures Obtained from Field Cores. *Journal of the Association of Asphalt Paving Technologists*, 75, 815–852.
- Walls, J., & M. R. Smith (1998). *Life-cycle cost analysis in pavement design in search of better investment decisions* (FHWA-SA-98-079). Federal Highway Administration, Washington, DC.
- Walubita, L. F., A. N. M. Faruk, G. Das, H. A. Tanvir, J. Zhang, & T. Scullion. (2012). *The Overlay Tester: A Sensitivity Study to Improve Repeatability And Minimize Variability In The Test Results* (Report FHWA/TX-12/0-6607-2). Texas Department of Transportation, Austin, TX.
- West, R., J. R. Willis, & M. Marasteanu. (2013). *Improved Mix Design, Evaluation, and Materials Management Practices for Hot Mix Asphalt with High Reclaimed Asphalt Pavement Content* (NCHRP Report 752). Transportation Research Board, Washington, DC.
- Zhang, K., S. Batterman, & F. Dion. (2011). Vehicle emissions in congestion: Comparison of work zone, rush hour and free-flow conditions. *Journal of Atmospheric Environment*, 45, 1929- 1939.
- Zhou, F, S. Im, L. Sun, & T. Scullion. (2017). Development of an IDEAL cracking test for asphalt mix design and QC/QA. *Road Materials and Pavement Design*, 18(Sup 4), 405-427.
DOI:10.1080/14680629.2017.1389082
- Zhou, F., & T. Scullion. (2005). *Overlay Tester: A Rapid Performance Related Crack Resistance Test* (Report FHWA/TX-05/0-4667-2). Texas Department of Transportation, Austin, TX.
- Zhou, F., D. Newcomb, C. Gurganus, S. Banihashemrad, E. Park, M. Sakhaeifar, & R. Lytton. (2016). *Experimental Design for Field Validation of Laboratory Tests to Assess Cracking Resistance of Asphalt Mixtures* (Final Report for NCHRP Project 9-57). Transportation Research Board, Washington, DC.
- Zhou, F., S. Hu, & T. Scullion. (2006). *Integrated Asphalt (Overlay) Mix Design with Balancing Rutting and Cracking Requirements* (Report FHWA/ TX-06/0-5123-1). FHWA, Texas Department of Transportation, Austin, TX.

Zhou, F., S. Hu, & T. Scullion. (2010). Advanced Asphalt Overlay Thickness Design and Analysis System. *Journal of the Association of Asphalt Paving Technologists*, 79, 597-634.

Zhou, F., S. Hu, T. Scullion, M. Mikhail, & L. Walubita. (2007). A Balanced HMA Mix Design Procedure for Overlays. *Proceedings of the Association of Asphalt Paving Technologists*, 76, 823-850.